System Level Investigations of Television Based Bistatic Radar

Ching-Wei, Wesley Chang

A dissertation submitted to the Department of Electrical Engineering,
University of Cape Town, in fulfilment of the requirements
for the degree of Master of Science in Engineering.

Cape Town, December 2005

Declaration

I declare that this work done is my own, unaided work. This dissertation is being submitted to the Department of Electrical Engineering, University of Cape Town, in fulfilment of the requirements for the degree of Master of Science in Engineering. It has not been submitted for any degree or examination in any other university.

Signed by candidate

Signature of Author

Cape Town
2005

Abstract

This dissertation is presented to introduce the reader to the techniques used and the technology of a Television Based Bistatic Radar system. Technology such as this one makes use of a non-cooperative television transmitter as an illuminator for the bistatic radar system investigated. Both technical and theoretical information about the topic will be introduced.

The dissertation starts off with a brief introduction to its structure, and evolves into a historical overview of multistatic and bistatic radars. Certain techniques about bistatic radars used in the past will be discussed; their advantages and disadvantages of the various techniques will also be shown. The geometrical design and the various effects of the bistatic radar arrangement will be discussed.

A simulator created to plot various SNR patterns over the Western Cape was also developed to estimate the input SNR value received at the receiver. This simulator is flexible in the sense that the transmitter and receiver locations can be arbitrarily placed around the Western Cape. The estimated SNR values for different ranges are then plotted over the mapped area. Not only does the simulator show the SNR plots, it also indicates the coverage area of both the receiver and the transmitter. The target flight path of aircrafts flying into Cape Town can also be included in the simulation.

This dissertation will then focus on the actual simulation of the receiver designed for the purpose of airborne target surveillance. These simulations involves actual receiver components used at the system level, with the created television input signal, as well as recorded data. The discussion will then focus on the use of an ordinary pc TV-card which was used as a receiver, whereby measurements were taken for actual targets landing into Cape Town International Airport. These target signals were recorded and analysed. A discussion surrounding this topic was included for the ambiguity analyses of the recorded data.

This dissertation is concluded by discussing the conclusions of the research as well as making some recommendations for future work which could be done to improvement the measured results for a television based bistatic radar system.

Acknowledgements

I would firstly like to thank my supervisor, Professor Mike Inggs for his immense wisdom and guidance which enabled me to complete this research. I would also like to thank Dr. Richard Lord and Thomas Bennett for their guidance and support, their input was most valuable to the research. Special thanks also go to Professor Chris J. Baker of the University of College London for his advice and wisdom.

I would also like to thank my family and friends for their support throughout this period and lastly to the colleagues in the radar lab for their contributions.

Contents

List of Figures

List of Tables

List of Symbols

Symbol	—	Definition
α_R	—	Receiver look angle
α_T	—	Transmitter look angle
β	—	Bistatic angle
δ_T	—	Transmitters' bistatic angle
δ_R	—	Receivers' bistatic angle
$\Delta\psi$	—	Calculated phase difference between two channels
ΔR_B	—	Bistatic system resolution
ΔR_M	—	Monostatic system resolution
ΔT_{rt}	—	Signal interval measured at the receiver of the transmitted pulse from the target
ΔT_{tt}	—	Transmitted pulse and received signal interval
ϵ	—	Error factor
κ	—	Bistatic maximum range product
λ	—	Wavelength
ω_c	—	Cutoff frequency
ω_{D_a}	—	$\frac{-2V_a\omega_c}{c}$
ω_{D_H}	—	$\frac{-2V_H}{c}\omega_c$
Φ	—	Noise free phase difference
σ_B	—	Bistatic radar target cross section
σ_M	—	Monostatic radar target cross section
τ	—	Compressed radar pulse width
θ	—	Antenna beamwidth
θ_R	—	Receiver look angle
θ_s	—	Directive angle of the antenna
θ_T	—	Transmitter look angle
c	—	Speed of light
d	—	Element spacing of the Yagi antenna
e	—	Eccentricity
f_d	—	Doppler frequency
f_{TV}	—	Television RF frequency
h_t	—	Target altitude
h_R	—	Receiver antenna altitude

Symbol	—	Definition
h_T	—	Transmitter antenna altitude
k	—	Boltzmann's constant
r_R	—	Coverage area of receiver
r_T	—	Coverage area of transmitter
t_o	—	Integration time through which the data is recorded (sampling period)
v_t	—	Target velocity
A_C	—	Common coverage area
AF	—	Pattern array factor
B_n	—	Receiver noise bandwidth
B_R	—	Receiver beamwidth
B_T	—	Transmitter beamwidth
C	—	Cut angle
F	—	Triangulation factor
F_T	—	Transmitter pattern propagation
F_R	—	Receiver pattern propagation
G_T	—	Gain of the transmitters' antenna
G_R	—	Gain of the receiver
K	—	Bistatic radar constant
L	—	Baseline
L_M	—	Losses in the system for the monostatic case
L_R	—	Losses in receiver
L_T	—	Losses in transmitter
N	—	Number of elements in the Yagi antenna
P_{av}	—	Average power
P_R	—	Received power
P_T	—	Transmitted power
R_M	—	Target distance for the monostatic case
R_R	—	Receiver to target distance
R_T	—	Transmitter to target distance
R_x	—	Receiver
T_s	—-	Receiver noise temperature
T_x	—	Transmitter
$\left(\frac{S}{N}\right)$	—	Signal to noise ratio
V_a	—	Target radial velocity
V_H	—	One-way radial velocity
V_R	—	Receiver velocity vector
V_T	—	Transmitter velocity vector

Nomenclature

Ambiguity functions—A function which shows the results of convolving a range of frequency shifted signals with a fixed reference signal.

Azimuth—Angle in a horizontal plane, relative to a fixed reference, usually north or the longitudinal reference axis of the aircraft or satellite.

Baseline—The identified distance between the transmitter and receiver locations for the bistatic scenario.

Beamwidth—The angular width of a slice through the mainlobe of the radiation pattern of an antenna in the horizontal, vertical or other plane.

Coverage area—This is defined as the area which is illuminated by the transmitter, as well as the receiver, which is under surveillance.

Doppler frequency—A shift in the radio frequency of the return from a target or other object as a result of the object's radial motion relative to the radar.

Ovals of Cassini—This is identified as the locus of the vertex of a triangle when the product of the sides adjacent to the vertex is constant and the length of the opposite side is fixed.

Monostatic radar—The most common radar system configuration, whereby the receiver and transmitter are located at the same location.

Passive radar—Passive radar is a type of radar system which uses one or more receivers, but lacks an active transmitter. The system detects ambient radio signals emanating from nearby radio transmitters. The receiver is either bistatic or multistatic, since it is positioned elsewhere. The system is not restricted to one receiver - several receiver systems may be operated in conjunction with one or many transmitters.

Resolution—The minimum spacing between two targets which allows them to be distinguished, by the radar.

ACMA	—	Analytical Constant Modulus Algorithm
AF	—	Pattern Array Factor
AM	—	Amplitude Modulated
AOA	—	Angles of Arrival
CFAR	—	Constant False Alarm Rate
CW	—	Continuous Wave
DBM	—	Double Balanced Mixer
DBS	—	Direct Broadcast by Satellite
DERA	—	Defence Evaluation and Research Agency
DOA	—	Direction of Arrival
DOT	—	Doppler Only Tracking
DSB-AM	—	Double Sideband Amplitude Modulation
FFT	—	Fast Fourier Transform
FM	—	Frequency Modulated
FSK	—	Frequency Shift Keying
IF	—	Intermediate Frequency
LO	—	Local Oscillator
LOS	—	Line of Sight
MUSIC	—	Multiple Signal Characterisation
NEC	—	Numerical Electromagnetic Code
PAL	—	Phase Alternating Line
PC	—	Personal Computer
PDF	—	Probability Density Function
RCS	—	Radar Cross Section
TDOA	—	Time Difference of Arrival
SNR	—	Signal to Noise Ratio
SSB	—	Single Side-Band
SSB-SC	—	Single Side-Band Suppressed Carrier
TV	—	Television
UCL	—	University College London
UHF	—	Ultra High Frequency
VHF	—	Very High Frequency
VXI	—	VMEbus Extensions for Instrumentation

Chapter 1

Introduction

1.1 Background to Bistatic Radars

Bistatic radars are systems whereby the transmitter and receiver are separated by a distance that is comparable with the maximum range of target detection with respect to the transmitter and receiver sites. The separation between these sites, introduces certain factors which have to be taken into consideration. The main difficulty with this separation in bistatic systems is the synchronisation between the transmitter and receiver locations. This has to be achieved in order to lock onto a specific signal at any particular point in time for target tracking purposes.

Various forms of bistatic radars have been developed over the past few years, of which, the most significant would be the multistatic radar. Multistatic radar is a form of bistatic radar with one transmitting site, and various receivers. The advantages and disadvantages of using such systems are discussed in detail in Chapter 2.

This dissertation investigates the literature review of bistatic radars, as well as a system level investigation for the bistatic radar receiver. Systems which were designed in the past are reviewed and analysed for compatibility with the receiver to be designed. The designs for this receiver system are discussed and simulated. The results for these simulations will be presented and discussed in detail.

1.2 Advantages of Bistatic Systems

Bistatic systems have many advantages when compared to monostatic systems, to list a few:

- Bistatic systems has its transmitter and receiver located at separate sites, and therefore is not susceptible to external jamming. If for any reason should the transmitter be destroyed, the receiver can be easily adapted to receive signals from another transmitting site.

- Another advantage is that multiple receivers can share a common transmitter. This is beneficial in the sense that these transmitters can be isolated, but yet still operational.
- Economic cost of such a system is also a main advantage since such a system does not require the transmitter if it makes use of existing transmissions, and hence consist of only the receiver costs.

1.3 The Objectives of the Research

The objectives of the research are:

1. To give the history and background to bistatic radars, and to give some examples of their uses in the past.
2. To determine the advantages and disadvantages of the system and their uses.
3. To describe the geometry of a bistatic radar system, and the theory behind such a system.
4. To create a signal to noise ratio (SNR) simulator for these SNR predictions.
5. To design and simulate the bistatic receiver system.
6. To analyse and process the recorded and simulated data.
7. To draw conclusions and make recommendations about the research.

Much of the predictions of the signal levels for the radar receiver were implemented in software. This simulator, which is mentioned in point 6 above, is able to predict signal-to-noise ratio values for targets at specific distances away from the receiver, this will be discussed in detail in Chapter 4, as well as some simulated predictions will be presented. A simulation of the receiver chain designed was also implemented in software, and the results from this analysis is also discussed later.

Not much work has been done to date in the radar field with regards to the use of Doppler and Bearing tracking (DBT), Doppler-only tracking (DOT) or Bearing only tracking (BOT), although much attention has been paid to it in the context of passive sonar systems [20]. The main method used within this research will be based on Doppler, as well as the Bearing information.

The potential rewards for this research are no costly transmitter required, and no-one can detect the presence of the receiver. The challenges are however equally as difficult since there is no dedicated transmitter, one is forced to use commercial transmitters. This proves to be challenging in the respect that no synchronisation exists between the transmitter and receiver, and synchronisation between the two respectively is difficult to achieve.

The techniques and recordings are demonstrated using the vision carrier of the PAL-TV signal used in South Africa. With this technique, together with the correct equipment, this research will show that Doppler extraction of airborne targets can be achieved. Much of the information gathered to complete this dissertation was based on various books as well as several papers published.

1.4 Plan of Development

Chapter 1 is the basic introduction to the research. This chapter also investigates the problem at hand and defines the objectives of the dissertation.

Chapter 2 reviews the published material on bistatic, and passive radar[1] techniques to provide the background information to the techniques used within the research. This chapter begins by defining multistatic radars and their uses. The discussion then evolves and concentrates on areas of bistatic radars, the types of operational modes as well as the various advantages and disadvantages for the system. Thereafter, the history of bistatic radars is discussed, ranging from the first use of these systems to modern day systems. Various applications of bistatic radars were then described, both for military uses as well as non-military uses. These applications were presented to show how bistatic radars have been of use to us, with the inclusion of some possible future products for both military and non-military applications of bistatic radars. Some of the enhanced techniques of bistatic systems are also discussed with regards to the performance of these bistatic systems compared to monostatic systems.

The overview of television based bistatic radars is then discussed in detail. There were four main groups of researchers involved and contributed to the area of bistatic research. Firstly, it was Griffiths and Long [14] of the University College London (UCL). This work performed in 1986, exploited pulse-like nature of parts of the television waveform for bistatic use. Various parts of the television signal was exploited to show the ability of the system to receive clutter from surrounding buildings. With the addition of some processing techniques, Griffiths and Long were able to successfully 'track' moving targets, however, this system was deemed unpractical since it required a special transmission waveform and only had a range resolution of 1800m and a range ambiguity of 9600m.

One of the major difficulties encountered within the research was the limited capability to capture long periods of data. In addition to that, was the limited dynamic range of the moving target indicator (MTI) to cope with the high clutter/signal ratio of this type of system. This research was concluded by stating that since the illuminator was not radar-like, however, an autocorrelation function could still be performed on the transmitted waveform. This indicated broad peaks at 64 μs intervals which corresponds with the line

[1] "Passive radar is a type of radar system which uses one or more receivers, but lacks an active transmitter. The system detects signals reflected from targets emanating from nearby radio transmitters. The receiver is either bistatic or multistatic, since it is positioned elsewhere. The system is not restricted to one receiver - several receiver systems may be operated in conjunction with one or many transmitters." [42]

sync pulses of the television signal (more detail about television signals can be found in Chapter 3). Their research also led them to using the multiburst test signal of the television transmission to increase the performance, however, possibly due to the lower energy of the multiburst pulse compared to the sync, moving targets were still unresolved. This research was extremely valuable in the sense that it was the first attempt of using television broadcasts as the transmission for the radar system in the time domain.

Griffiths, Garnett, Baker and Keaveney [13] later returned to research using television transmissions as the source of the radar transmitter using a sophisticated correlation technique on Direct Broadcast Satellite (DBS) television signals. The receiver system used had two receiving channels. One of the signals were received directly from the transmitter, while the other was from the target flightpath. Cross-correlation between these two channels produced a compressed waveform which essentially increased the processing gain for the system. This amount of gain however was still insufficient to detect targets successfully.

Another group of researchers related to this bistatic radar field were two French researchers, Poullin and Lesturgie of ONERA [28], who described their system to be a multistatic passive system. Their system were also based on television transmissions, with the exception that for each of the television transmitters used, they had a two channel receiver system, with one of the antennas pointed directly at the transmitter, while the other was pointed in the surveillance region. The signals captured were sampled, and the FFT was taken to determine the spectrum around vision carrier of the television signal. The spectrum of the signal captured from the channel pointed directly at the transmitter was subtracted from the signal captured from the surveillance channel to extract the Doppler shifted echoes of the target. In order for their system to work, the bistatic system would require four or more transmitters. The extracted Doppler values from each of the receiver channels would be used to solve the target location.

The technique used by these French researchers were interesting in the fact that target location could be acquired by the use of only the Doppler information. However, this system was impractical in the sense that it required a minimum of four transmitters at any time in order for the system to work. This, in the real world is not very practical. Another difficulty perceived from their system was that the researchers did not indicate how the Doppler profiles extracted from each of the transmitters would be used for target location if multiple targets were to occur in the same area.

Carrara, Toutier and Pecot of THOMPSON-CSF [5], had also performed a study on exploiting the practicalities of the frequency division multiplexed digital waveform produced from television systems. The system designed by them, extracted target echoes, which was used in a correlator based FFT to achieve sample in range and Doppler. The detection of the target would require the signals to be acquired directly from the transmitter as well as the target, to establish the bistatic range. Two types of receiver configurations for target acquisition were proposed by them, and more detail of this is described in

The final researcher who exploited television signals as a form of transmission for the bistatic system was Howland [20, 21]. His work, unlike others, assumed the system to have only one transmitter and one receiver. From his experiments, he was able to demonstrate how a target's velocity and location can be estimated from the measurement of target Doppler and Direction of Arrival (DOA). The extracted results were from a series of measurements taken by him, based on the fact that the Doppler and DOA for a target echo with time was uniquely determined by the target course and velocity. His experiment did not require any timing measurements, and therefore no synchronisation between the transmitter and receiver were required, provided that the carrier frequency of the signal was stable enough, and known.

The data captured by him was done via a two channel, two downconversion receiver. These signals were then further downconverted in signal processing to baseband and thereafter processed taking the FFT. From the FFT of the results, the Doppler estimates were extracted. The spectrum of the FFT results from the two channels were then subtracted from one another to calculate the bearing of the target. Some of the difficulties experienced in his research was the mutual coupling which occurred at the antenna, this however was resolved and described in Chapter 2. Much of the work performed by Howland had significant overlap with the work performed by Griffiths and Long [14], with the exception that Howland's work was performed in the frequency domain.

After the review of the past systems used, the chapter describes some of the advantages and disadvantages noted for the Television Based Bistatic System. The chapter then begins to describes the coordinate system, overall geometry and equations for bistatic systems. This section covers with emphasis on the significant difference between bistatic and monostatic system, both within the arrangement of the geometrical setup of the system, as well as the equations attached to the system. The received power levels of the system were also described in significant detail here, and the associated equations for the bistatic configuration to calculate power levels were included.

Target location and the coverage area are of great importance for the system. The equations associated for target location and coverage were presented here. The equations used for the coverage area had a great impact on the system, since this was an estimation of the area at which a target could be realistically tracked for our system.

A section on Doppler and DOA estimates was also presented within this chapter. This section contains some equations and theoretical background to the Doppler values extracted and showed how these values relates to the bistatic radar configuration which was conducted in the experiment. With a radar receiver to be designed, the signal to noise ratio measurement was required to be known at the radar receiver. However, with the knowledge of the geometry and configuration of the system, this could be accurately estimated. This accuracy could effect the measurements of Doppler and DOA for the target. These effects on the measurements were explained in detail within this chapter.

This chapter was concluded in noting the significant difference between bistatic and monostatic systems. The cause of this difference was contributed mainly by the geometry of the system. This chapter also proves that the performance of the bistatic system can never exceed that of a monostatic system, however, there are distinct applications whereby bistatic systems supersedes that of the monostatic system. Much of the literature and techniques researched within this section was taken into consideration for the design of the system.

Chapter 3 presents the theory of Television Based Bistatic Radar. The objectives of this chapter are to provide an in-depth analysis of Howland's system, whereby Doppler and DOA information of the targets flightpath was successfully extracted. This chapter also introduces the theory of the television waveforms used in the research. The typical modulation scheme used for television systems is discussed, with emphasis on the type of modulation used on South African television signals (PAL). Waveforms of a typical television signal will be shown as well as the frequency band of the signal. The bandwidth of the signal as well as the location of the carrier is required in order to track targets. The details of the television signal is required as this is the foundation of looking into which portion of the television signal is stable enough, and could be used for target detection.

A simulation was also created within Systemview to simulate the television signal used. The simulated signal represented the same carrier suppression used within the actual modulated television signals recorded. The output of this simulation will provide the input signal to the receiver simulation designed, which is identified in Chapter 5. The design of the system as well as the results from the simulation are shown in Chapter 5. The theory and background to the SNR simulator created in Chapter 4 are also presented in this chapter.

Chapter 4 describes the SNR simulator which was created. The details of the transmitter will be provided in chapter which will be used for the calculation of SNR values, and coverage areas. This signal to noise ratio simulator was created in package called IDL. The purpose of this simulator was to predict SNR values for the coverage area of the system. Included within this simulator is the aircraft flightpath into Cape Town as well as the coverage areas of both the transmitter and the receiver. The image shown in Figure 1.1 indicates the output of the simulation. Adjustments can be made within the software to create various plots over the mapped area.

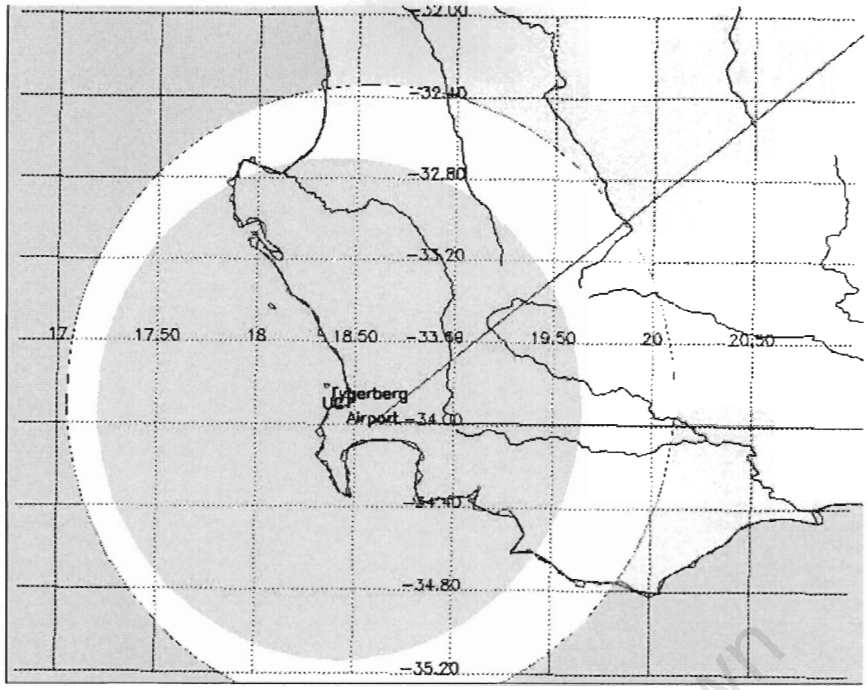

Figure 1.1: Mapped area created from the simulator.

As can be seen in Figure 1.1, the vertical lines are the longitudes, while the horizontal lines represents the latitudes. The two lines shown on the image indicates target flight-paths of targets flying into the Cape Town Airport. The inner shaded ring represents the coverage area of the receiver, while the outer shaded ring represents the coverage area of the transmitter. The coverage area mentioned for both the transmitter and receiver are defined as the radar horizon coverage for targets entering into Cape Town. The coverage areas were calculated with targets at altitudes of roughly 1500 feet, roughly 451 m. Details of how the simulator was created, and a description of the specific equations used is presented in this chapter. This chapter also describes how the simulator can be modified such that the SNR estimate can be plotted with the use of either an omnidirectional receive antenna, or a directional antenna for the receiver measurement. The results indicated from the simulation were also referenced via calculations with the equations used which can be found in this chapter.

In Chapter 5, is an overview of the proposed, two-channel, television-based bistatic radar receiver system designs. The receiver designed is for a system which could be built at the University of Cape Town, primarily used for air-surveillance purposes. This system will essentially 'hitchhike' off existing non-cooperative television transmitters located around Cape Town. The receiver system will essentially detect airborne targets by focusing on the vision carrier of the television signal transmitted. The decision for this design was based on the research conducted on past experimental systems which tracked targets successfully, but primarily concentrating on work performed by Howland. The block diagram of the receiver architecture is shown in Figure 1.2.

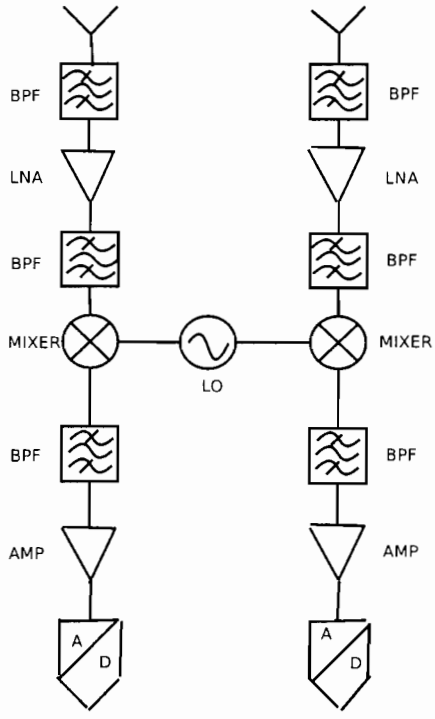

Figure 1.2: Block diagram of the designed receiver chain.

Included within this chapter, is an analysis of the signal through the receiver chain designed. The analysis of the signal is an indication of how the Doppler and bearing estimates of a target would be extracted from the system designed. This chapter also includes specifics of the hardware components to be used within the system. A brief overview of the antenna structure is also presented here, with consideration of the types of arrangements used in the past. More details of the antenna arrangements can be referred to [31].

The simulation of the receiver chain was also performed in Systemview. This simulator allows actual component values to be included within the simulation, therefore an accurate analysis of the signal can be presented. The results of these simulations are indicated in this chapter, concentrating on the extracted Doppler shifted signals. The limitations encountered with the use of the Systemview simulations are all discussed within this chapter.

This chapter also includes some real-time data which were recorded with the use of a Pinnacle PCTV television card. This card was modified such that there was an output which was connected directly at the IF of the card. The data captured was recorded with the Tektronix TDS5000B Digital Phosphor Oscilloscope and then further processed in IDL. The spectrum of the recorded signals are shown in this chapter as well as a detailed analysis of the data. This data was then basebanded, and the Doppler shift caused due to a target leaving the Cape Town airport was extracted. An ambiguity analysis study of the data captured as well as the results expected was discussed. The ambiguity plot for the e-tv television signal was presented.

The dissertation ends with a chapter describing the conclusions drawn from work completed, and looks into further improvements which can be made to the system for further reliable, television-based bistatic radar measurement purposes.

Chapter 2

Overview of Bistatic Radar

If the transmitter and receiver of a radar system, is separated by a distance that is comparable with the expected maximum range of target detection, the system is known as bistatic. This type of radar system is also defined as an active radar system (a system which is not dependent on deliberate or incidental electromagnetic emissions from the target of interest) whereby significant separation between the transmitter (illuminator of opportunity) and the receiver site exists [15].

Target detection of such a system is achieved when the signal transmitted from the 'illuminator of opportunity' (transmitting site), is scattered back from the target and received by the receiver. The physical separation of the transmitter and the receiver means that the electro-magnetic isolation between the two points are good, and therefore continuous transmissions are possible [20]. The arrangement of this type of radar system offers strategic and economic advantages. The main disadvantage in bistatic systems, is the synchronisation between the two locations.

This chapter is written to give the reader background information (historical and technical) on bistatic radar. This particular system to be built is a Television-Based Bistatic Radar system to be used for air surveillance purposes.

2.1 Definition of Multistatic Radar

Multistatic radar systems are generally systems which have a higher complexity with multiple transmitter and receiver subsystems employed in a coordinated manner at more than two sites [15]. All the units involved, contribute to the collective target acquisition, detection, position finding and resolution, with simultaneous reception at the receiver sites. In a simpler sense, multistatic radars are systems which have two or more receiving sites with a common spatial coverage area employed, and data from these coverage areas are combined and processed at a central location [40]. These systems are considered to be multiple bistatic pairs. Multistatic radar systems have various uses, some of which includes the prevention of jamming, and anti-radar munitions.

Multistatic radar units are transmitters, receivers, or both. These units include components such as antennas which is used for detection, position finding, or resolution of targets at electromagnetic frequencies. Different ways of co-operation between multistatic radars can be used [15]:

- operation of the radar by transmission of signals and reception of echo from reflecting targets.

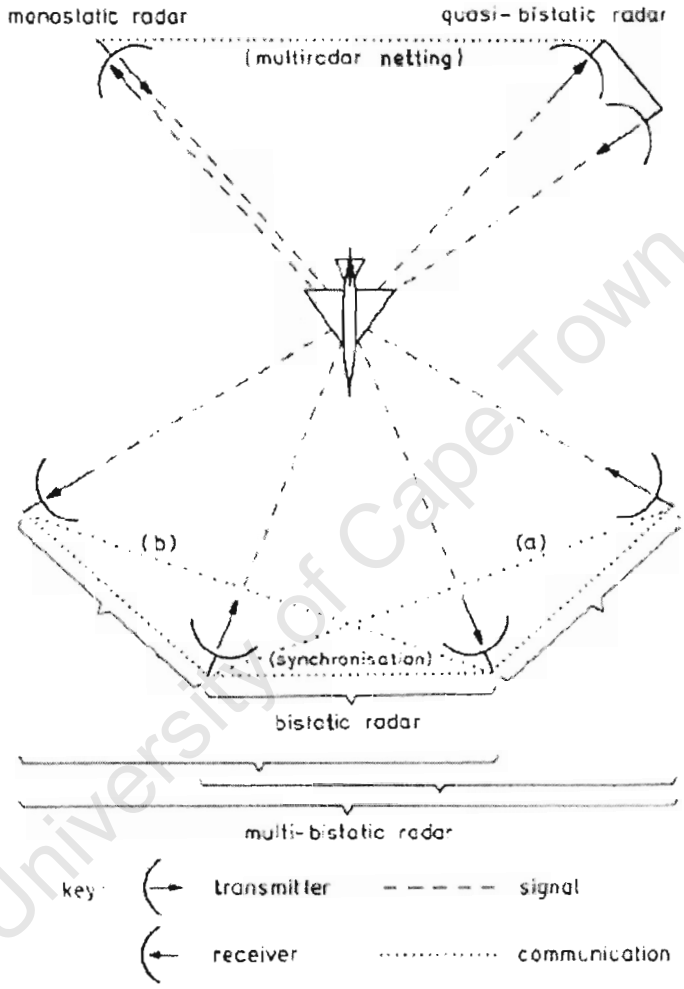

Figure 2.1: Survey of multistatic radar configurations. [15]

- common alternating transmission.
- simultaneous reception with common data processing with sensor netting.

Additional combination of bistatic pairs can results in the following advantages [15]:

1. Energy which is reflected by a target from the transmitted signal can be used by several receivers, therefore reducing the overall power needed for the coverage area, and thereby reducing the mutual interference.

2. Due to the positioning of the bistatic system, target echoes from different aspect angles reduces the probability of target loss. This is due to a cross-section minimum at one aspect angle if multistatic reception or netting is implemented. The main point being that multistatic reception avoids the null position being created between the target and the receiver. This is particularly useful for targets designed to have a low monostatic RCS. These are referred to as stealth techniques.

3. The dispersion of transmission and or reception from many directions can also be used for the purpose of increased detection performance, high resolution, target classification purposes, and imaging. The bistatic signature of the target is different to that of the monostatic case. Therefore, more information about the target can be obtained in the multistatic case. Furthermore, the stealth techniques described, is designed specifically for the monostatic case, and therefore is not stealth like anymore if the system is multistatic. Imaging for multistatic systems could generate better 3D information about the target, and hence better classification and detection.

2.1.1 Advantages and Disadvantages of Multistatic Radars

Their advantages are [24, 7, 44]:

- receiver sites can be placed anywhere, and cannot be located, therefore is safe from attack.
- the transmitter can be placed in a radio-noisy location, therefore, the transmission frequency can be diverted amongst other broadcasting channels - by utilising this factor, transmitters are not easily detected, and therefore not easily targeted.
- increased immunity compared to other systems - because of their multiple locations, jamming of the system is virtually impossible, unless omni-directional jamming was implemented with an increased power source to cater for the omni-directional jamming.
- receiver requires no protection from the transmitted pulse - no large amplitude, close range echoes, and the dynamic range requirement is less than for the monostatic case.
- simplified resolution and range ambiguities due to triangulation of target.
- the advantage of spectrum conservation is achieved.
- no transmitter to receiver switch or duplexer - these are expensive, lossy and heavy.

- configuration wise, they have less transmitted power than the monostatic case.
- high PRF used, since bistatic systems do not suffer from same range blindness.
- several receivers increase their probability of detection.
- multiple measurements improves accuracy and consistency.
- bistatic radars measures the Doppler component between transmitter and receiver - one of the major advantages is that one could use an extremely narrow-band, CW waveform, and therefore transmit with a low peak power, but still reasonable average power, and not use up much bandwidth.

There are also various disadvantages, those of which include [24, 44]:

- geometry of the entire system is more complicated.
- synchronisation between transmitter and receiver is complicated.
- need for co-operation between the sites.
- multi-beam receivers are required for some multistatic systems, these tend to be expensive.
- two radar sites required, this is even more expensive.
- for the system to work, both radar sites must see the target, some problem arises with different terrains, and co-ordinate conversion is difficult.
- deadzone.
- should be only one-way sidelobe protection against clutter.

2.2 Definition and Requirements of Bistatic Systems

Skolnik [35] defines bistatic radar as:

> "...a bistatic radar is assumed to be one in which the separation between the transmitter and receiver is comparable to the target distance."

If the transmit and receive antennas are on the same site, the system is then considered to be monostatic, according to the above definition. These systems are also known as "quasi-bistatic" [15]. Bistatic radars can operate in any of the following three modes [44], mainly:

1. **Dedicated** - The dedicated mode is defined as being under both design and control of the bistatic system.

2. **Cooperative** - This type of system is designed for other functions, but is found suitable for bistatic operations, and the transmitter can be controlled to do so.

3. **Non-cooperative** - This system is designed for other use and is suitable to support bistatic operation, however the transmitter cannot be controlled.

In order to determine target location, the transmit azimuth, elevation and timing of the transmitted signal must be known. For matched filter operation, the transmitted waveform must be available, and for coherent receiver operation, the phase of the transmitted waveform must be known to the receiver. Therefore, for bistatic or multistatic radar system, synchronisation between the receiver and transmitter must be maintained [44, 15]. This can be achieved in three ways:

1. **Direct synchronisation** is a technique used when the signal is sent from the transmitter to the receiver. This signal is used to synchronise a clock. Various methods can be used for this type of synchronisation, of which includes, the use of a communication link, a land line, or the receiver can be directly synchronised at the transmitters RF, if an adequate line of sight exists between the transmitter and receiver.

2. **Indirect synchronisation.** This method is achieved by using identical stabilised clocks at both the receiving and transmitting site. The clock however must be periodically synchronised.

3. **Direct breakthrough synchronisation.** This type of synchronisation is achieved when the transmitting beam scans past the receiving site, given an adequate line of sight. The receiver then synchronises on the pulses received during the main beam illumination period (dwell period).

2.2.1 Advantages and Disadvantages of Bistatic Systems

Some of the factors below apply mostly to bistatic systems.
Advantages of bistatic systems:

- In a military case, normal radar systems which have co-located receiver and transmitter are susceptible to external interferences, such as jamming devices. With the huge power emission, the transmitter clearly advertises it position and therefore could be in threat. With bistatic systems, this is not the case [22].

- In both military and civilian environments whereby there are several airfields nearby, each airfield will have their own receiver, while the incoming targets will be illuminated by a single high power transmitter covering the required coverage area. The advantage of this is that the mutual interference between transmitters and receivers will be eliminated, and better utilisation of the spectrum is achieved [22].

- If a multistatic radar system as described above is netted, the probability of target detection is improved immensely. In addition to this, range resolution is improved by triangulation and co-operation between the units can be achieved [15].
- When the bistatic angle approaches 180^o,the bistatic radar cross section RCS increases when compared to the monostatic RCS due to the forward scatter phenomenon [22]. In this region, the forward RCS is 15 dB's greater than the backscatter RCS measured by a conventional monostatic radar [9]. The magnitude of the forward scatter return is not dependent on the targets material, therefore detection of an object with a monostatic RCS reduced by absorbent material and re-shaping, is possible.
- Continuous-wave operation is possible, modulated or unmodulated [15].
- No transmit-receive switching by a duplexer is necessary [15].
- Transmit and receive antennas can be optimised and implemented differently, mobility can be increased, especially for receivers [15].
- Demands in clutter suppression are generally reduced by smaller dynamic range [15].
- Various other advantages due to their triangulation arrangement can be found in [15].

Disadvantages of bistatic systems are:

- The cell (area covered by the transmit and receiver beams) resolution degrades as the bistatic angle approaches 180^o [22].
- If the receiver has a wide beamwidth, it is more susceptible to noise interferences directed towards the receiver, transmitter antenna sidelobe clutter and by target echoes from wrong areas. For a bistatic radar to compete with a monostatic one, pulse chasing techniques with a narrow beam receive antenna is required [15].

2.3 History of Bistatic Radar

The first radar system designed back in 1904, and detected ships, was developed by a German engineer, Christian Hulsmeyer [22]. This system was bistatic in nature. Thereafter certain radar systems were constructed simultaneously in Germany, United Kingdom, Russia, Japan and the United States whereby they had their transmitter and receiver on separate locations for technical reasons, i.e. avoidance of transmit / receive switching and the use of continuous wave [15]. These radars are known as continuous-wave (CW) interference detectors, consisting of widely spread transmitters and receivers. These systems

designed detected objects as they crossed the transmitter-to-receiver baseline by measuring the beat frequency of its Doppler shifted reflection and the direct signal propagating from the transmitter to the receiver [9].

In 1922, A. Taylor and L.C. Young of the US Naval Research Laboratory detected a wooden ship by using a CW bistatic system. Later in 1930, L.A Hyland, of the Naval Research Laboratory accidentally detected aircraft by using a direction-finding apparatus at 33 MHz [9].

During World War 2, the first non-cooperative bistatic system was built by the Germans, the 'Klein Heidelberg' [44]. These devices were placed along the coast of Western Europe and could detect targets, of distances up to 450 kilometres. It used the British Chain Home radar transmissions. The receivers set up were then able to detect Allied bombing raids while still over the English Channel, without compromising their ground sites.

The Soviet Union also explored bistatic CW radar (RUS-1) in 1934 which operated at 4m (75 MHz) with a 35 km separation between each transmitter and receiver pair. This system was later accepted by the Soviet military in 1939. Forty-five of these systems were employed in the Far East and Caucasus at the time of the German invasion of the Soviet Union [9].

Professor Okabe from the University of Osaka in Japan developed a bistatic CW radar which was later deployed in the Pacific for detection of Allied forces. These systems achieved detections of up to 400 km, and operated between 40 - 80 MHz with an omnidirectional transmitting antenna, and a rotatable directional receive antenna [44].

In 1936, the invention of the duplexer was achieved at the US Naval Research Laboratory, and it was at this point, bistatic radar systems became virtually dormant. This duplexer allowed both the receiver and transmitter to share a common antenna, therefore be on the same site, and this system eventually led to the monostatic radar system [44].

A great deal of research development was also done in semi-active homing missile detectors, at this time, Navspuv was developed [9]. This system was used to detect ballistic missiles and orbiting objects as they passed over the United States. Also developed was systems such as AZUSA, the Udop and the Mistram which were multistatic radars, and were used for precision measurements of trajectories at missile test ranges [22].

Later in the 1970's, the development in bistatic radar research was revived, whereby the research primarily focused on theory and measurement, forward scatter fences, semi-active homing missiles, and multistatic radars [44]. This move was initiated due to the fact that the transmitters used, were targeted easily by enemies. Missiles were targeted at the transmitter radiation which was irradiated from the transmitter site. To make transmitters less vulnerable, they had to move the sites away from battlegrounds, into a sanctuary. A second threat which began to emerge was the radar jammers. These were essentially high gain jamming antennas directed towards the monostatic radar. These jamming systems caused problems for monostatic radar systems. By using the correct bistatic arrangement, these directive jamming effects can be reduced. Research into clutter tuning also began.

Bistatic pulsed Doppler radar was also developed by the military for protection of its grounded aircrafts, this system is known as aircraft security sensor (ASR). Five portable transmitter-receiver units were placed at 65 m intervals surrounding the base. Each of the transmitters would service the adjacent receiver. These were configured for near forward scatter operations [37].

Systems such as the TRADEX L-Band and ALTAIR UHF monostatic radars are also used in multistatic configurations [9]. The configuration was developed to track ballistic missile skin echoes. This system which was developed in 1980, was projected to measure three dimensional positions and velocity with accuracies better than 4 m and 0.1 m/s respectively throughout re-entry.

In one US experiment [44] in the early 1980's, a bistatic radar test bed called Bistatic Alerting and Cueing (BAC), in the diagram blow, used E-3A Airborne Warning and Control System (AWACS) and an emulation of cooperative transmitters. The ground-based receiver detected and processed the signals received from short-range air and moving targets.

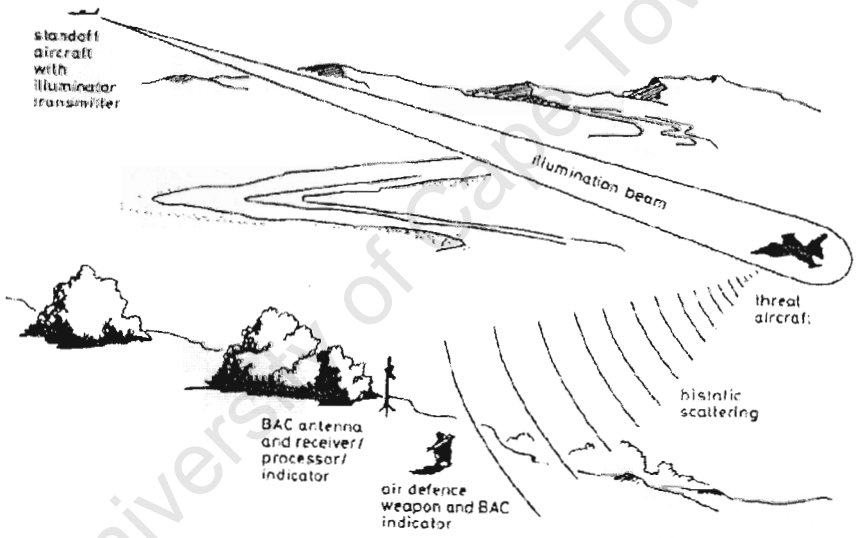

IEE PROCEEDINGS, Vol. 133, Pt. F, No. 7, DECEMBER 1986

Figure 2.2: The BAC Concept. [9]

Systems hitchhiking off other illuminators of opportunity were also developed, such as the system by Griffiths et al. [14]. Various other systems were designed in later years with much improvement. All of these can be referred to in [9, 44].

2.4 Applications in Bistatic Radar

There are many applications of bistatic radars. These can be split mainly into military and non-military applications. The following sections below, briefly discusses these applications.

2.4.1 Special Applications of Bistatic Radar

One of the special applications of bistatic radar, by Hanle [15], amongst others, is a quasi-bistatic radar system. This system is a form of a bistatic radar which tends towards a monostatic radar when the baseline seen from the target is small compared to the half range sum to the target [15]. Theses types of radars have the benefits of bistatic systems caused by the transmitter and receiver separation, but not the characteristics caused by triangulation. The benefits of the system usually exceed the disadvantages, and this can be seen in [15].

2.4.2 Military Applications

1. Semi-active missile seekers have been used since 1950's [9]. These systems employ ground based transmitters which illuminates an object, and the receiver carried by the missile, targets these locations. The rear-facing antenna is usually a data link for command guidance etc., as well as for deactivation.

2. When a target crosses a line joining the transmitter and receiver (baseline), the radar system is operated in a forward scatter mode. In this instance, the bistatic radar cross section (RCS) is larger than that of the monostatic case. The improvement is called the forward scatter phenomenon [22]. Hence, the detection of a stealth-protected object is possible.

3. The transmitter of the radar system can be placed within a secure location which will avoid any possible attack, while the receiver system monitoring the covered area is just as well protected.

4. A receiver can be placed on an aircraft which then uses illuminators of opportunity to detect any incoming aircrafts or missiles. This concept is called passive situation awareness (PSA) [44].

A possible future military system would be to have hybrid radars with both monostatic and bistatic modes of operation. With this system, its usual mode of operation would be the bistatic mode, making use of its surrounding illuminators of opportunity [9].

2.4.3 Non-Military Applications

1. Systems based on very-low frequencies (VLF), i.e. uses lightning as its illuminator of opportunity is able to detect abnormal or disturbed characteristics of the ionospheric D and E regions [9].
2. Bistatic radars have been used in planetary explorations [9].
3. Civilians are able to use the bistatic system for air-traffic control for a common area. In such an instance, there is a common shared transmitter, and various receivers at their specific locations (i.e. airports). Aircrafts entering the main coverage area will be illuminated by the transmitter, and can be tracked there onwards. This method reduces the mutual interference caused between multiple transmitters.
4. Synthetic Aperture Radars (SAR) can be produced by placing transmitters and receivers on separate aircraft platforms. This configuration causes the velocity vectors to change, or be controlled. This concept is known as clutter tuning [22].

Some potential non-military applications have been listed below:

- Topographic imaging bistatic radars can be deployed on spacecrafts for imaging of water resources, soil moisture, etc.
- Automobile or aircraft avoidance and collision systems.
- Intrusion detection systems.
- Global ionospheric monitoring networks.
- Low cost radar system in boats for navigation and weather detection.

2.4.4 Enhanced Techniques of Bistatic Radar Systems

Bistatic radars have certain techniques which leads to enhanced performance compared to monostatic radars [9].

1. Improved resolution in the vertical plane.
2. Glint reduction.
3. Clutter tuning - side looking moving target indication (MTI) radar and forward looking synthetic aperture radar (SAR).
4. Radar cross section (RCS) enhancement.

2.5 Overview of Television-Based Bistatic Radar

There has been a growing interest for the past 20 years in applications of bistatic and multistatic radars for both long range and short range surveillance. By utilising any convenient 'radar-like' illuminator of opportunity, the system has the merit of being completely covert, therefore does not advertise the presence of the receiver and transmitter stations [14]. Various methods of this nature have been proposed and conducted, and the methods used are described below.

A number of experimental bistatic systems have been built and evaluated, by Schoenenberger and Pell [33, 1]. The majority of their work had been based on existing transmitters, or on dedicated transmitters whereby the characteristics of these transmitters were optimum for bistatic systems.

Much work was also performed at the University College London (UCL) with the use of other people's transmissions for bistatic use. The topic of television-based bistatic radar was done in 1986 by Griffiths and Long [14] of the University College London (UCL) as a result of a research agreement with the Royal Signals and Radar Establishment (RSRE) [20]. The work done by them was based on exploiting the pulsed-like nature of parts of the television waveform for bistatic use. Their first investigation was on the "sync plus white" waveform, and showed the ability to receive clutter from the surrounding buildings. With off-line processing, they implemented a simple two pulse MTI canceller, and were able to "track" moving targets. This system was unpractical in the sense that they required a special transmission waveform and only has a range resolution of 1800m and range ambiguity of 9600m.

The work done by them had a few difficulties, one of them being that they found it difficult to capture adequate long data records. This factor caused most of the data to be proved negative. Another factor which contributed to this was the dynamic range of the moving target indicator (MTI) cancellation system used was inadequate to cope with high clutter/signal ratios of the quasi-CW radar system. The positive results obtained occurred on the few occasions when the target aspect gave a high value of bistatic cross-section, the receive antenna direction coincided with that of the target and the data were satisfactory recorded [14].

This paper was concluded by stating that the use of a pulse radar transmitter as the illuminator is the simplest form, however when the illuminator is not radar like, then the key importance is the autocorrelation function of the transmitted waveform. Some of the conclusion drawn by them with regards to the desirable property of transmitters, which includes [14]:

1. The transmit power should be commensurate with the coverage required. In the case of complex modulation functions such as the television, the calculation is made on the basis of the power of that part of the modulation spectrum used for radar purposes.

2. Radiation pattern of the illuminator should be either omnidirectional (floodlight coverage), or pencil-beam.

3. The modulation bandwidth should commensurate with the required range resolution.

The autocorrelation performed on the television signal by Griffiths, showed broad peaks at 64 μs intervals corresponding to the line sync pulses. If however these line sync pulse were gated out, the autocorrelation function of the signal would appear to be sharper (depending on the picture content), but still occurring at 64 μs intervals [14]. They also stated within the research that with the transmitter which was used, the transmit power was high and the azimuth coverage was omnidirectional, but the elevation plane had been deliberately restricted. The multiburst test signal was then used in the attempt to increase performance, but this was still unable to resolve moving targets, possibly due to the lower energy of a multiburst pulse compared to the sync (the television signal is discussed more in Chapter 3). This work was valuable because it was the first attempt of using television broadcasts as the transmission for a radar system in the time domain.

A later paper produced by Griffiths, Garnett, Baker, Keaveney [13], returns to the use of television transmissions in the time domain using sophisticated correlation techniques which were applied to Direct Broadcast by Satellite (DBS) TV signals. The receiver used by them had two receiving channels, one receiving the direct signal from the transmitter while the other was received from the target. Cross-correlation between the target and the television signal was done to achieve a compressed waveform, which ultimately increases the processing gain. From this research conducted, a target of 20 dBm^2 at 100 km would require a processing gain of 80 dB, however, the level of gain which was achieved was at a level of 45 dB, some 35 dB short of what was required. This level of gain was required to achieve a probability of detection of 90% with the probability of false alarm (P_{fa}) of 10^{-6}. A possible method of achieving this additional gain was through a technique which compensates for Doppler and range migration, however, the authors does not demonstrate this.

At an International Conference on Radar held in 1994 in Paris, France, there were three papers on television based bistatic radar. The first paper included work done by Howland [18], his work will be described in more detail below. The other two papers were presented by French researchers.

One of the papers presented was by Poullin and Lesturgie of ONERA [28] who described their system to be a multistatic passive system which used non-cooperative television transmitters. For each of the television transmitters used, they proposed to have a two channel receiver system, whereby the one of the antennas would be pointing in the surveillance region while the other, directly at the transmitter. The signals captured were sampled using a 12 bit A/D converter, and then the FFT was taken to determine the spectrum around the vision carrier of the television signal. The spectrum of the signal pointed directly at the transmitter was then subtracted from spectrum obtained from the channel

pointed in the surveillance region. This was performed to remove the unwanted television frame rate information from the spectrum of the received data, and leaving the Doppler shifted echoes of targets within the surveillance region.

In order for these target echoes to be tracked, the authors proposed a technique which requires four or more transmitters. The Doppler shift of the target would be measured for each of the transmitters, and equations were formulated for the targets position and velocity relative to the transmitters and the measured Doppler shift. These equations were then solved for the location of the target, but the velocity was not estimated. This technique is interesting as it only makes use of the Doppler information to locate and track targets, however, the system was impractical in the sense that at any time, a minimum of four transmitters were needed for the system to operate correctly, and in reality, it is quite difficult for a location to have four transmitters.

Even if the system was possible, Poullin and Lesturgie did not specify how the Doppler profiles extracted from each transmitter would be associated to each target, if multiple targets were present. Due to the fact that the tracking algorithms were essentially formulated as simultaneous equations, there was no scope for redundancy in the data, and therefore these algorithms were dependent on high signal to noise ratios for their success. This could be one of the causes to their limited range abilities for target detection.

The television based bistatic radar system was then further investigated by Howland [20, 21], also making the use of a non-cooperative television transmitter as the illuminator of opportunity. His research was made possible by utilising a simple receiver system, comprising of a radio receiver, and a pair of simple Yagi antennas. Much of the work presented by him consisted of signal processing techniques used for target tracking.

Howland's work assumes that there is only one receiver system, and one remotely located television transmitter. His research shows how a target's velocity and location can be estimated from measurements of bearing and Doppler shift of target echoes of the vision carrier from terrestrial television signals. His research was not based on a single measurement of Doppler shift and DOA of the target echo, as little information can be extracted from this. His research was based on a series of measurements for Doppler and DOA with time to know the behaviour of the target to accurately locate it. This was based on the fact that the change in Doppler shift and DOA of a target echo with time was uniquely determined by the targets course and velocity.

His research did not require any timing measurements to be made, and therefore no synchronisation between the transmitter and the receiver was made, provided that the television carrier frequency was known and stable enough. The carrier being stable widens a number of possible transmissions to be exploited, not only limited to television signals, but to any transmitter of opportunity with a stable CW, AM, narrowband PM or narrowband FM signal.

The signal was captured through a two channel downconversion stage receiver, first at 290 MHz, and thereafter at 29 MHz. This signal captured was then fed into a digital HF re-

ceiver card which further downconverts the signal to baseband through signal processing with a bandwidth of 100 Hz to 16 kHz. The signals received at baseband in each channel are then processed, using the FFT of these signals, he was able to extract the Doppler and bearing estimates of the target. A constant false alarm rate was then used to reject the unwanted harmonics and noise levels, and the target echoes were extracted. Thereafter a Kalman filter based tracking scheme was used to associate the Doppler and bearing estimates of the same target. More signal processing was done thereafter to extract the tracking algorithms and plots, of which this research will not cover.

The spectrum of the FFT extracted was complex, therefore the difference between the two channels can be used to calculate the bearing of the target. Analysis of the extracted signals can be seen in Chapter 4. Due to the close spacing of his antennas, his measurements had some degree of error due to the mutual coupling which occurred between the antennas, and caused severe tracking errors. This however was resolved by modelling the antennas with the method-of-moments numerical electromagnetics code (NEC) version 4 [4]. Much of the work done by Howland had some correlation to Griffith's and Long's work, with the exception that his work was done in the frequency domain. Howland, however criticises some of the work done by Griffiths and Long, and states that the time domain of terrestrial television transmissions cannot be sensibly used for bistatic radars.

This research is based on the vision carrier of the domestic television broadcast as radar transmissions, using a passive receiver to detect target echoes. The television signal is essentially pulsed in nature, and certain ghosting effects can be seen on any domestic television sets, showing that this is effectively a simple radar system.

2.5.1 Advantages of the Television-Based Bistatic Radar System

- The receiving system is completely passive, simple and cheap.
- Dynamic range of signals used is reduced due to the defined minimum range.
- Milne discussed several configurations of transmitters and receivers. Azimuthal discrimination at both transmitter and receiver is desirable, otherwise system is vulnerable to response from sidelobes. The form of scanning required for the antenna, follows the position of the RF pulses through space. This is known as pulse chasing [14].
- Target bistatic cross-section σ_B is not the same as for monostatic case, although the target will be comparable with range of values from monostatic cross-section [36]. Therefore a target is unlikely to present a low cross-section for more than one bistatic configuration.
- The receiving or transmitting antennas can be used interferometrically to obtain high azimuthal discriminations. These sources of interference can be located by triangulation and passive techniques, to locate noise-like sources [14].

- A high pulse repetition frequency (PRF) may be used, and range ambiguities resolved by triangulation from several receivers or by a staggered pulse repetition interval (PRI's) [14].
- Transmitters can be located remotely.

2.5.2 Disadvantages of the Television-Based Bistatic Radar System

- It is necessary to synchronise the received signal with the transmitted signal - could be difficult to implement.
- There is a coordinate distortion effect - targets on the transmitter to receiver baseline have zero bistatic range [14].

2.6 Coordinate System, Geometry and Equations

Due to the separate positioning locations of the transmitter and the receiver, the coordinate system and the geometry of a bistatic radar system can be complex in a way. The signals between the stations can be compromised even further if direct line-of-sight is not achieved. All of this will be discussed in the sections below.

2.6.1 Coordinate System and Geometry

The coordinate system used to describe the geometry will be in a two dimensional case, a north referenced coordinate system. The bistatic plane, is the plane on which the transmitter (Tx), receiver (Rx) and the target (on the edge of the range ring) lies. On this particular plane, the ellipse with its foci at Tx and Rx is also present (the range ring). This ellipse has its midpoint located between the Tx and Rx stations.

All the ellipses have a common transmitting and receive site foci, and therefore a common baseline. The bistatic system is shown in the diagram below, and is known as the bistatic triangle.

As shown on the diagram, the baseline (L) is the distance between the transmit (Tx) and receive (Rx) stations. The distance from the receiver to the target is defined as R_R and from the transmitter to the target is R_T.

The bistatic angle is C, or β, which is also known as the cut angle, is the angle between the transmitter and the receiver, with the vertex at the target. The transmitter look angle is α_T and the receiver look angle is α_R. The look angles are taken as positive in a counter-clockwise direction. They are also known as the angles of arrival (AOA) [44]. Note also that:

$$\alpha_T + \alpha_R = C = \beta \tag{2.1}$$

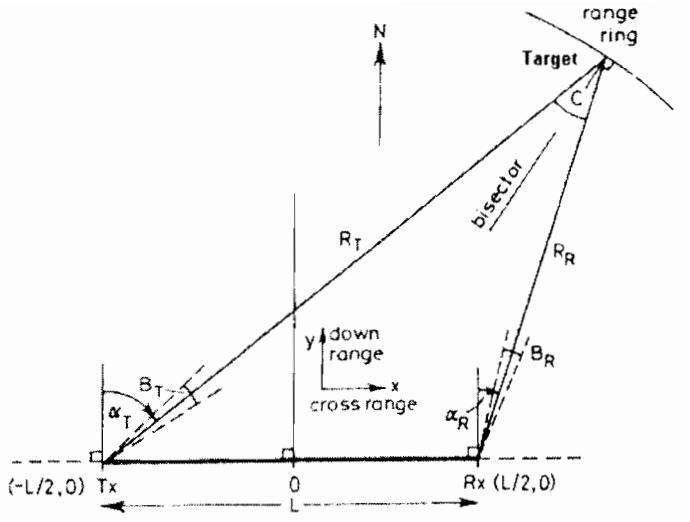

Baselength = L, beam azimuths = α_T, α_R, beamwidths = B_T, B_R, cut angle $C = \alpha_R - \alpha_T$, ranges = R_T, R_R

Figure 2.3: Geometry of a bistatic radar, North referenced coordinate system. [23]

In a general case, the bistatic system works the same, irrespective of whether the target lies above or below the baseline. This is due to its symmetrical nature of their geometry.

2.6.2 Bistatic Radar Range Equations

Bistatic radar range equations are derived exactly the same way as in the monostatic case. The derivation of this equation can be found in [17]. Several differences does occur within the equation, and will be discussed later. The bistatic range equation, from Willis [44], is shown below.

$$(R_T R_R)_{\max} = \left[\frac{P_T G_T G_R \lambda^2 \sigma_B F_T^2 F_R^2}{(4\pi)^3 k T_s B_n \left(\frac{S}{N}\right)_{\min} L_T L_R} \right]^{\frac{1}{2}} \tag{2.2}$$

$$(R_T R_R)_{\max} = \kappa \tag{2.3}$$

where

R_T = transmitter to target range
R_R = receiver to target range
P_T = transmitted power
G_T = gain of the transmitter's antenna
G_R = gain of the receiver's antenna
λ = wavelength
σ_B = bistatic radar target cross section
F_T = transmitter pattern propagation
F_R = receiver pattern propagation
k = Boltzman's constant
T_s = receiver noise temperature
B_n = receiver noise bandwidth
$\left(\frac{S}{N}\right)_{\min}$ = signal to noise ratio needed for detection
L_T = losses in transmitter (cables, signal processing, etc.)
L_R = losses in receiver (cables, signal processing, etc.)
κ = bistatic maximum range product

The television broadcast antenna is assumed to be omni-directional, and therefore assumed to have a gain of 0 dBi. Also, for calculation purposes, we first assume the pattern propagation factors $F_R = F_T = 1$. For this bistatic range equation to be reduced for the monostatic case, the following needs to be changed [44]:

1. $\sigma_M = \sigma_B$
2. $L_T L_R = L_M$
3. $R_T^2 R_R^2 = R_M^4$

Note also that $(R_M)_{max} = \sqrt{\kappa}$. This factor is called the equivalent monostatic range.

The pattern propagation factors take into account the gains of the transmit and receive antennas as a pointing angle. Also taken into account are the losses in the signal (atmospheric, absorption, etc) while propagating through the atmosphere. More about propagation factors can be found in [44]. In practice, the curvature of the earth means that low flying / altitude targets may not be illuminated by both the transmitter and the receiver at the same time, and therefore not observed by the radar. In order to model and obtain the correct results, the effects of the curved earth, diffraction of the radar energy around the earth, target altitude, and the pattern of antennas will be considered.

2.7 Contours of Constant Range and Power

In bistatic radars, the range of the target found from the scattered pulses, or rather the delay between reception of a hypothetical direct signal from the transmitter to receiver, and the echo depends on the total path instead of $2R_M$ in the monostatic case [23]. By

keeping total path (T) constant, constant range sum ellipses (isoranges) can be formed. The transmitter (Tx) and receiver (Rx) forms the foci of the ellipses. The total distance travelled by the signal from the transmitter to the receiver is:

$$T = R_T + R_R \tag{2.4}$$

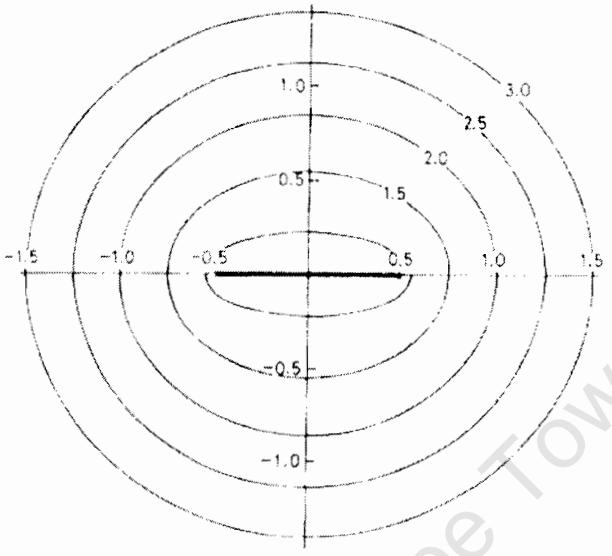

Figure 2.4: Constant range contours. [23]

Note from the diagram above that the bistatic angle is orthogonal to the tangent of the isorange contour at any point on the contour [44]. The following equation represents the general Cartesian coordinates for these ellipses.

$$\frac{x^2}{a^2} + \frac{y^2}{b^2} = 1$$

Within the above equation, a is the semi-major axis of the ellipse and $b = \left(a^2 - \frac{L^2}{4}\right)^{\frac{1}{2}}$ is the semi-minor axis of the ellipse. The origin is the midpoint between the transmitter and receiver site, as stated above. Also note that $(R_T + R_R) = 2a$. The eccentricity of the ellipse shown can be represented by:

$$\begin{aligned} e &= \frac{L}{(R_T + R_R)} \\ &= \frac{L}{2a} \\ &= \frac{\sqrt{(a^2 - b^2)}}{a} \end{aligned} \tag{2.5}$$

The value of e lies in the range $0 < e < 1$. When $e = 0$, then $L = 0$, and the ellipse is then

a circle, therefore becoming monostatic in nature. An IDL software simulation for range contours over the specific geometry for which the system is designed was developed and the output of the simulation is shown below. The details with regards to the simulation development will be explained in detail in Chapter 4.

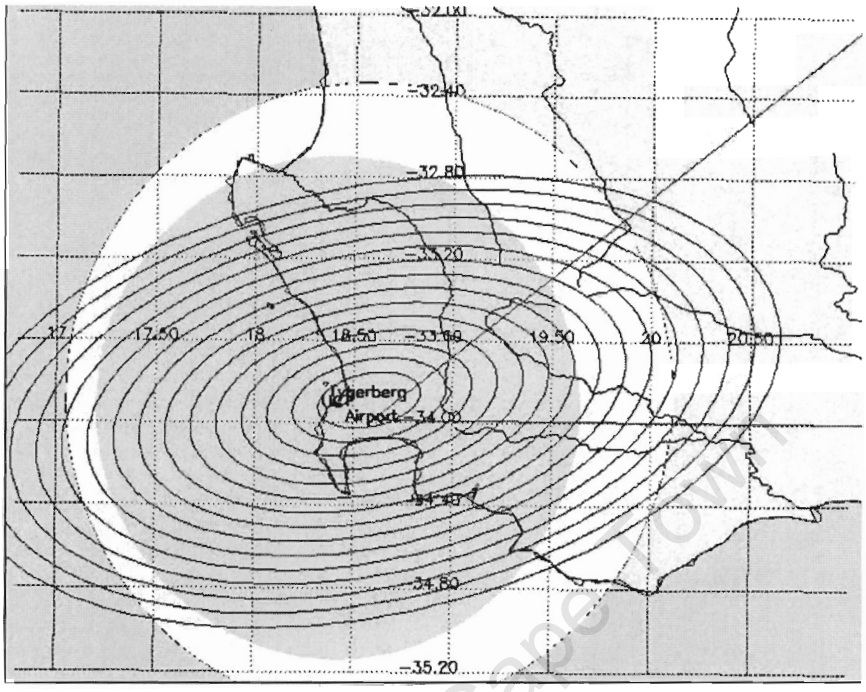

Figure 2.5: Diagram showing the range contours over the Western Cape.

The echo power received for a bistatic case is different to that of a monostatic case. This is due to the path loss factors, for the bistatic case, it is $\frac{1}{R_T^2 R_R^2}$ and for the monostatic case, it is $\frac{1}{R_M^4}$ as shown from the equation in Section 2.6.2. These signal to noise ratio contours, whereby $R_T R_R$ is kept constant for each contour are called ovals of Cassini. To obtain these curves, you would have to solve the radar range equation in Section 2.6.2 for the SNR.

$$\frac{S}{N} = \frac{K}{R_T^2 R_R^2} \tag{2.6}$$

whereby

$$K = \frac{P_T G_T G_R \lambda^2 \sigma_B F_T^2 F_R^2}{(4\pi)^3 k T_s B_n L_T L_R} \tag{2.7}$$

and the minimum SNR contour can be obtained from [44], and is shown below. This K term is called the bistatic radar constant, and is related to the bistatic maximum range product κ.

$$\left(\frac{S}{N}\right)_{min} = \frac{K}{\kappa^2} \tag{2.8}$$

A convenient way to plot the ovals of Cassini is in a polar coordinate (r, θ) system. The geometry of this system can be seen in [44]. Converting R_T and R_R into polar coordinates gives:

$$R_T^2 R_R^2 = \left(r^2 + \frac{L^2}{4}\right)^2 - r^2 L^2 \cos^2\theta \tag{2.9}$$

therefore

$$\frac{S}{N} = \frac{K}{\left(r^2 + \frac{L^2}{4}\right)^2 - r^2 L^2 \cos^2\theta} \tag{2.10}$$

These ovals of Cassini (signal to noise ratio contours) for $10\,dB \leq \frac{S}{N} \leq 30\,dB$, can be seen in Figure 2.6.

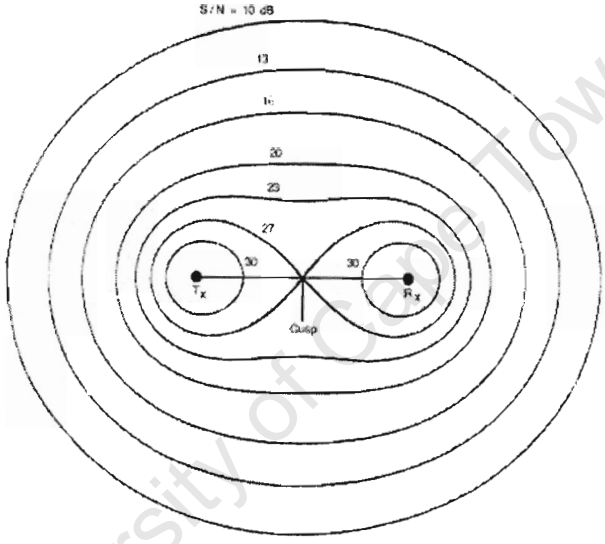

Figure 2.6: Contours of constant received power. [23]

As shown on the diagram, the oval shrinks and finally collapses around the transmitter and receiver as the SNR increases. This same effect occurs if the baseline is increased. The point on the baseline where the oval breaks into two parts is called the cusp. The oval is now called a lemniscate (of two parts) at this S/N. At this point, r = 0, and from the $\frac{S}{N}$ equation above, $\frac{S}{N} = \frac{16K}{L^4}$. Assuming that $\left(\frac{S}{N}\right) = \left(\frac{S}{N}\right)_{min}$, the lemniscate yields, $L = 2\sqrt{\kappa}$ [44].

From these equations, three main operating regions can be defined [44], namely:

1. The receiver centred region - occurs when $L > 2\sqrt{\kappa}$ and $R_T \gg R_R$, hence the oval breaks into two parts.

2. The transmitter centred region - occurs when $L > 2\sqrt{\kappa}$ and $R_R \gg R_T$, hence the oval breaks into two parts.

3. The cosite region - occurs when $L < 2\sqrt{\kappa}$, therefore the oval remains single (oval doesn't develop a cusp or breaks into two parts, refer to Figure 2.6).

Another method of characterising SNR contours, is to plot it as a function of its increasing baseline [44]. With this in mind, a program has been developed in IDL programming language to create the signal to noise ratio plot of the corresponding locations of the transmitter and the receiver. The separation between the two sites corresponds to the distance between our present transmitter and receiver. A more advanced version of the software was implemented for the purpose of plotting estimated SNR values over the Western Cape. Both these programs will be discussed in more detail in Chapter 4, as well as the results achieved from the simulations will be shown.

Theoretically, these SNR predictions are performed by using the signal to noise ratio predictions for various transmitter to target, and target to receiver distances. These SNR predictions, are calculated with the following equation [44]:

$$\mathrm{SNR} = \frac{\mathrm{P_t G_t G_r \lambda^2 \sigma F_t^2 F_r^2}}{(4\pi)^3 k T_s B L_t L_r R_t^2 R_r^2} \tag{2.11}$$

where:

P_t = transmitted power
G_t = transmitter antenna gain
G_r = receiver antenna gain
λ = wavelength
σ = radar cross section
F_t = transmitter propagation factor
F_r = receiver propagation factor
k = Boltzman's constant
T_s = system temperature
B = bandwidth
L_t = transmitter losses
L_r = receiver losses
R_t = transmitter to target range
R_r = receiver to target range

2.8 Target Location and Coverage

In bistatic radar system, one normally wants to know the target range and azimuth (R_R) relative to the receiver. This section covers most of the equations needed for these calculations, and also discusses the coverage constraints.

In order for us to resolve a target location, certain parameters must be defined. These parameters are the baseline (L), transmitter azimuth (θ_R) and range sum. The receiver look angle can be either measured or, θ_T can be converted to θ_R. The baseline length can

be measured with the transmitters location, or could be already set. With this in mind, there are two main methods of determining the range sum:

1. **The direct method** [37]. This method allows the receiver to measure the time interval, ΔT_{rt} between the reception of the transmitted pulse and target echo (also known as the timing sequence method). This method can be used with any transmitter configuration, given an adequate line-of-sight (LOS) between transmitter and receiver. The following equation can be used to calculate the range sum:

$$(R_T + R_R) = c \cdot \Delta T_{rt} + L \tag{2.12}$$

2. **The indirect method** [37]. This method utilises stabilised clocks between the transmitter and the receiver. The receiver measures the time interval (ΔT_{tt}) between the transmitted pulses and the received echo signals returned by the target. With this method, the transmitter-to-receiver LOS is not required for measurement. However, a LOS will be required if periodic synchronised clocks are implemented over the direct path. The range sum can be calculated from:

$$(R_R + R_T) = c \cdot \Delta T_{tt} \tag{2.13}$$

whereby $c = 2.998 \times 10^8$

The following equations are derived from the bistatic triangle as shown in Section 2.6.1. This equation can be used to calculate R_R and θ_R.

$$R_R = \frac{(R_R + R_T)^2 - L^2}{2\,(R_T + R_R + \mathrm{Lsin}\theta_R)} \tag{2.14}$$

$$R_R = \sqrt{(R_T^2 + L^2 - 2R_T\mathrm{Lsin}\theta_T)} \tag{2.15}$$

$$\theta_R = \theta_T - 2 \cdot \arctan\left(\frac{\cos\theta_T}{\left(\frac{c\cdot\Delta T}{L} + 1 - \sin\theta_T\right)}\right) \tag{2.16}$$

Several other techniques can be used for target location, but these mainly depend on the geometrical location of the receivers. In some occasions, multiple receivers are required, this can be found in a netted bistatic radar arrangement. Some of these systems can be found in [44] and [37].

Coverage is an important factor in bistatic radars, and this can be defined as the area on the bistatic plane whereby the target is visible to both the transmitter and the receiver. Bistatic coverage is detected in two ways [44]:

1. **Detection-constrained coverage**. This type of coverage is constrained by the maximum range of the oval of Cassini $(R_R R_T)_{max}$. When the oval of Cassini encapsulates both the transmitter and the receiver (the cosite region), the coverage area can

be approximated by:

$$A_{B1} \approx \pi\kappa \left\{ 1 - \left(\frac{1}{64}\right)\left(\frac{L^4}{\kappa^2}\right) - \left(\frac{3}{16384}\right)\left(\frac{L^8}{\kappa^4}\right) \right\} \tag{2.17}$$

But when the oval of Cassini surrounds the transmitter and receiver with two separate circles, the coverage area is approximated by:

$$A_{B2} \approx \left(\frac{2\pi\kappa^2}{L^2}\right)\left(1 + \frac{2\kappa^2}{L^4} + \frac{12\kappa^4}{L^8} + \frac{100\kappa^6}{L^{12}}\right) \tag{2.18}$$

In a monostatic case, L = 0, and becomes:

$$\begin{aligned} A_M &= \pi\kappa \\ &= \pi(R_M)^2_{max} \end{aligned} \tag{2.19}$$

this is expected, as the oval becomes circular in shape. In Figure 2.7, it is shown how coverage area varies with respect to the monostatic area A_M, as a function of the baseline, L. It is assumed that a suitable LOS exists between target, transmitter and receiver [44].

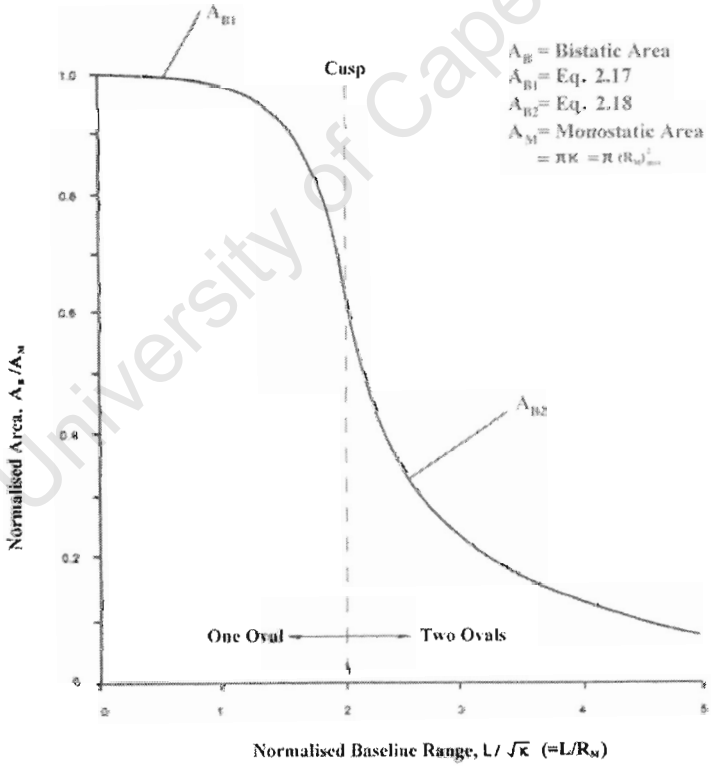

Figure 2.7: Ratio of bistatic area (oval of Cassini) to monostatic area. [44]

2. **Line-of-sight constrained coverage**. For any given target, transmitter, and receiver

altitudes, the target must be in the LOS of both the transmitter and receiver sites. For a flat earth, these requirements are established by coverage circles centred at each site.Targets in the area common to both circles, A_C, have a LOS to both sites as shown in Figure 2.8, [44].

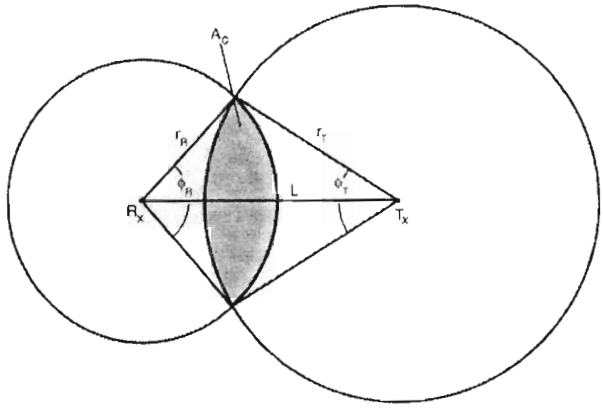

Figure 2.8: Geometry of a common coverage area, A_C. [44]

Realistically, our coverage area is as shown in the graph created by the IDL program in Figure 2.5 of Section 2.7. This coverage area shown is the effective radar horizon coverage area for a smooth earth model, as shown from the equations to follow. In usual circumstances, the coverage area is affected by multipath, refraction, diffraction, shadowing and earth curvature. For a $\frac{4}{3}$ earth model, and ignoring multipath lobing, the radius of the coverage areas can be approximated in kilometres by the following equations [44].

$$r_R \propto 130\left(\sqrt{\sqrt{h_t}+\sqrt{h_R}}\right) \tag{2.20}$$

$$r_T \propto 130\left(\sqrt{\sqrt{h_t}+\sqrt{h_T}}\right) \tag{2.21}$$

where

r_R = coverage area of the receiver.

r_T = coverage area of the transmitter.

h_t = target altitude (km).

h_R= receiver antenna altitude (km).

h_T= transmitter antenna altitude (km).

These derivation of these equations can be obtained in Willis [44]. The common area between the transmitter and the receiver is the intersection area between the two circles.

$$A_C = \frac{1}{2}\left[r_R^2\left(\phi_R - sin\phi_R\right) + r_T^2\left(\phi_T - sin\phi_T\right)\right] \tag{2.22}$$

where

$$\phi_R = 2\arccos\left(\frac{r_R^2 - r_T^2 + L^2}{2r_R L}\right)$$
$$\phi_T = 2\arccos\left(\frac{r_T^2 - r_R^2 + L^2}{2r_T L}\right)$$

Theses equations are valid for $L + r_R > r_T > L - r_R$ or $L + r_T > r_R > L - r_T$. Whenever the right-hand side of either inequality is not satisfied such that $r_T + r_R \leq L$ then $A_C = 0$. This means that the coverage areas do not intersect. When the left-hand side of the first inequality is not satisfied, then $A_C = \pi r_R^2$. Similarly, with the second inequality, $A_C = \pi r_T^2$. This is because the transmitter's coverage includes the receiver's coverage, and vice-versa.

For our particular system, the direct method will be used to calculate the range sum, and the coverage area for the moment could be line-of-sight constrained. Our coverage area is also mainly dependent on our antenna system. The designs for the antenna system will be discussed later.

2.9 Target Resolution and Target Cross Section

The definition of bistatic target resolution is the same as that of the monostatic case [44]. It is similar in the sense that two or more targets (of equal amplitude and arbitrary constant phase) may be separated in one or more dimensions, such as range, angle, velocity (or Doppler), and acceleration [44]. In a monostatic case, the target separation is referenced to radar-to-target LOS, while in the bistatic case, target separation can conveniently be referenced to the bistatic bisector.

2.9.1 Range Resolution

For both monostatic and bistatic cases, adequate separation between the two target echoes at the receiver is taken to be $\frac{c\tau}{2}$, where τ is the compressed radar pulse width. To be able to generate a $\frac{c\tau}{2}$ separation at a bistatic receiver, two-point scattering targets must lie on a bistatic isorange contour with a separation ΔR_B. In a monostatic case, the distance between the two circles are constant, whereby in a bistatic case, it is not so. The equation for a monostatic system resolution is given in the equation below:

$$\Delta R_M = \frac{c\tau}{2} \tag{2.23}$$

whereby τ is the pulse width [37]. For a bistatic radar given a constant pulse width τ, separation between the ellipses depend on the bistatic angles. As the bistatic angle increase, so does the distance between the isorange contours, and vice versa. Eventually on an extended baseline, or long ranges, they become equi-spaced, and start to represent

a monostatic case. An approximation for ΔR_B is [37]:

$$\begin{aligned} \Delta R_B &= \frac{\Delta R_M}{\cos\left(\frac{\beta}{2}\right)} \\ &= \frac{c \cdot \tau}{2\cos\left(\frac{\beta}{2}\right)} \end{aligned} \tag{2.24}$$

The above equation is based on the monostatic case by a factor of $\cos\left(\frac{\beta}{2}\right)$. This factor is also carried through to other operations as well.

It was stated previously that as the bistatic angle increase, or the eccentricity of the ellipses increases the bistatic error approximations. The maximum error for $\Delta R_B\,(\epsilon_{max})$ occurs on the perpendicular bisector of the baseline, given as [37]:

$$\epsilon = \frac{a(a'-a)}{b(b'-b)} - 1 \tag{2.25}$$

where

a = semi-major axis of inner ellipse.

a'= semi-major axis of outer ellipse.

b = semi-minor axis of inner ellipse.

b'= semi-minor axis of outer ellipse.

Here we see that ϵ_{max} is always positive, therefore, the expression for ΔR_B yields a separation which is always greater than or equal to the exact value. The actual area illuminated by both the transmitter and the receiver, is dependent on their respective beamwidths. This leads to the topic of cell area resolution. Just to comment briefly on this topic, cell area resolution is divided into two groups, namely beamwidth-limited, and range-limited. Within beamwidth-limited cell area resolution, the cell area is the intersection between the transmit and receive antenna beams. For the range-limited resolution, it is similar to that of the beamwidth-limited resolution, but with the addition of the pulse width taken into consideration. More of this can be found in [44, 23].

2.9.2 Target Cross Section Characteristics

The bistatic radar cross section of a target, σ_B, is the measure, as is in monostatic RCS, σ_M, of the energy scattered from the target in the direction of the receiver [17]. Bistatic cross sections are more complex than monostatic RCS in the sense that additional factors such as aspect and bistatic angles need to be taken into consideration. Three regions of the bistatic RCS need to be taken into consideration: pseudo-monostatic, bistatic, and forward-scatter (sometime known as near-forward-scatter) [44].

The pseudo-monostatic RCS region.

An equivalence theorem for monostatic-bistatic developed by Crispen and Seigel applies for this particular region, and it states [44]:

> "For vanishing small wavelengths, the bistatic RCS of a sufficiently smooth, perfectly conducting target is equal to the monostatic RCS measured on the bisector of the bistatic angle."

It is shown that this region varies with different objects. In the case when smaller objects are being detected, compared to the transmitted wavelength, smaller pseudo-monostatic regions are returned. For more complex structures, the extent of this region is considerably reduced. A variation of the equivalence theorem for more complex targets was developed by Kell [44], and it states:

> "For small bistatic angles, typically less than 5^o, the bistatic RCS of a complex target is equal to the monostatic RCS measured on the bisector of the bistatic angle at a frequency lower by a factor of $\cos\left(\frac{\beta}{2}\right)$."

Kell's complex targets are defined as an assembly of discrete scattering centres. Various targets, such as planes, ships, etc. are appropriate for this model, due to the fact that the wavelength is small compared to the target size. Both versions of the equivalence theorem are valid when the positions of the transmitter and receiver are interchanged. It is also possible to derive bistatic RCS data from monostatic RCS data whenever the equivalence theorem is valid via a simple method developed by Kell [44].

The bistatic RCS region.

The bistatic angle at which the equivalence theorem fails to predict the bistatic RCS defines this region. In this region, the bistatic RCS diverges from the monostatic RCS [44]. Kell identified three sources of divergence from complex targets for and for a target aspect angle fixed with respect to the bistatic-bisector [44].

1. Changes in the relative phase between discrete scattering centres. This source is similar to fluctuations in the monostatic RCS as the target aspect angle changes, but now the effect is caused by changes in the bistatic angle.

2. Changes in radiation from discrete scattering centres. This occurs for example, when discrete centres re-radiates energy toward the transmitter, and the receiver is positioned on the edge of, or outside, the retroflected beamwidth, and thus the received energy is reduced.

3. Changes in the existence of centres - appearance of new centres or disappearance of those previously present. This can be caused by shadowing which does not occur within the monostatic case.

In general, the bistatic RCS is lower than that of the monostatic case. Sometimes exceptions do occur in instances such as an object deliberately shaped to have a low monostatic RCS, but a high bistatic specular RCS or shadowing which sometimes occurs in the monostatic geometry and not in the bistatic case.

Another advantage for bistatic RCS is glint reduction. In a monostatic radar, phase interference from two or more scatters causes a distortion of the echo signal [37]. This causes the target aspect angle with respect to the radar, to cause the apparent phase centre of the radar reflection to wonder. This random wondering of radar reflecting centres, leads to jittered angle tracking, known as target glint [9].

Forward-scatter RCS region.

This region occurs when the bistatic angle reaches 180^o. Within this region, the RCS can be more than 15 dB larger than that of monostatic RCS. The magnitude of the object's forward scatter return does not depend on the material composition, therefore irregular shaped objects, and radar-absorbent materials used on targets are still able to be detected. The equations associated with forward-scatter can be found in Barton [2].

Any target illuminated by the transmitter on the baseline, when the targets dimensions are larger than the transmitted wavelength, produces a shadow. This shadow region occurs on the opposite side of the target from the transmitter. By using Babinet's principle [1], it is possible to resolve forward-scatter RCS [44].

2.10 Ambiguity Analysis for Bistatic Systems

The basic definition of an ambiguity diagram is a three-dimensional plot which shows the results of convolving a range of frequency shifted signals with a fixed reference signal [25]. The ambiguity function is basically the result of matching the received signal corresponding to the actual total delay and Doppler still remains.

The waveform sent out by the radar itself is used as the reference waveform. This waveform is used to generate the impulse response to the matched filter used for the ambiguity diagrams. This signal is then convolved with several different frequency-shifted versions of the reference signal, which represents the types of waveforms that represents a moving target.

The ambiguity diagram portrays two important properties of a waveform. These properties are the waveform's range and Doppler properties [25]. It can be shown that ambiguity functions arises naturally from the detection and parameter estimation problems associated with a slowly fluctuating point target being observed in additive white Gaussian noise [41]. Ambiguity function plots are examined for qualitative determination of the suitability of different waveforms meeting various requirements [37].

The ambiguity function is defined as [41]:

[1] "Babinet's principle is an approximation according to which the amplitude of near-forward scattering by an opaque, planar object is the same as that of an aperture of the same shape and size. Babinet's principle is sometimes combined with Fraunhofer diffraction theory in the development of an approximate theory of the corona" [10].

$$\theta(\tau_H, \tau_a, \omega_{D_H}, \omega_{D_a}) = \left| \int_{-\infty}^{\infty} f\ (t-\tau_a)\, f^*(t-\tau_H) \exp\left[-j\,(\omega_{D_H} - \omega_{D_a})\, t\right] dt \right|^2 \quad (2.26)$$

$\omega_{D_H} = \frac{-2V_H}{c}\omega_c$

$\omega_{D_a} = \frac{-2V_a}{c}\omega_c$

From the equation above, it can be conveyed that for the monostatic case, the ambiguity function plot is the manner at which the receiver responds to target returns at various values of delay and Doppler using a candidate signal. In the case of bistatic systems, the positions of the transmitter and receiver are not at the same place, and therefore requires some suitable point of reference.

Tsao et al [41], have performed experiments and analysis on the bistatic ambiguity functions. For their particular research, the point of reference used was the receiver location. Tsao et al. [41], have looked at the form of the ambiguity function for bistatic radar, and have shown that the bistatic geometry of the system can have a significant effect on the shape of the ambiguity function, since the relationships between ω_D and v , and between τ and R, are nonlinear. They proposed that the ambiguity function should be expressed as:

$$\left|\chi\left(R_{R_H}, R_{R_a}, V_H, V_a, \theta_R, L\right)\right|^2$$

$$= \left| \int_{-\infty}^{\infty} \tilde{f}\left(t-\tau_a\left(R_{R_a}, \theta_R, L\right)\right) \tilde{f}^*\left(t-\tau_H\left(R_{R_H}, \theta_R, L\right)\right) \exp\left[-j\left(\omega_{D_H}\left(R_{R_H}, V_H, \theta_R, L\right) - \omega_{D_a}\left(R_{R_a}, V_a, \theta_R, L\right)\right)t\right] dt \right|^2$$

with the receiver as the reference point, where:

R_{R_a} = target distance from the receiver

R_{R_H} = one − way range

V_H = one − way radial velocity

V_a = target radial velocity

θ_R = receiver look angle

L = baseline length

$\tau_a = \frac{2R_a}{c}$

$\tau_H = \frac{2R_H}{c}$

ω_c = cuttoff frequency

$\omega_{D_H} = \frac{-2V_H}{c}\omega_c$

$\omega_{D_a} = \frac{-2V_a\omega_c}{c}$

The "one-way" mentioned above, refers to the signal travelling from the receiver / transmitter to the target. As an example, they calculated and plotted an ambiguity of a simple Gaussian pulse for various different bistatic geometries.

Radar systems transmitted waveforms are mainly selected for their ability to satisfy the requirements for measurement accuracy, detection, ambiguity, and clutter rejection [41]. It is important to know the properties of these ambiguity functions with time, as the variation in the form of the ambiguity function would determine the radar's performance.

2.11 Doppler Relationships and DOA Estimations

In Figure 2.9, the geometry and kinematics for bistatic Doppler when the target, transmitter, and receiver are moving. The velocity vector of the target is V, and the aspect angle δ referenced to the bistatic bisector. The velocity vectors and bistatic angles of the transmitter and receiver are V_T & V_R and δ_T & δ_R referenced to the north coordinate system of the figure.

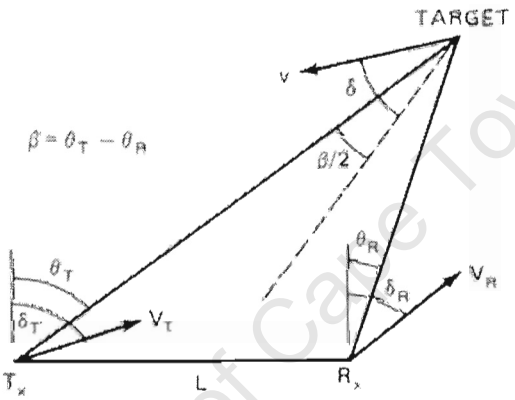

Figure 2.9: Geometry for bistatic radar. [37]

The consistency of Doppler shift in monostatic radars are not the same as that in bistatic systems. This complexity which is dependent on all the characteristics of the target position will be explained by the example of Doppler frequency in bistatic systems. Firstly, an equation is given to represent the definition or measurement of the bistatic triangle, commonly called the triangulation factor [37].

$$F = \sin\left|\frac{(\theta_R - \theta_T)}{2}\right| \tag{2.27}$$

This Doppler frequency can be split into three parts [15]. Firstly, an expression for the bistatic Doppler frequency.

$$f_d = f_o D\cos\delta \tag{2.28}$$

where $f_0 = \frac{2 \cdot v}{\lambda}$ is the maximum Doppler frequency of a target flying with a velocity v

observed at a radar wavelength λ [15]. The direction related to the elliptic system is:

$$\delta = \psi - \frac{\varphi_R + \phi_T}{2} \tag{2.29}$$

meaning that paths of zero Doppler shift are ellipses and paths of maximum Doppler shift are hyperbolas orthogonal to the ellipses. The third part is a Doppler reduction caused by the triangulation factor F:

$$\begin{aligned} D &= \cos\left(\frac{\varphi_R - \phi_T}{2}\right) \\ &= \sqrt{(1 - F^2)} \end{aligned} \tag{2.30}$$

The curves of constant Doppler frequency reduction, and the location above the angles are shown in Figure 2.10.

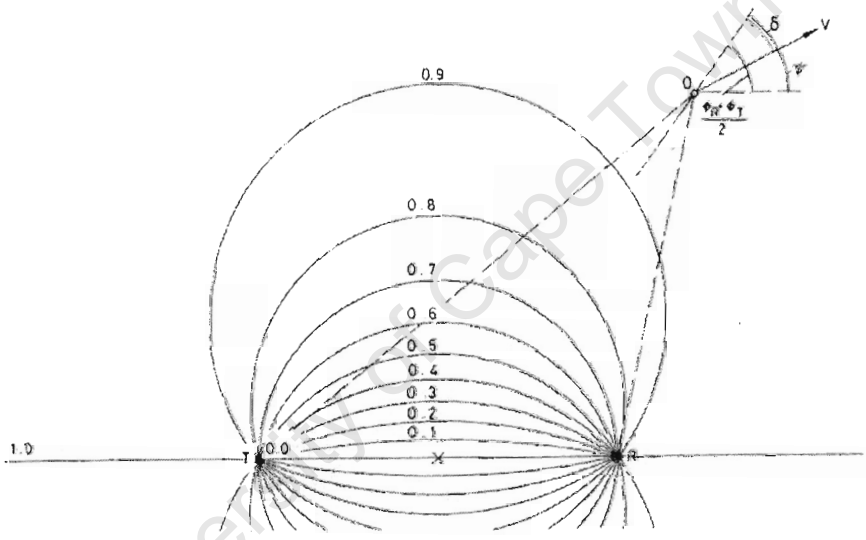

Figure 2.10: Curves of constant Doppler frequency reduction. [15]

When a target flies in a hyperbolic trajectory, the Doppler frequency corresponding to flight in a monostatic system, varies from monostatic maximum values at large ranges to a value of zero when it crosses the baseline. On the one hand, this Doppler variation can be used to extract additional information on target trajectory, while on the other hand, it limits the estimation of the target velocity [15].

Note also that when $-90^o < \delta < 90^o$, the bistatic target Doppler is positive, therefore for a closing target, the bistatic bisector generates a positive or 'up' Doppler. When $\delta = \pm 90^o$, the bistatic Doppler is zero (i.e. when the target flies on the isorange Doppler - the ellipse) [36].

With the system being developed, the signal received by the two channels will be down-converted and processed to provide the Doppler and bearing estimations for DOA. In

order to reject picture harmonics, and to identify target echoes, a time-acting constant false alarm rate detection scheme needs to be developed (CA-CFAR). In order to do this, a processing scheme that derives the Doppler shift and DOA expressions needs to be developed. For this research, this processing scheme will not be considered.

Certain assumptions are made in this research, one of them being the earth is considered as a flat surface. Another assumption is that the target is flying at a constant velocity, and in the same direction throughout the period at which it is tracked. This assumption is made for large commercial aircrafts only, not including military aircrafts.

The assumption of a flat earth is due to the fact that if the curvature of the earth is considered, then low altitude targets may not be simultaneously illuminated by both the transmit and the receive antennas, therefore not seen by the radar. In order to model this properly, the effects of the curved earth, diffraction of the radar energy around the earth, target altitude, the lobed elevation patterns of the antennas should all be considered.

The assumption of the target flying at zero altitude can also be assumed because zero altitude flying targets causes a small systematic error for high-altitude targets close to the receiver [20]. In this instance, the radial velocity in the direction of the receiver (which is a cause of the Doppler shifted echo) and the apparent measured DOA returned will be affected by the target's non-zero altitude [20].

2.11.1 Isodoppler Contours

The term isodoppler occurs when the target is stationary, and the transmitter and the receiver are moving (e.g. airborne), the bistatic Doppler shift at the receiver site is:

$$f_{TR} = \left(\frac{V_T}{\lambda}\right)\cos\left(\delta_T - \theta_T\right) + \left(\frac{V_R}{\lambda}\right)\cos\left(\delta_R - \theta_R\right) \tag{2.31}$$

whereby the terms are defined in Figure 2.9. In this research, the isodoppler contours do not apply.

2.12 Impact of SNR on Measurements

Signal to noise ratios (SNR) at the radar receiver can be predicted with the knowledge of the geometry and configuration of the radar system. It is important to know how the SNR's accuracy can effect the measurements of the Doppler and the Direction of Arrival (DOA).

2.12.1 Effect of SNR on Doppler Measurements

In Howland's thesis [20], he describes the time histories of the Doppler shift of the target echoes are determined by using discrete Fourier transform, applied to sequential blocks of data. Spectral components whose SNR exceeds a certain threshold are defined as targets, while using a constant false alarm rate (CFAR) threshold scheme. By this, we can declare that targets have positive SNR's, typically above 6 dB. The higher the noise level, the more number of false targets generated. These can be removed automatically later by processing.

The accuracy at which the frequency can be calculated is by using a parameter known as the effective time duration of the signal. In the thesis by Howland [20], he indicates the minimum RMS error in measurement of the carrier frequency, based on details from Skolnik's book [36], is:

$$\delta f = \frac{\sqrt{3}}{\pi \mathrm{T}\sqrt{\frac{2\mathrm{E}}{\mathrm{N}_0}}} \tag{2.32}$$

where $\frac{\mathrm{E}}{\mathrm{N}_0}$ is the SNR. In Howland's thesis's description of SNR [20], it is roughly estimated at:

$$\frac{\mathrm{E}}{\mathrm{N}_0} = \frac{3}{2\pi^2} \tag{2.33}$$

2.12.2 Effect of SNR on DOA Measurements

The greatest effect of an echo's SNR is on the accuracy with which the direction of arrival (DOA) can be estimated. In order to compute this fact, it is necessary to derive the probability density function (PDF) of DOA errors in terms of the SNR of the target echo after coherent integration. The way this was done by Howland [20], was to consider the process by which DOA is estimated. For this purpose, the calculation was split into three stages:

1. Phases of a target echo on the two channels of an interferometer are measured.
2. Phase difference of the echo between channels is found.
3. Phase difference is transformed into DOA using a non-linear function.

In order to derive the probability density function (PDF) of the errors in DOA[2], it is necessary to consider the PDF of each stage of the process.

[2]This work was not performed in this research. For more details on this, refer to work performed by Howland [20].

It can be shown that for a signal arriving at an angle θ_t, the phase difference between the two antennas of the interferometer will be $\Phi = \frac{2\pi d}{\lambda}\sin\theta_t$ (in a noise free situation) [20]. Therefore the DOA of the arriving signal calculated from the channel phase difference is by using:

$$\theta_t = \sin^{-1}\left(\frac{\lambda\Phi}{2\pi d}\right) \tag{2.34}$$

where Φ is the noise free phase difference, and d is the spacing between the two antennas. In order to avoid any directional ambiguities, $-\sin^{-1}\left(\frac{\lambda}{2d}\right) < \theta_t < \sin^{-1}\left(\frac{\lambda}{2d}\right)$. In practice, the signal will be corrupted by noise, and therefore the DOA of the signal will be estimated using:

$$\theta = \sin^{-1}\left(\frac{\lambda\Delta\Psi}{2\pi d}\right) \tag{2.35}$$

where λ is the wavelength, and $\Delta\Psi$ is the calculated phase difference between the two channels.

2.13 Maximum Unambiguous Range and PRF

In the monostatic case, the range beyond which targets appear as a second-time-around echoes is called the maximum unambiguous range [36], which is given as:

$$(R_M)_u = \frac{c}{2 \cdot \mathrm{PRF}} \tag{2.36}$$

where PRF is the pulse repetition frequency in Hz. The corresponding bistatic unambiguous range is:

$$(R_T + R_R)_u = \frac{c}{\mathrm{PRF}} \tag{2.37}$$

which is an ellipse, or isorange contour, of major axis length $\frac{c}{\mathrm{PRF}}$. The PRF can be significantly increased when the operation is constrained to a small column beam volume. However, problems due to these high gain beam scans can arise, and one solution would be to implement pulse chasing, which in turn establishes its own requirements on PRF. Pulse chasing by definition is a process whereby a second receiver is equipped with a staring array of antenna to switch rapidly through them at an appropriate rate, following the region illuminated by the transmitter pulse [24]. This method effectively reduces the complexity and cost of multibeam bistatic receivers. Their fundamental effectiveness and requirements have been defined by [23].

For bistatic radars, operating in the cosite region, PRF_uvaries as a function of its geome-

try.

$$\begin{aligned}(\mathrm{PRF}_B)_u &= \frac{c}{(R_R + R_T)_{max}} \\ &= c\left[L^2 + 2\kappa\left(1 + \cos\beta\right)\right]^{-\frac{1}{2}} \end{aligned} \tag{2.38}$$

where $(\mathrm{PRF}_B)_u$ is the maximum unambiguous range PRF for the bistatic system operating at a maximum range product κ. Note that this PRF is a minimum when $\beta = 0^o$ or when the target is on the baseline, the pseudo-monostatic case. This PRF would be a maximum when β is maximum, which is when the target is located perpendicular to the bisector of the baseline [44]. Two special bistatic radar configurations also establish a maximum PRF: high gain transmitting and receiving beam antennas, and single beam pulse chasing. More of this can be found in [44].

2.14 Target / Clutter Ratios

The received signal at any location is the RF sum of the direct signal and of the multipath propagation [14]. Most of these multipath signal energies would result from reflection off fixed objects, such as, buildings, other large objects, other aircrafts, etc. To reduce multipath from various directions, one solution would be to have a pointing reference antenna, but this is not a perfect solution, as it will pick up narrow-angle multipath as well and possibly even the target signal via sidelobes.

According to Griffith, et al. [14], the power returned from the illuminated ground clutter is equal to that of a target of $\sigma^o A$ where σ^o is the relative reflectivity, and A is the area illuminated. For low grazing angles, Skolnik [37], gives values of σ^o of -20 dB for a city, and -30 dB for a cultivated terrain. This has been taken into consideration by us when calculating the equations. Due to the fact that ground clutter is not confined to a specific area, we are unable to ascribe an effective area to it. The target / clutter ratio is given by:

$$\frac{\text{target power}}{\text{clutter power}} = \frac{\frac{G_r \sigma_B}{(r_{1t} r_{2t})^2}}{\int\int \frac{G_r \sigma^o}{(r_1 r_2)^2}\, dA} \tag{2.39}$$

where r_{1t}, r_{2t} are the target-to-transmitter and target-to-receiver distances. By taking no clutter returns within 1 km of the receiver, an approximate solution is:

$$\frac{\text{target power}}{\text{clutter power}} \simeq \frac{2.4 \times 10^7}{\sigma^o \theta} \frac{\sigma_B}{\left(r_{1t} r_{2t}\right)^2}$$

whereby

θ = antenna beamwidth

σ_B= 20 m^2(this is according to the paper presented by Griffiths [14])[3]

[3]This value was chosen since there isn't really any standard value for bistatic RCS. This value used is

With a television illuminator, unlike normal pulsed systems, the target return is compared with a fixed clutter level rather than one that decreases with range. For a high probability of detection of targets at further distances, the signal processing following the detector must use features of the waveforms to realise more than 50 dB processing gain [14].

2.15 Other Aspects of Bistatic Systems

Bistatic radars are more prone to sidelobe clutter unlike monostatic systems. They also suffer from scan to scan coverage losses. Bistatic systems will never exceed the target-receiver capabilities of the monostatic radar [7]. Two methods of improving bistatic systems are listed below.

2.15.1 Beam Scan on Scan

This method is usually used for surveillance purposes. Radar energy is inefficiently used when using high gain scanning antennas for the transmitter and receiver. This is due to the fact that only the volume common to both beams (the bistatic footprint) can be observed at any given time. Targets illuminated by the transmit beam outside the footprint are not detected. There are fours techniques which can be used to resolve this [37].

1. **Step scan.** This occurs only when the transmitter beam is fixed, and therefore giving the receive beam time to scan the surveillance frame. The transmit beam then stepped into the next frame and fixed while the receive beam scans this area and so on. The disadvantages of such a system is that there is an increase in surveillance time per frame, and a dedicated transmitter would be required.

2. **Multiple simultaneous beams-receiver-signal process.** This method utilises various receive beams to simultaneously scan the transmit beam and complete the surveillance frame. The main disadvantage of such a system is the cost in having separate receivers for each beam.

3. **Pulse chasing.** A disadvantage of this system is the expensive inertialess antenna (phased array) is required with precise and complex beam scheduling. This is described in more detail in Section 2.15.2 below.

4. **Floodlight beams.** Two scenarios are allowed for this method, either the transmit or receive beams floodlight the surveillance area and then the receive or transmit beams scan this area respectively. Disadvantages of this system is that it reduces the SNR and effective gain of the system.

for a standard commercial passenger aircraft. The work performed in this research, has some correlation to some degree, to work performed by Griffiths, et. al. and is along the same lines of the work performed by Howland [14, 18, 20, 21].

2.15.2 Pulse Chasing Techniques

This concept is introduced to reduce the complexity and cost of multibeam bistatic receiver, which is one of the solutions to the beam scan on scan problem. In Figure 2.11 below, the single receive beam rapidly scans the volume covered by the transmit beam (essentially chasing the pulse as it propagates away from the transmitter). This is done to improve the performance of the bistatic radar (the radar system utilises all the available target-scattered energy which arrives at the receiver).

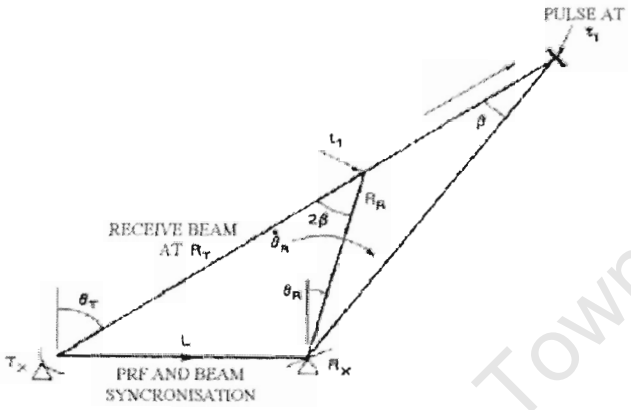

Figure 2.11: Pulse chasing for the single-beam, continuous-scan case. [37]

This method causes the receiver to look at the radar cell from which the target echoes caused by the illumination from the transmitted pulse can arrive. In order to do this a high gain steerable receive antenna is required. As the pulse is transmitted, the receivers antenna will "follow / chase" the pulse in oder to cover the sensitive sector from which the echoes might arrive.

The required azimuth coverage of the receive antenna changes while it "chases" the pulse in order to illuminate the correct range cell. The beamwidth of the receiver is dependent on two criteria, namely the transmitter beamwidth and pulse duration [23]. The image to follow, Figure 2.12, indicates the geometry of the transmit and receiving arc.

The beamwidth of the receiver is [23]:

$$\Delta\theta_R = \frac{((\Delta\theta_{R1} R_R) + (\Delta\theta_{R2} R_R))}{R_R} \tag{2.40}$$

where

$\Delta\theta_{R1} = \frac{\Delta\theta_T R_T}{R_R}$

$\Delta\theta_{R2} = \frac{(c \cdot \tau \cdot \tan(\frac{\beta}{2}))}{R_R}$

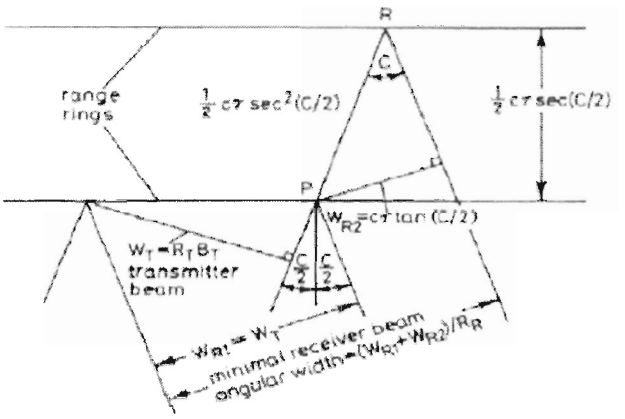

Figure 2.12: Receiving arc due to transmitter beamwidth and pulse length. [23]

From Section 2.4, the receiver's beamwidth, $(\Delta\theta_{R1})$ will be reasonably narrow except near the receiver. If the target is in its immediate vicinity to be detected, then the instantaneous receiving beamwidth must be very wide unless the transmitter's beamwidth is narrow. The receiver's beamwidth, $(\Delta\theta_{R2})$ is the reciprocal of the distance from the receiver. This receive beam-scanning rate must be the transmitter's pulse propagation rate, modified by the usual geometric conditions. The requirement of the receiver's beamwidth is small when the receiver and transmitter's line-of-sight is nearly parallel. For a detection at the baseline, it is large at the receiver end. For typical geometries, $\Delta\theta_{R2}$ can vary from $1^o/\mu$s to $0.01°/\mu$s. This type of rate change requires an inertialess antenna, such as phased array and fast diode phase shifters.

Due to pulse propagation delays from the target to the receiver, the pointing angle of the receive beam θ_R must lag the actual pulse position. Note also that the echo received from the target comes from the point behind the transmitted pulse, where the transmitter beam intersects the appropriate range ring. The distance by which the receiver trails the transmitted pulse is equal to the receiver range from which a target echo can originate from. It is also noted that the rate at which the receiver's azimuth changes is determined by [23]:

$$\frac{\mathrm{d}\theta_{\mathrm{R}}}{\mathrm{dt}} = \frac{\mathrm{c}\cdot\tan\left(\frac{\beta}{2}\right)}{\mathrm{R_R}} \quad \text{degrees}/\,\mu\mathrm{s} \tag{2.41}$$

For the receiver to meet these requirements, it will either need a fast switch over narrow beams or electronic scanning, because mechanical scanning cannot meet these requirements. Phased array antenna would probably be most suited [15].

2.15.3 Passive Tracking Techniques

This type of tracking techniques measures the coordinates of a moving target. This is done via measurement of Doppler shifts, DOA, and range estimations. In this particular type of system, it is always best to maximise the SNR, therefore, the antenna of the system will be directed at the target path area. Error signals and error corrections for this system can be produced and done. There are three main methods of passive tracking [36]:

1. **Sequential Lobing.** This type of method can obtain the direction and magnitude of the angular error in one coordinate by alternately switching the antenna between the two positions.

2. **Conical Scanning.** A logical extension of the simultaneous lobing technique described in the point above, is to rotate continuously an offset antenna beam rather than to discontinuously step the beam between the four discrete positions.

3. **Monopulse Tracking Radars.** For both the sequential lobing and conical scanning systems, they require a minimum number of pulses in order to extract the angle-error signal. In this technique, multiple beams are used to find the angular position of the target. The RF signals received from the two offset antenna beams are combined to produce the sum and the difference channel, and obtained simultaneously. The signals are then multiplied through a phase sensitive detector to obtain both magnitude and the direction of the error signal.

The type of system we are interested in for our research is monopulse tracking radars. There are two specific types of monopulse radar systems:

1. **Amplitude comparison.** This technique of monopulse system employs two overlapping antenna patterns to obtain the angular error in the one coordinate. Both the sum and the difference patterns are produced from this system. The signals received from the antennas are fed into a hybrid junction to produce these sum and difference channels. The sum pattern received is used for range measurement, and is also used as a reference to extract the error sign, while the difference channel is used for the measurement of the error in angular measurement. More information on this can be found in [37, 36]. Amplitude-comparison monopulse radars can also be defined as when the beams of the system have a common phase centre [34].

2. **Phase comparison.** The techniques discussed above were based on amplitudes of the signal. The difference in amplitudes in several antennas is proportional to the angular error. The angle of arrival from one direction can also be determined by comparing the phase difference between the two antennas. The antennas used in this system is not offset from the axis as opposed to the amplitude comparison situation. In this instance, the antenna boresight axes of the antenna are parallel,

and therefore causing a far-field radiation to illuminate the same volume in space. Therefore this essentially produces signals of the same amplitude, but difference in phase. Essentially, the illuminated beams of the phase-comparison monopulse system are parallel and identical except for lateral displacement of their phase centres on opposite sides of the axis [36, 37, 34].

The passive tracking techniques mentioned above, refers to the three main measurement types [20]:

- Time difference of arrival (TDOA)
- Direction of Arrival (DOA)
- Doppler shift

TDOA systems measures the time difference received from the signals at the receivers. Each signal measured locates the target on an ellipsoid whose foci are the two receivers. In order for the target to be unambiguously located, more receivers could be used, or the receivers needs to take azimuthal and elevation measurements. This method was researched by Griffiths [14].

DOA tracking systems operates by looking at the DOA of the target signal varying with time. For the source to be unambiguously located, the DOA measurements should be taken from more than one location. This can be achieved by using two or more receivers, or the receiver must be moving itself.

Doppler tracking systems works on a similar basis as the DOA system, but measures the variation of Doppler shift of the signal with time. Doppler measurements from a single fixed receiver is ambiguous, and therefore two or more receivers are required, or the receiver must be moving [20].

The system to be built at the University of Cape Town will be DOA and Doppler based.

2.16 Conclusions

From the details included in this chapter, one notes that the concept of bistatic radar is significantly more complex than monostatic radars. This is mainly caused due to the geometry of the bistatic system. The separation between the transmitter and the receiver gives the bistatic radar distinct advantages and certain disadvantages. Some of these advantages and disadvantages are listed in Section 2.2.1 in this chapter.

It is also evident from this chapter that the performance of bistatic radars can never exceed that of the monostatic system. Although this is true, there are some distinct applications within the bistatic system which cannot be implemented by monostatic radars. An example whereby bistatic systems are a major advantage, is using such a system to detect

stealthy aircrafts. Although stealth aircrafts are designed to have a low RCS, in the monostatic case, the bistatic system however, illuminates the targets from all directions, and therefore the unique design of the stealth aircraft is not "stealth-like" to bistatic systems. It must also be noted that as the bistatic angle tends towards zero, or the target range becomes large, the bistatic theory tends towards that of the monostatic case. Various definitions of bistatic systems have been given, along with some methods, and considerations which is taken into consideration for the design.

Bistatic systems which have been implemented was also presented, and this showed that there were a few systems designed in the past specific for certain tasks. However the system adapted in this research will be based on Howland's method, as it proved to be the most viable system with regards to the tracking accuracy, as well the distance at which targets were detected. His method was also analysed and proved to be more possible and the most logical implementation for this type of system. The implementation of these methods will be discussed in more detail in the chapters to follow. The design of a bistatic receiver will be discussed, as well as the results will be shown from the simulations executed.

Chapter 3

Theory of Television Based Bistatic Radar

The objectives of this chapter are to present the theory of Television Based Bistatic Radar. This chapter will present work performed by Howland. The overview of his work includes its theory, and his receiver architecture for signal extraction. Much of his work involves signal processing of the signal after extraction. However, this research will concentrate mainly on the receiver itself. The theory to Howland's system forms the background theory of the system to be designed.

This chapter also contains the details of the television modulation schemes used for PAL transmissions. The properties of these signals and their application to the radar system are identified. Analysis on both the television signal, as well as the audio signal is presented here. A simulation of the television signal was also performed in Systemview. This simulated TV signal will be used as the input signal for the receiver simulation in Systemview.

Most of the details of the 625-line PAL television transmission system used in South Africa are obtained from Slater [38]. Various transmitters around Cape Town have been identified as a possible illuminator. However, the Tygerberg transmitter, on top of Tygerberg Hill, Cape Town, was used as the main transmitter. This transmitter site has an advantage of being in a direct line of site with the University of Cape Town.

The theory involving the calculations of the SNR values received are also presented in this chapter. These predictions are vital in the sense that they provide the signal levels which are to be detected at the receiver. The theory described in this section are used to create to SNR simulator for SNR predictions. More about the simulation will be explained in Chapter 4.

3.1 Background Theory for the Proposed Receiver System

There were various projects of this nature performed in the past, [14, 20, 28], but the approach adopted will be based on the research done by Howland [20, 21]. His method proved to be more feasible and had less complications. The aim for his research was to track airborne targets using two domestic television aerials, a receiver system and a desktop computer. The potential rewards for his research were great in the sense that no costly transmitter was required and no frequency allocations were necessary, therefore no one could detect the radar's presence. This however was equally challenging in the sense that no dedicated transmission was available. His research was mainly aimed at using the carrier of French television and the carrier of the British television, however, any amplitude modulated (AM) broadcast would also do.

Howland's method was based on obtaining a series of measurements, and therefore making a *priori* knowledge of the target's Doppler and DOA measurements which increases the chances of target detection. This was base on the assumption that the Doppler shift and DOA of a target echo with time is uniquely determined by the targets course and velocity . Mathematical expressions for Doppler and DOA profiles were then determined for the behaviour of targets which was entered into matched model for target estimations [20].

The data used in his work was collected using the receiving equipment based at DERA Malvern and DERA Pershore. His final results were collected with a more sophisticated and compact VXI mounted digital receiver system, with Yagi antennas mounted 18 m high.

His system consisted of two identical channels to down-convert the received target echoes from their transmitted frequency (200 - 800 MHz) to baseband, where they were sampled, digitised and stored on a 386/25 PC. Each channel was fed from a standard Yagi antenna with its elements spaced half a wavelength apart, and used as an interferometer in order to estimate direction of arrival [20, 21].

In each channel, the signal was first passed through a low noise tunable bandpass filter, and then passed into the front-end box. This front end box consisted of a low noise broad band amplifier with 27 dB gain and then a bandpass tunable bandpass filter to reduce the image noise, before being mixed down to IF of about 20 MHz. The Rohde and Schwartz synthesiser provided the extremely stable local oscillator, which was used to phase lock onto other synthesisers and receivers in the system. Once the signal has been downconverted to a frequency of 20 MHz in a bandwidth of 10 MHz, the signal was then fed into a Rohde and Schwartz HF receiver which was used to further downconvert the signal to 1 kHz, in a bandwidth of about 2 kHz. This output was then fed into a PC based analogue to digital converter which sampled the signal at rates of up to 6 kHz, and stored the data in the PC for subsequent processing [20, 21].

A Racal-Dana synthesiser and a variable attenuator was used to provide the calibration tone. This was used to asses the phase difference between the two channels and ensures accurate estimates of DOA. This however, was injected after the tunable bandpass filter, and therefore did not fully calibrate the entire system. The Hewlett-Packard analogue and digital spectrum analysers were available to view the frequency spectrum of each channel. Processing off-line was performed on the DEC Alpha 3000 model 600 workstation, running Digital UNIX, using software written in DEC Fortran and Mathematica [20, 21].

The later system was upgraded to using a more compact VXI mounted digital receiver system. This systems has the identical performance as the earlier equipment with the exception that it was controlled in Windows. The VXI unit contains a number of cards which replaced the earlier equipment. This unit consisted of a National Instruments 100 MHz 80486 controller PC, two Watkins-Johnson digital HF receivers, a Marconi signal generator and a Roke Manor VHF/UHF to HF low noise down-conversion unit [20, 21].

As this system operates in the VHF/UHF frequency bands, multipath propagation is a potential cause of low-level [1] coverage. In order to improve the low level coverage and reduce the effects of elevation lobing, the antennas were mounted on a 18 m high mobile tower. The low noise mast head down-conversion unit performed the initial two stage downconversion, at 290 MHz and 29 MHz. The signal was then relayed at 29 MHz down low-loss semi-rigid coaxial cables to digital HF receivers in Portacabin 50 m from the antennas. The digital HF receiver then downconverted the signals to baseband with a bandwidth of 100 Hz - 16 kHz, before providing the output in the form of 16 bit quadrature samples. The data was stored on a 2 Gb disk attached to the VXI controller PC. This whole system was locked to an oven controlled 10 MHz reference provided by a Racal-Dana or Rohde and Schwartz SMGHU synthesiser [20, 21].

The Time/Doppler history of the signal is calculated using a mixed radix FFT. This basically involves taking a two second sample on each channel and thereafter applying the Hamming weighting, and calculating the FFT of each, and then the process repeats. As the spectrum for the FFT is complex, the phase difference between the channels can be used to calculate the bearing of the target, using the equation:

$$\theta = \sin\left(\frac{\lambda\Delta\phi}{2\pi \mathrm{d}}\right) \tag{3.1}$$

where

λ = radar wavelength

d = spacing between the two antennas

$\Delta\phi$ = phase difference between the two channels

In Howland's paper [21], he states that it is assumed that $-\sin^{-1}\left(\frac{\lambda}{2\mathrm{d}}\right) < \theta < \sin^{-1}\left(\frac{\lambda}{2\mathrm{d}}\right)$ to avoid any directional ambiguities. Though in practice, close spacing of the Yagi an-

[1] This low-level coverage refers to the coverage area, as the coverage area calculated is based in a function of the receiver, transmitter and target altitudes, as referred to in Chapter 2, Section 2.8.

tennas reduces directional ambiguities, but resulted in severe mutual coupling. This will cause problems with the estimate of target bearings as it moved off boresight, and therefore possibly cause severe tracking errors. These concerns will be addressed by my colleague who will be dealing with the tracking algorithm for the research [30].

After the data was captured, downconverted and stored, he then used processing schemes to provide a track estimation from his measurements of the Doppler shift and DOA of targets echoes from the television's sound or vision carrier. Processing of the data was split into several steps. The signal is first received on two channels, and downconverted to baseband through a low noise VHF down-conversion unit and digital HF receivers. Signals from each channel are then processed using fast Fourier transforms (FFT) to provide bearing and Doppler estimates. Each FFT requires 1-2 sec worth of data. A constant false alarm rate (CFAR) was used to identify the target echoes and reject the unwanted carrier harmonics. A Kalman filter based tracking scheme was then used to associate detections belonging to the same target. The Doppler and DOA samples for each target are then passed to a three stage track estimation process which estimates the target Cartesian coordinates and velocity components [20, 21]. Figure 3.1 is a summary of Howland's receiver system.

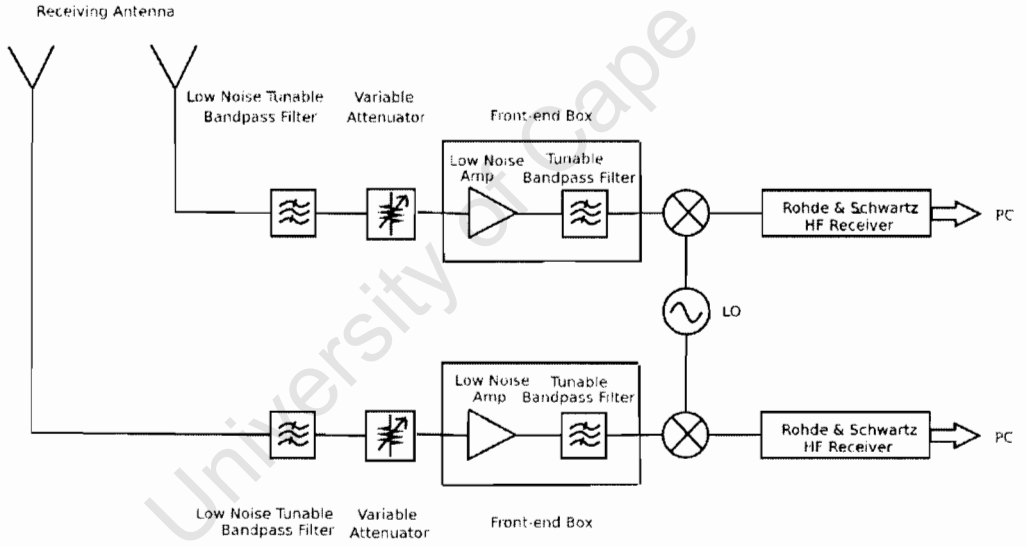

Figure 3.1: Block diagram of Howland's receiver architecture.

Howland's work was mainly based on work performed by Griffiths and Long [14]. Their published work was the first mention in the open literature of television-based bistatic radars. Their work explained the pulse-like nature of television signals for radar use, which enabled them to receive clutter from local buildings. With off-line processing, they implemented a two pulse MTI canceller to resolve moving targets. However, this system was impractical in the sense that it required a special transmission, but yet having only a range resolution of 1800 m and a range ambiguity of 9600 m.

Griffiths, et al. [14], also implemented experiments in using only the test signal, which was made available by television stations transmitting these multiburst signals outside programme times. Frequency filtering was performed on the received signals by tapping off the signal just before IF and routing it to a spectrum analyser. Their final result was that they were not able to detect any Doppler frequencies consistent with aircraft targets. Factors which could have been the cause of this is the energy level of the individual multi-burst pulse is less than the actual level of the sync pedestal used for their previous tests. To base our receiver to be designed on the multiburst test signal is almost impossible, since we do not have the resources for this kind of arrangement with television stations to transmit multiburst signals.

The experimental system implemented by Griffiths et al. consisted of two parallel receiver channels. The one channel of this receiver would receive the direct signal, while the other would receiver the radar echoes. Their receiver blocks were built based on standard commercial tuners and IF units. This was a simple way of assembling a working system, however, noise figures and intermodulation products were inferior to custom products. The video output was not the full 5.5 MHz bandwidth, in particular the colour sub-carrier had been filtered out. Their Yagi antenna was mounted on the roof top of their experimental location which received the transmitted signal. Figure 3.2 shows their system architecture.

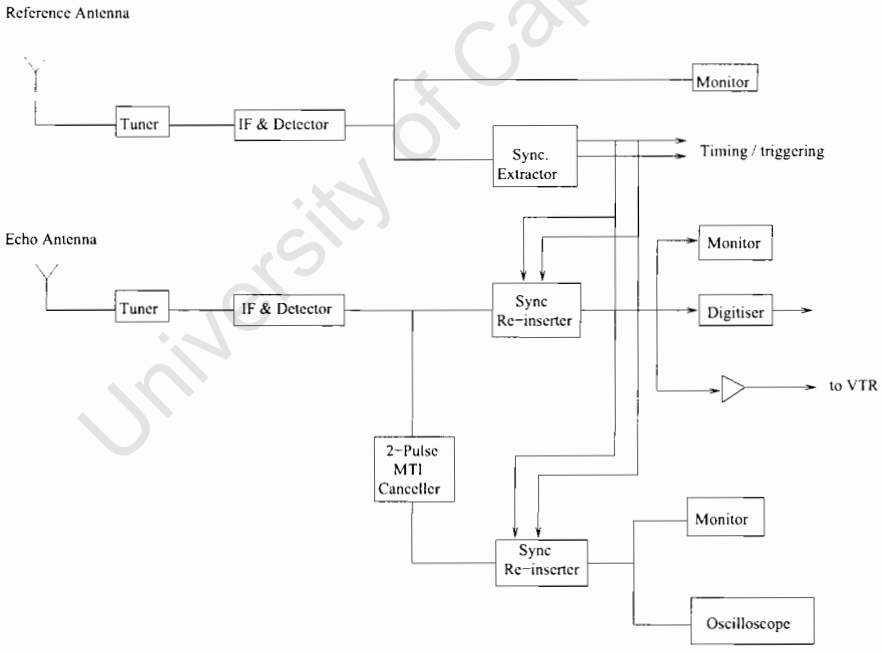

Figure 3.2: Block diagram of Griffith's et al. receiver system.

3.2 Theory on the Television Modulation Scheme

The transmitted TV signal is essentially a filtered AM signal, and the waveform shown is the signal received in an ideal receiver with the correct frequency response [14]. With the method used to create a television transmitted signal, the result should be the same as that using a video signal to amplitude-modulate the vision carrier fully, and passing this through a filter [14]. This can be shown in Figure 3.3.

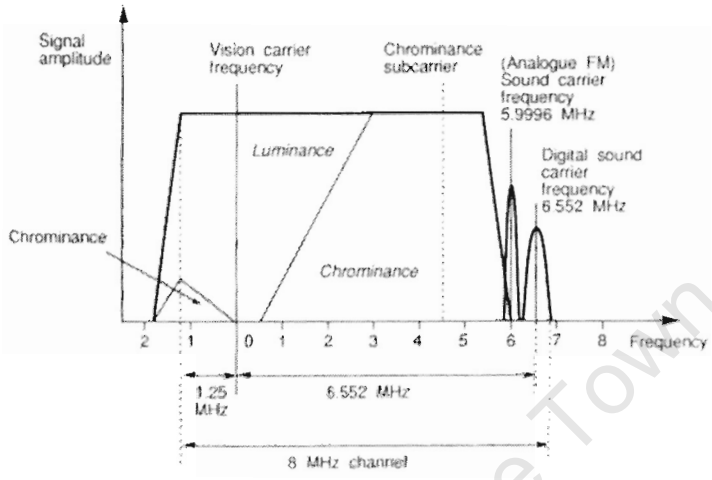

Figure 3.3: Frequency band of the television signal. [38]

Figure 3.4 is an image of the idealised carrier amplitude for a picture of line colour test bars.

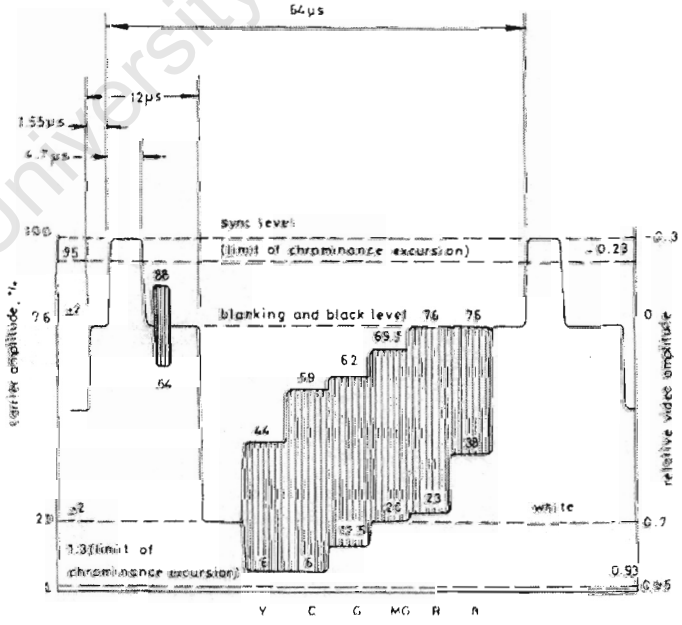

Figure 3.4: Waveform showing a variation of carrier amplitude with time. [38]

From conventional modulation techniques, the difficulty with the TV vision signal, is that the signal changes from AM to single-side band (SSB) [2] as the video frequency rises. Below 1.25 MHz, the signal is pure AM; from 1.75 MHz to 5.5 MHz it is pure upper sideband [14]. The result of this is that the lower video frequencies can modulate the carrier fully, while only 50% can be reached by the higher ones. A typical television signal is shown in Figure 3.5.

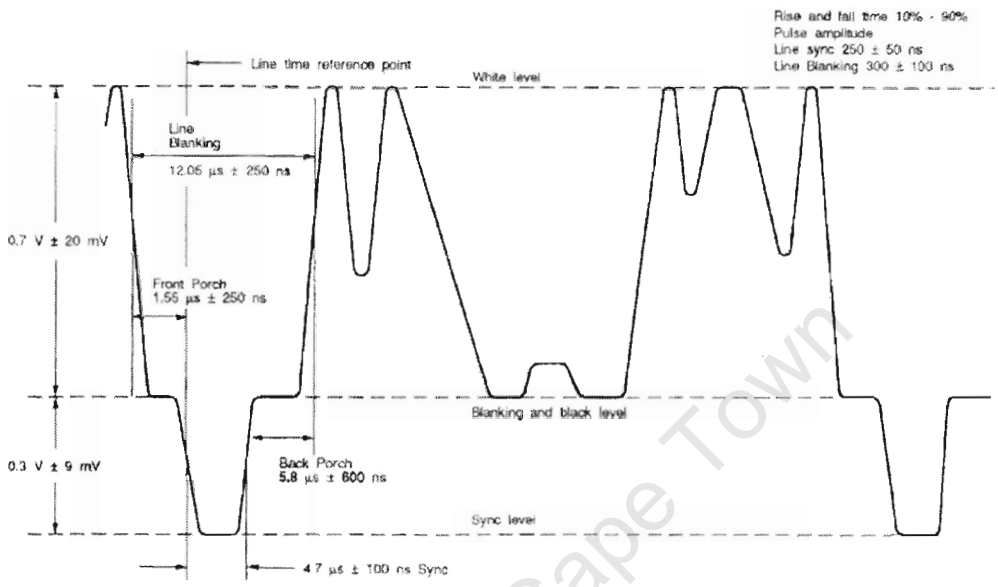

Figure 3.5: TV-line waveform. [38]

The amplitude indicated in Figure 3.5, at any instant determines the brightness of the display, this amplitude coincides with the voltage shown as the blanking level. The line blanking pedestal is at the black level of 76% of peak, but the sync part itself is blacker than black to the 100% level.

3.2.1 Analysis of the Television Signal

The dominant feature of the TV signal is the line sync pedestal and pulse (this is the negative part of the signal as shown in Figure 3.5, and in Figure 5.7). The sync portion of the signal is essentially the line blanking interval, whereby the electron beam uses this time to end off a line and return to the start of the next line. This portion of the signal occupies $4.7\mu s$ of the total $64\ \mu s$ television signal. By using Equation 2.23. The resolution of using the sync pulse can be calculated to be 704.53m whereby $\tau = 4.7\mu s$. Although

[2] Single-sideband modulation (SSB) is a refinement of the technique of amplitude modulation designed to be more efficient in its use of electrical power and bandwidth. It is closely related to vestigial sideband modulation (VSB). A vestigial sideband (in radio communication) is a sideband that has been only partly cut off or suppressed. Television broadcasts (in NTSC, PAL, or SECAM analog video format) use this method if the video is transmitted in AM, due to the large bandwidth used. It may also be used in digital transmission [43].

this proves to be of poor resolution, however, this is better than using the entire signal which has a resolution of 9593.6 m. The resolution was obtained by using the monostatic resolution equation because the bistatic system has the best performance when it behaves monostatically.

The time domain plot for the signal captured is shown in Figure 3.6. This signal was captured using a video recorder connected to a 60 MHz oscilloscope. The television signal captured was the SABC 2 channel from the Tygerberg transmission. Figure 3.6 shows that the received signal follows the same format of the theoretical signal, indicating the sync pulse, the back porch with the colour burst, and the luminance and chrominance region.

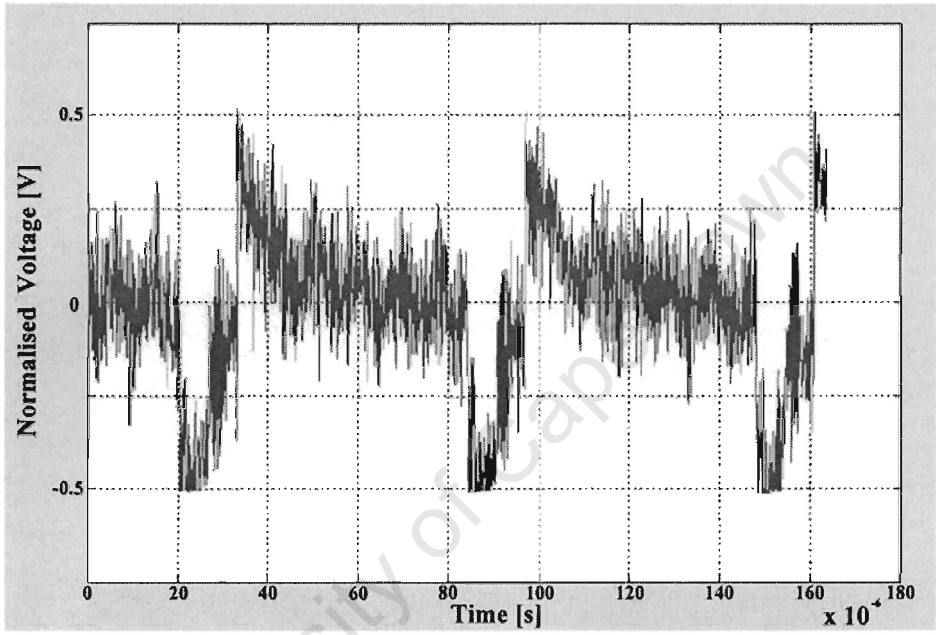

Figure 3.6: Time domain plot of the received TV signal data.

3.2.2 The Audio Signal

The sound carrier of the signal sits at roughly 6 MHz above the vision carrier, with a power level approximately one fifth of the peak vision carrier. This can be seen in Figure 3.3. The sound carrier however has a modulation limit of 15 kHz, and therefore not suitable for matched filter pulsed compression techniques, as poor radar resolution will be obtained (roughly 20 km) [14]. In more advanced systems, a new digital audio carrier is implemented, and this is also shown in Figure 3.3. However, the signal level of this new digital audio signal is even lower than that of the original analogue FM sound carrier and therefore is also unsuitable for this usage.

3.2.3 The Simulated Television Signal

The PAL television signal was simulated using Systemview. The PAL system used in South Africa uses vestigial sideband amplitude modulation for the picture, and FM for the sound. This type of modulation was also simulated. Figure 3.7, is the image of the television signal simulation, with the components which were used. The television signal used in the simulation is indicated in Figure 3.8, with the complex FFT of the output signal sitting at the respective frequency below that.

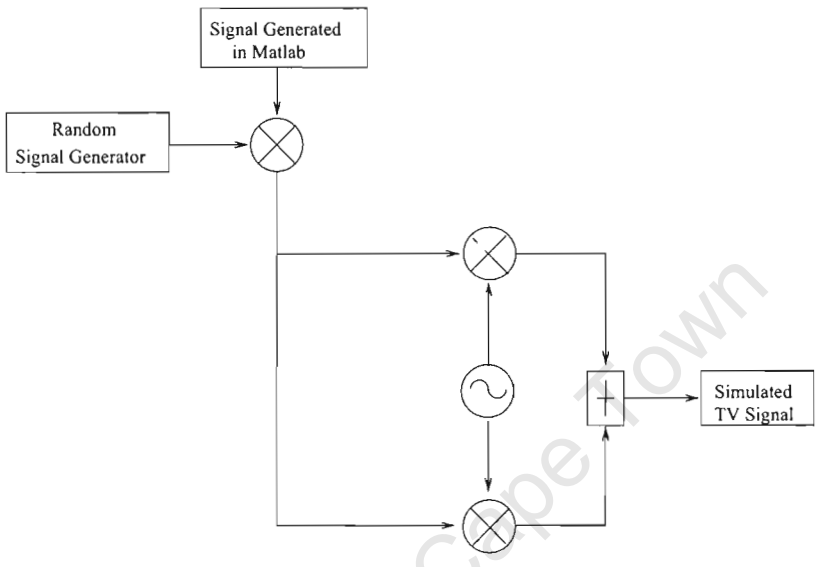

Figure 3.7: Simulation of the television signal with SSB modulation.

The television signal was created by writing a single line television signal in Matlab. This signal created is similar to the one shown in Figure 3.5, with the exception that the portion after the back porch is at a constant level. This portion essentially represents the line information of the TV signal and changes from line to line. This signal was imported into Systemview and mixed with a random generator, which provided the random rise and fall time for the constant level, essentially simulating the line information changes. In reality, the content within this rise and fall time within the white level of the television signal does have some coherency from line to line, however this information is extremely difficult to simulate. The simulated signal is then mixed with a signal which is at the specified frequency of the transmission to create the completed television signal located at RF. The output of the created television signal is shown in Figure 3.8. This simulated waveform has significant association to that of the theoretical form.

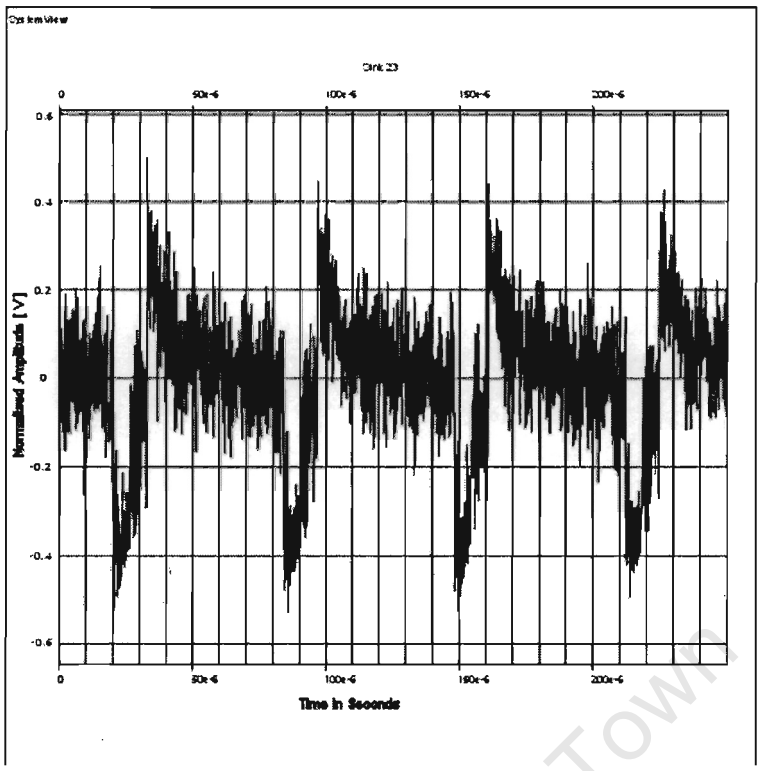

Figure 3.8: Time domain waveform of the simulated television signal.

3.3 Theory for SNR Calculations

The SNR values are calculated for specific R_T & R_R. These predicted SNR values allows us to evaluate the signal levels received for a target at that location. The SNR value is generally calculated with the following equation from Skolnik [37], also shown in Section 2.7.

$$\mathrm{SNR} = \frac{\mathrm{P_t G_t G_r \lambda^2 \sigma_B F_t^2 F_r^2}}{(4\pi)^3 \mathrm{k T_s B} \left(\mathrm{R_t R_r}\right)^2 \mathrm{L_t L_r}} \tag{3.2}$$

The main difference when compared to monostatic systems, is that this equation caters for the bistatic range at which the signals have to travel. Equation 3.2 is dependent on the bandwidth throughout the system, and provides the minimum SNR value for a target at a maximum distance away.

From Barton [2], a more convenient method of calculation is used whereby the SNR is measured at the final stages, after processing. The advantage with this method is that not only all the gain for the various stages are considered, as well as their bandwidths, but more importantly, considerations have also been accounted for the processing gain. This gain factor is incorporated with the integration time for which the target is recorded.

These factor are shown in Equation 3.3, and can be referred from Barton [2].

Barton's theory for matched filters, in this instance, states that the maximum output SNR is equal to the ratio of the total received energy to noise spectral density [2, 24]:

$$\left(\frac{S}{N}\right)_{mf} = \frac{E}{N_0}$$

The SNR values predicted for the simulator are based on this particular SNR equation. This equation is used for systems which are similar to a continuous wave (CW) or coherent pulse radars, whereby the signal is integrated through an observation time t_o in the prediction filter, therefore, the received energy ratio and matched filter SNR output is:

$$\left(\frac{S}{N}\right)_{mf} = \frac{P_{av} t_o G_T G_R \lambda^2 \sigma}{(4\pi)^3 (R_T R_R)^2 k T_S} \tag{3.3}$$

whereby

P_{av} = Average transmitter power

t_o = Integration time through which the data is recorded

G_T = Transmit antenna power gain

G_R = Receive antenna power gain

λ^2 = Wavelength

σ_B = Bistatic target radar cross − section

T_S = Receive system noise temperature

R_T = Transmitter to target distance

R_R = Receiver to target distance

k = Boltzmann's constant

The length of time required for recording the data, was derived from the fact that a target travelling into Cape Town will not be travelling extremely fast (at ±150 m/s for a target at 8-12 miles out of the airport). Ordinary commercial aircrafts don't have large fluctuations for 1 m displacements, therefore, these targets can be tracked at every 1 m displacements, until it reaches its destination, Cape Town.

$$v_t = \text{target velocity} \pm 1\ \text{ms}^{-1}$$

With the above assumption, the Doppler resolution of the target can be calculated to be 4.48 Hz, with a minimum sampling period of 223 ms.

$$\delta f_d = \frac{2 \cdot v}{\lambda} \tag{3.4}$$

$$\delta f_d = \frac{1}{t_0} \tag{3.5}$$

whereby

t_o = sampling period

The velocity used in this instance is the 1 m displacement mentioned, and $\lambda = \frac{c}{f}$, whereby the operating frequency is 671.25 MHz. Ideally, at least 223 ms of data needs to be recorded, however, certain limitations restricts this from happening. These limitations will be explained further in Chapter **5.**

3.4 Conclusions

This chapter provided the background theory of Howland's system. Howland's [20, 21, 19, 18] research proved the feasibility of using a non-cooperative transmitter as an illuminator of opportunity for bistatic radar systems. The receiver designed was able to adequately capture signals from airborne targets whereby both Doppler and DOA profiles were extracted successfully with only using a bandwidth of a few kilohertz. His tracking techniques allowed targets to be detected several hundreds of kilometres away using only the vision carrier of television transmissions.

Included in this chapter was also a brief introduction on basic concepts of television systems and their modulated signals. The locations of the precise carrier frequencies were shown, as well as the frequency band of these television signals. Certain sections of the television signal seems viable for usage in this research. A simulation in Systemview was introduced in this chapter which simulated the television signal. This signal will be used as the input to the receiver system to simulate the Doppler shifted television signal for the experiment.

Chapter 4

Signal to Noise Ratio Simulator

This chapter is describes the signal-to-noise ratio simulator which was created in IDL. Two different programs were created for the purpose of SNR estimations, and the results achieved by both will be shown. The simulator was designed for both the omni-directional and directional receive antenna arrangements. Both of the outcomes of these simulations will be shown in this chapter. The equations and background theory for this simulator was presented in Chapter 3.

This simulation produces expected signal-to-noise ratio values for a target at various distances from the receiver and the transmitter. The simulation also shows both the coverage area of the transmitter as well as the coverage area of the receiver. Indications of the flight paths of targets coming into Cape Town Airport are also shown for a target flight-path coming in from Johannesburg and Port Elizabeth. The SNR levels produced in the simulation are shown in dB's, and these levels have been overlaid over the mapped area of the Western Cape.

SNR predictions have a great impact on the overall design of the system. The analysis of these signal to noise ratio values at the radar receiver can be predicted with the knowledge of the geometry and configuration of the radar setup. These estimated SNR values also helps with determining the accuracy at which the Doppler measurements of targets echoes are made.

This chapter begins by providing the details of the transmitter used. The Tygerberg transmitter was selected for the main transmitter of usage since it has a direct line of sight advantage to the receiver location, therefore most of the details here will be based on this transmission station. The chapter then begins to describe some of the theory of how the simulator was created, along with the equations which were used. Descriptions for both the omni-directional, as well as the directional antenna were given. The associated target Doppler resolutions and SNR values are indicated within this chapter.

4.1 Transmission Parameters

Although the research is based on the receiver only, details of the transmitter needs to be known in order to calculate various SNR values at the receiver, as well as the power levels at the receiver. Most of the details about the television signals themselves were dealt with in Chapter 3.

The parameters for the various transmitters' location around the Western Cape was made available by Sentech. The parameters of main concern will be the Tygerberg transmitter. This can be seen in the table below.

Table 4.1: Table showing the transmitter parameters.

Station Name	Tygerberg
Frequency Vision Carrier (MHz)	671.25
Bandwidth (MHz)	8
Effective Radiated Power (Watts)	2000
Site Height (m a.s.l)	398
Mid Antenna Height (m a.g.l)	75
-3 dB Beamwidth	360^o
Vertical Radiation Pattern Tilt	-1.2^o

The frequency of the vision carrier varies from station to station as well as for different transmitting sites. The E-tv channel was chosen for the experiment as it has most of it's vision carrier located within a closer band. These carriers are located in the range of 500 - 700 MHz. By utilising this factor, we will be able to maximise the signals received from a single antenna for the different transmission sites.

4.2 SNR Plots and Assumptions for an Omni-Directional Receiver Antenna

This particular software developed needed to estimate the SNR value received at the receiver for various distances at which the target position would be when compared to the receiver and the transmitter. Certain assumptions and estimations had to be used for the purpose of creating the simulator. Most of the values used and estimation are strictly for standard commercial aircrafts, and does not cater for any military aircraft, or any other light aircrafts.

The software developed for these SNR estimations at particular distances out from the receiver is based on the maximum coverage range of the receiver. An image of the simulations is shown below, with flight path coming into Cape Town, and coverage areas of the respective receiver and transmitter.

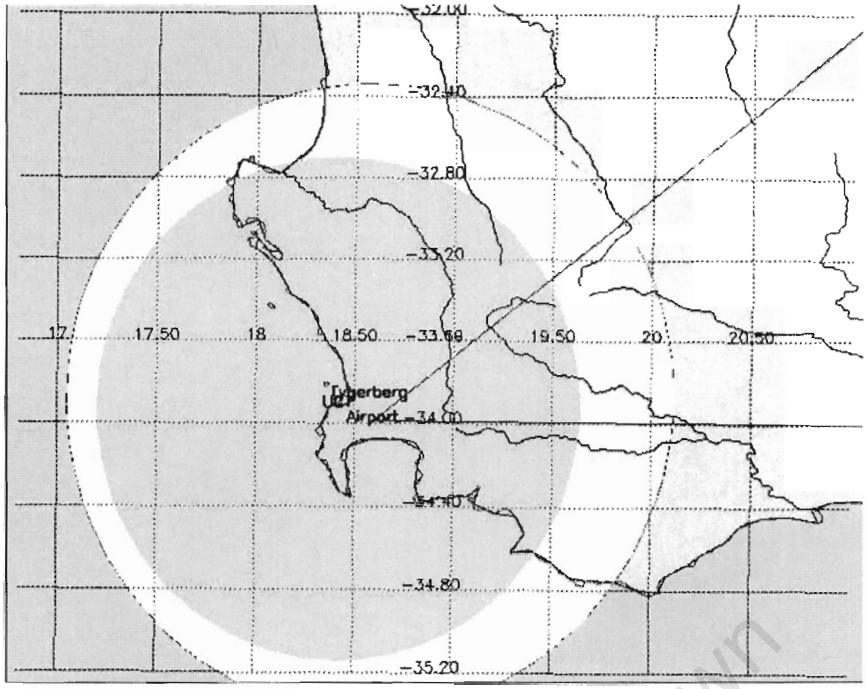

Figure 4.1: Coverage area for the receiver and transmitter using the Tygerberg transmitter station.

In Figure 4.1, there are legends shown for the latitude and longitude values on the map. The image also shows the coverage area of both the transmitter and the receiver. The coverage calculated are for targets simultaneously within the LOS to both the receiver and the transmitter. The targets are assumed to be at an altitude of roughly 1500 feet, which is 451 m for targets entering into Cape Town. For a smooth earth, these LOS requirements are established by coverage circles centred at each site. The shaded outer ring represents the coverage area of the transmitter, while the inner ring, represents the coverage area for the receiver. The coverage areas of both the transmitter, as well as the receiver plotted takes into consideration of the target altitude, as well as the receiver and transmitter altitude positions, therefore, this effectively is the radar horizon coverage area for the transmitter and the receiver. Targets within the common coverage area (common overlapping area of both the transmitter and receiver coverage) are in line with both the transmit and receive antennas, and therefore could be detected with sufficient RCS. The equations and considerations used for the coverage plot was discussed earlier in Section 2.8.

From the various parameters calculated, the predicted coverage for a bistatic configuration is shown below. The software used for the creation of this prediction was done in IDL along with a more advanced version, which is shown further on in this chapter. Figure 4.2 represents only a small portion of the actual coverage area.

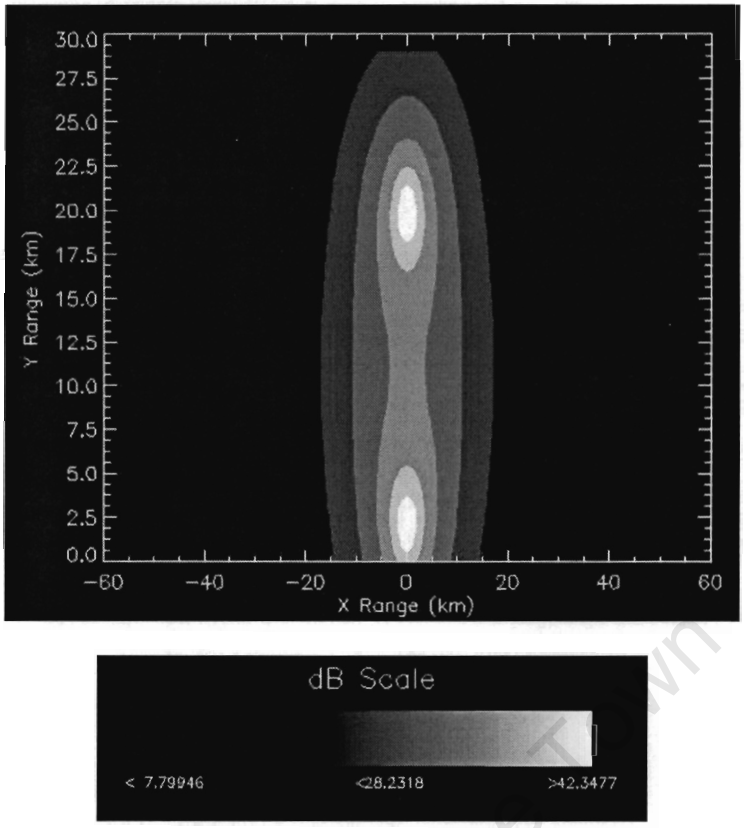

Figure 4.2: Predicted coverage for a bistatic configuration.

The scale in the image above represents the SNR levels in dB's, as indicated, it can also be seen in the plot that the separation between the two points of the highest SNR is the transmitter and receiver locations. The separation between the two locations was calculated as accurately as possible using converted co-ordinate values. For the verification of the simulation, a point calculation is shown below. $R_{T_X} = R_{R_X} = 40\,\text{km}$ and $R_{T_Y} = 5.5\,\text{km}$, therefore $R_T = 40.37\,\text{km}$. $R_{R_Y} = 12.5\,\text{km}$ therefore the distance from the receiver to the target, $R_R = 41.91\,\text{km}$.These values are used in Equation 3.3 to give a total $\frac{S}{N} = 9.42\,\text{dB}$. The above calculated value corresponds to the value on the image relative to a target distance at roughly 40 km away from both the transmitter and the receiver. The approximated bistatic radar cross section is $20\,\text{m}^2$, this value was the estimated RCS of a standard commercial aircraft [14]. Other values used in the equation are referenced in Appendix A, Algorithm 1.

A more advanced version of software shown above was created for a plot of the SNR over a map of the Western Cape and these predictions are shown in Figure 4.3.

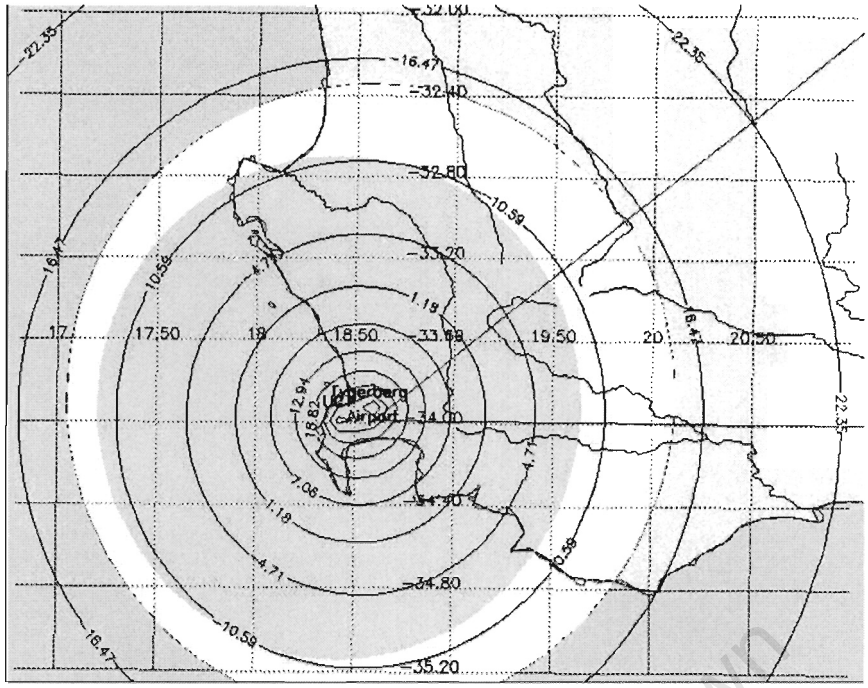

Figure 4.3: SNR plot over the Western Cape from the simulation, using the Tygerberg transmitter.

The values calculated in Appendix A, Algorithm 2, indicates a value of -10.01 dB at the outer boundary of the receiver coverage. This value can be cross referenced to Figure 4.3. The radius of the receiver is calculated to be at 135.069 km away, while the transmitter is at a distance of 117.261 km away from the target. Other figures used in the equation are shown in the Appendix. Although the values shown at the outer boundaries of the coverage area does not reflect positive results, however, these results still reflect that target detection can be achieved at distances up to 80 km since the SNR level sits at roughly 7 - 10 dB, which is ideal for detection. These SNR calculations reflects thats this system is a viable system for target detection.

Mismatch losses of the integrating filters for the system are represented in the equation, as $L_m L_f$. The advantage of approaching the SNR calculations through the matched-filter SNR, is that loss factors for the system can be minimised. These mismatch losses seldomly exceed 2 or 3 dB. It should also be noted that the above analysis, as well as the image plotted refers to a purely omni-directional antenna used. The image created and SNR estimations for a directional antenna will be shown in the following section.

Figure 4.4 is another plot of the estimated SNR values to be received, but with the use of the Paarl transmitter. Here you can see that the coverage area of the transmitter has shifted significantly, but this coverage area is still wide enough to cover most of the receiver's coverage area. The effective coverage area of this arrangement would be the effective covered area of the transmitter overlapping the receiver coverage. It should also be noted that the range of SNR predictions have also changed due to the nature of the positioning

of the transmitter location.

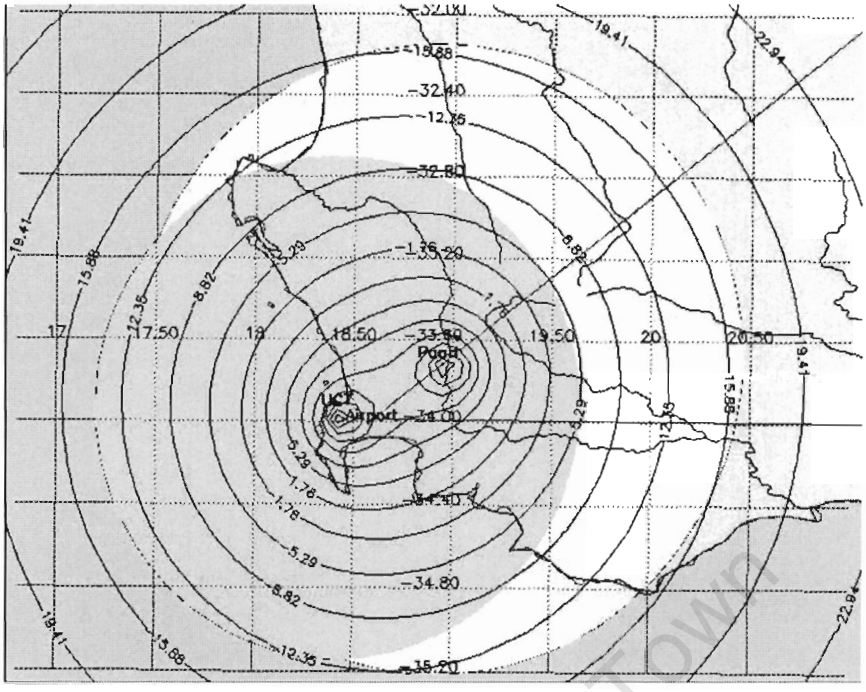

Figure 4.4: SNR plot over the Western Cape using the Paarl transmitter.

As shown in Figure 4.4, the SNR projections exceeds the coverage areas themselves, but these SNR values are much lower than those calculated within the coverage area. Ultimately, the SNR predictions of interest are those values which are within the radar horizon, therefore, from the image shown, only the SNR estimations within the coverage areas are needed. These SNR predictions does not include any propagation or path loss factors through air, so this should also be taken into account, therefore the predicted SNR values would decrease. However, these losses have only a minor effect on the actual values.

One of the most important factors surrounding the use of this particular equation, is that all the other alternative procedures which involve expressions for calculations of SNR which involve bandwidth and subsequent gain factors, are subject to misinterpretation, and larger errors due to the different bandwidths throughout the system [2].

4.3 SNR Plots and Assumptions for a Directional Receiver Antenna

The equations used for this portion of the simulator have been described previously, the only difference of this section is the inclusion of the antenna gain. For the previous section, this gain factor was assumed to be at 0 dBi for an omni-directional antenna.

The plot in Figure 4.5 is the predicted coverage for a bistatic radar including the antenna pattern factors. The assumptions used for Section 4.3, about the receiver system remains the same, with the inclusion of a 15 dB gain for the Yagi antenna.

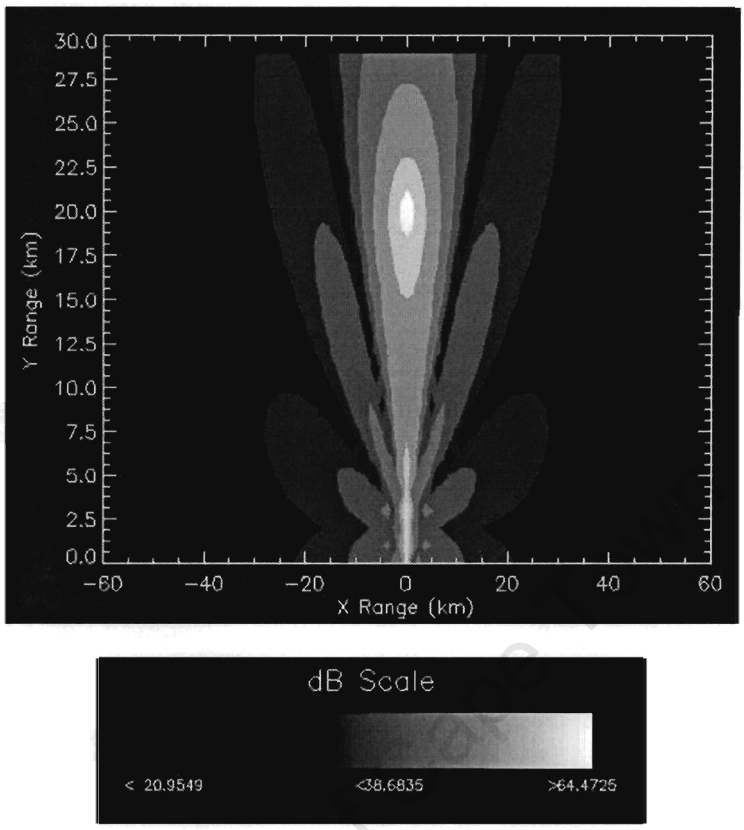

Figure 4.5: Predicted coverage for a bistatic radar including the antenna pattern factor.

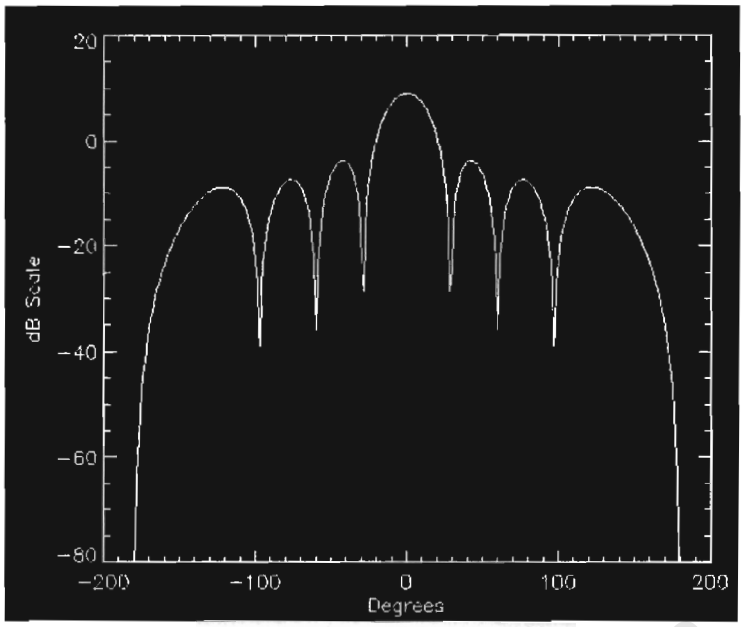

Figure 4.6: Receiver antenna pattern factor.

The associated antenna pattern for the prediction is also shown in Figure 4.6. The type of antenna pattern used, has an associated sidelobe level of -10 dB. The software created can be manipulated to adjust the directive angle of the antenna pattern, as well as changing the number of elements of the antenna. The scale shown in Figure 4.5 is presented in dB's, and the verification of the predicted SNR values are shown below. $R_{T_X} = R_{R_X} = 40\,\text{km}$ and $R_{T_Y} = 8\,\text{km}$, therefore $R_T = 40.79\,\text{km}$. $R_{R_Y} = 10\,\text{km}$ therefore the distance from the receiver to the target, $R_R = 41.23\,\text{km}$. The calculated $\left(\frac{\text{S}}{\text{N}}\right) = 24.472\,\text{dB}$. This calculation is presented in Appendix A, Algorithm 3.

This SNR value can be related to the relative position of Figure 4.5 to prove the accuracy of the simulation. Equation 4.1 below was used as the pattern array factor for the antenna in the simulation. This was obtained from Kingsley [24].

$$\text{AF} = \left| \sqrt{\text{N}} \frac{\sin\left[\text{N}\pi\left(\frac{\text{d}}{\lambda}\right)(\sin\theta - \sin\theta_\text{s})\right]}{\text{N}\sin\left[\pi\left(\frac{\text{d}}{\lambda}\right)(\sin\theta - \sin\theta_\text{s})\right]} \right| \tag{4.1}$$

whereby

AF = Pattern array factor

N = No. of elements in the Yagi antenna

d = Element spacing of the Yagi antenna

λ = wavelength

θ = Angle off boresight

θ_s = Directive angle of the antenna

This antenna pattern equation was incorporated into the software, and can be easily ad-

justed. Modifications to the equations, such as number of Yagi elements, wavelength, etc can also all be easily modified.

Figure 4.7 represents a more advanced version of Figure 4.5, this plot is similar to that of the one plotted for the omni-directional antenna plotted over the Western Cape.

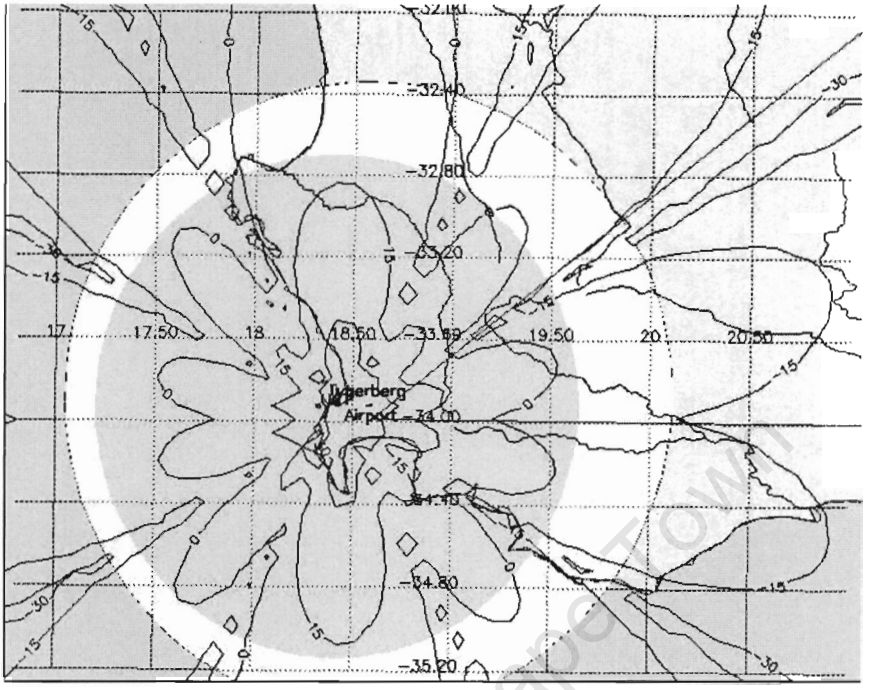

Figure 4.7: Directive SNR plot over the Western Cape using the Tygerberg transmitter.

From Figure 4.7, the yellow, outer ring, and grey, inner shaded area, still represents the coverage area of both the transmitter, as well as the receiver. But as can be seen in the image, the SNR pattern is now affected by the lobes of the antenna pattern, due to its directive nature of the antenna. The levels of SNR are also shown on the projection with the values of the respective layers shown in dB's. Some of the SNR values at the same ranges could vary, and this was mainly caused due to the antenna gain with respect to azimuth angle. This basically means that the antenna gain is maximised at a 0 degree azimuth pattern, and this value increases or decreases with respect to the angle as well as the number of lobes expected for the pattern. The antenna pattern used to plot the image was shown in Figure 4.6. With the use of Equation 3.3, the minimum SNR at the maximum receiver range is calculated to be at 4.993 dB. This calculation can be referred to in Appendix A, Algorithm 4.

In Figure 4.7, the antenna is directed in a northerly direction. Although most of the gain in the antenna is directed in a northerly direction, there are still certain, lower SNR values received behind the antenna due to the nature of the antenna, as well as due to the gain provided by the receiver itself. The simulation of this directive antenna pattern shown above, in Figure 4.7, can be modified such that the antenna can be directed in any direction, therefore providing a directive SNR estimation for the coverage areas.

4.4 Conclusion

A simulator was created for predicting SNR values for both omni-directional and directive gain antennas. This simulation allowed for arbitrary placement of transmitter as well as the receiver. Much of the parameters used within the simulation, such as the power levels, gains of the antenna, radar cross section, etc can all be adjusted within the code. The software developed can also be adjusted such that only the coverage is plotted, only directive SNR, etc. Most of these modifications are explained in detail within the code themselves.

The portion of the simulator which describes the SNR prediction with a directive antenna, also allows the controller to point the antenna in any arbitrary position. This is advantageous in the sense that the antenna could be pointed directly at the target, therefore receiving the maximum reflection off the target.

This chapter has described the capabilities of the simulator, and has shown that the simulated results relates to the theoretical calculated results. These values estimated from the simulator is vital to us as this is a first estimate to the type of signal levels which are expected for the different target distances. These estimations are used for the designs of the receiver, as well as sets the capabilities of the receiver.

Chapter 5

Bistatic Receiver System

This chapter covers the details of the research with regards to the receiver designed. This system was designed and simulated, but not built. A detailed overview of Howland's method is provided as well as the system architecture for Griffiths, et al. is defined. The architecture of the receiver will be presented with an analysis of the signal throughout the chain. The components used within the receiver designed are briefly introduced, and actual components have been selected to be used within the receiver. The data sheets for these components have been provided in Appendix C.

A simulation of the receiver chain design was also created. This simulation will be used to confirm that the system designed is able to extract Doppler estimates of target shifts as the project requires. The components used within this simulation are values extracted from the actual components selected. The simulation is used to detect any flaws in the design, if any, these can be corrected before the actual system is ready to be built and tested.

This chapter starts off with a description of the receiver system, both in the architectural side as well as the theoretical, and mathematical side of the signals received will be explained. Simulations for the receiver chain have been conducted in Systemview and will be presented. The analysis of the data recorded from both the simulation as well as actual data which was recorded will be discussed. The recorded data refers to the real-time data which was recorded with the use of a pc Pinnacle PCTV rave television card. Details of this card, along with how the signals were extracted will be mentioned within the chapter. The explanations for how the simulations were run, together with their restrictions will be indicated.

This chapter also aims to show the reader how a cost-effective proposed bistatic radar receiver system can be achieved without the involvement of complex circuitry.

5.1 Description of the Proposed Bistatic Receiver

The receiver designed, and located at the University of Cape Town is primarily used for air-surveillance purposes. The receiver chain would consist of two receiver channels. One would be used to receive the direct or reference signal, with minimal ghosting effects, while the other channel will be used to study the radar echoes and their effects. The antenna arrangement designed for this system will be placed on the roof of the Menzies building, at the University of Cape Town. This receiver is designed to "hitchhike" off various transmitters, which are non-cooperative, located around the Cape Town area.

The receiver required can be built with ordinary television demodulation blocks. Although these demodulation blocks are cheap, the disadvantage of using these commercial components are that the noise figures and intermodulation products might be inferior to 'custom' products. Another downside of this is that a prescribed passband shape would have to be used instead of a better suited one for AM reception around the vision carrier, as shown by work performed by Griffiths, et al [14].

The block diagram for this research, based on Howland's work as described in Section 3.1, is shown in Figure 5.1.

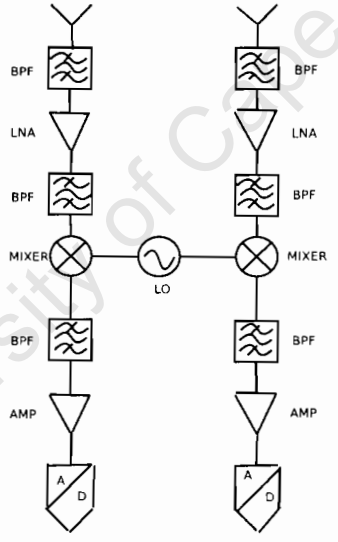

Figure 5.1: Block diagram of the proposed receiver system.

The signal received will be processed through a two channel, down-conversion receiver. These signals will be downconverted to an IF of 10.7 MHz, and then sampled by an ADC. The signals received from each of the channels will be processed using a Fast Fourier Transforms (FFT) technique to provide the Doppler estimates of the target flightpath.

The receiver will be required to down-convert the reflected RF signal, to an IF level whereby the signal can be stored and be used as a means of measuring the bearing of target echoes. In Howland's research, target bearing was achieved by using phase interferometry, with a pair of eight-element Yagi-Uda antennas [21]. The antennas to be used

for signal reception, can be mounted on top of the Menzies Building at the University of Cape Town. The height of this building could also help with reducing the low-level coverage and elevation lobing as mentioned by Howland in Section 3.1.

The receiver front end will be designed to maximise the sensitivity to obtain the maximum dynamic range. In order to prevent saturation of the receiver, variable gain amplifiers will be added into the system. This will prevent saturation obtained by the clutter, but will still maximise dynamic range.

Three important factors will be taken into account for the design in the bistatic system:

1. The complexity of the bistatic geometry is difficult to control.
2. There are various clutter rejection requirements.
3. The difficulty in implementation, i.e. synchronisation and isolation aspects.

It was then later discovered from a simulator created by Dr. N Morrison[1] that targets can be accurately tracked using only the Doppler information received from the recorded data. This was most helpful since the original design for the receiver can be stripped to a single chain, only if the exact LO located of the transmitted signal is known, and stable enough. This is also a major advantage in the sense that the cost implications for building such a receiver would reduce by half.

The design for the receiver system will however still remain a two channel receiver system, since bearing estimates received of target flightpath can be utilised. The extraction of the Doppler information as well as the method of extracting the bearing information will be shown in the sections to follow. However, for the sake of simplicity, much of the simulations and testing done will be based on only one receiver channel, therefore extracting only the relative Doppler information, and no phase information. No sophisticated antenna arrangement is required for this, which makes the measurements simpler.

5.1.1 Doppler and DOA Extraction from the Receiver

The calculations referred to in this section verifies the signal processing through the receiver chain, which was shown in Figure 5.1. This verification will prove that both the Doppler and DOA estimates can be extracted from the receiver designed in signal processing. These values can be extracted from the receiver by creating a difference and sum channel of the results. Since the system is bistatic, the LO for the transmitter and receiver are located at different locations. Therefore, stable synthesisers are required to produce stable clocks, at the respective sites. Howland suggested some methods of doing this, and this can be found in [21].

[1] Dr. N Morrison is a retired lecturer from the University of Cape Town, who now spends his time doing some contract work for the Radar and Remote Sensing Group.

Figure 5.2 is a representation of how the signals are received with the respective angles. V_A& V_B described in Appendix B are the signals received from the antenna structures. The bearing, or the direction of arrival, as mentioned above is represented by θ in the equations, and can also be seen in Figure 5.2.

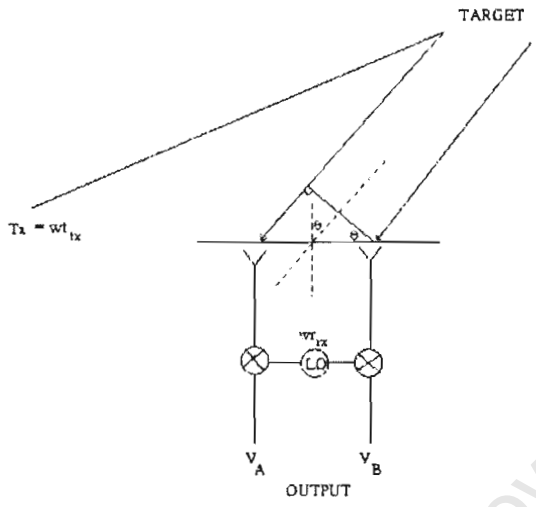

Figure 5.2: Figure indicating how the signals are received, with the relative angles.

The DOA bearing, θ, can be calculated by extracting the phase difference, $\Delta\phi$, from the two channels. The phase difference $\Delta\phi$ will be split into $\frac{\Delta\phi}{2}$ and $-\frac{\Delta\phi}{2}$ in the equations in Appendix B to simplify the mathematics. The positive and negative portions of this phase difference represents the positive and negative portions for the phase difference on either side of boresight to where the antennas are pointing. For instance, if the target was directly on boresight, there would be no phase difference between the channels, therefore $\Delta\phi = 0$ and $\theta = 0$.

It should also be noted that the amplitudes of the signal has been assumed to be of no great importance. This was established because the phase comparison monopulse system is used for the processing techniques, and the amplitudes will be normalised at the extraction of the phase difference information from the two channels. It is therefore assumed that the amplitude patterns are identical, therefore pure phase sensing can be achieved. This method of sensing was also demonstrated earlier by Rhodes [32]. Since only the phase of the signals will be considered, the amplitudes of the signals will be represented by A.

From the equations in Appendix B, it can be noted that the phase difference between the channels can be extracted by taking the normalisation factor between the difference and the sum of the two channels.

Amplitude monopulse radar techniques described by Rhodes [32] can also be used and in this case. However, the output result would be the amplitude ratio, which is $\frac{p(u)-1}{p(u)+1}$, where $p(u)$ is the amplitude ratio [32]. The significance between the two lies in the fact that they are both amplitude functions, except for the fact that the one lies on the real axis,

while the other is on the imaginary axis. The output of the phase normalisation between the channels is represented on the imaginary axis. These two types of techniques can be related as follows:

$$\tan\frac{\Delta\phi}{2} = \frac{p(u)-1}{p(u)+1} \tag{5.1}$$

It can be noted from the verification that the bearing estimate of the target can be obtained by taking the $\frac{\Delta}{\Sigma}$ factor from the output of the two channels, whereas the Doppler component of the signal can be observed in both the sum and the difference of the two channels. Extraction of the Doppler component from the signal is independent of the amplitude as well as the phase of the signal, since the frequency of the signal is of interest here. Therefore from the two signals below, amplitude and phase has no effect on the Doppler extraction.

$$\Delta = \mathrm{A}^2(\theta,\mathrm{d},\mathrm{t})e^{-j\omega_d t}\left[e^{j\theta_{A1}} - e^{-j\theta_{A2}}\right] \tag{5.2}$$

$$\Sigma = \mathrm{A}^2(\theta,\mathrm{d},\mathrm{t})e^{-j\omega_d t}\left[e^{j\theta_{A1}} + e^{-j\theta_{A2}}\right] \tag{5.3}$$

From Equations 5.2 and 5.3, it is shown that the Doppler and bearing estimates of the target flightpath can be extracted from the signal. These extractions were only possible with the assumption that the receiver LO is locked onto the transmitter LO, with minimal drift. Drift in the LO or the transmitted signal should be minimised to effectively record accurate measurements.

5.1.2 Receiver Requirements

Certain aspects for the receiver system needs to be met, for the bistatic system to be feasible. These criteria are listed below:

- Must illuminate the area of the target path.
- The system must not saturate when illuminated by the transmitter.
- The system must not saturate when receiving scattered clutter returns.
- Must have a high probability of detection, roughly 80%.

Maximum sensitivity will be obtained to obtain the maximum dynamic range. A variable gain amplifier will be included to prevent saturation of the receiver.

5.1.3 Components and Effects of the Receiver

The reception of the signals will be at a frequency, f_{TV}, and this received RF signal will be down-converted to an IF frequency of:

$$IF = RF \pm LO \tag{5.4}$$

where LO is the local oscillator frequency. Local Oscillator's such as the Rohde and Schwartz synthesiser can be used to provided the stable LO which a reference signal, which can be used to phase lock onto other synthesisers and receivers for the system.The signals received can then be manipulated in software to form a sum and difference channel, to extract Doppler and bearing estimates of a target.

The sum channel forms the beam which is the combination of the signal power of the two individual beams, and so improves the signal to noise ratio. This specific channel is used for target detection and also to measure the range and Doppler information. The gain of the sum channel gives monopulse systems the advantage over earlier techniques which the target was viewed off bore-sight [24]. However, the sum beam is wider than the original beam, and therefore it is not used for angle measurement. The difference channels produces a error voltage, which is roughly proportional to the angular deviation of the target from bore-sight [24], and no output is obtained when the target echo amplitude is the same in both antenna beams.

Two types of monopulse systems are known, and were described earlier in Chapter 2, Section 2.15.3.

The usefulness of such a system is limited however due to the fact of multipath effects that occurs when multiple signals are received from a single target, these effects are known as multipath effects. Another problem is the ambiguities in angular position, called grating lobes, that occurs when two widely spaced antennas are used [21, 24].

5.1.4 Mixers

In this type of receiver, a mixer is required to convert the incoming RF signal down to an intermediate frequency (IF). Any non-linear device can be used, as non-linearity is required for the production of frequencies not in the input [**?**]. More details on theory of the mixers can be found in [26]. Certain factors to consider when choosing a specific mixer is the minimum LO and maximum RF input power level, conversion loss, port-to-port isolation and return loss of conversion frequency. There are two main types of mixers which are available [29]:

1. **Single-balanced mixer.** A single-balanced mixer offers good isolation between LO and RF, but poor isolation between RF and IF (no balance).

2. **Double-balanced mixer (DBM).** DBM's allows the designer to achieve minimum levels of distortion with a high degree of isolation from interfering signals.

For this application, the main parameters to look at are the conversion loss and the dynamic range of the mixer. The conversion loss is a measure of the efficiency of the mixer

in providing frequency translation between the input of the RF signal and the output IF signal [26]. This is the basic indication of the noise figure and therefore determines the lower limit of the dynamic range. The upper limit of the dynamic range will be set by the conversion compression point [26]. In this instance, a double-balanced mixer will probably be ideal for this situation.

Frequencies which are generated by the double-balanced mixer ares:

$$f = n \cdot f_{LO} \pm f_{RF} \tag{5.5}$$

where n is odd. The unwanted frequencies which are produced could be filtered out by a matched filter. The frequency mixer chosen for the receiver is the ZX05-10 from Mini-Circuits, with its details defined in Appendix C. The conversion loss for this particular mixer is at 8.3 dB, and the 1 dB compression point is at 1 dBm. The noise figure of the mixer is at 6.8 dB and requires a LO level of 7 dBm to drive it. More details of this mixer can be seen in the Appendix, as mentioned.

5.1.5 Amplifiers

These amplifiers provide the main gain of the system. Certain amplifiers have automatic gain adjustments. These can be useful such that saturation of the amplifiers, which could even lead to damage, would not occur. Low noise amplifiers can also be mounted at the antenna to prevent any degradation in the noise figure of the system which may occur due to certain losses. These losses would primarily consist of losses caused by the cabling.

The front-end amplifiers which have been chosen are the AM-2A-0510 from Lorch. The operation of this amplifier is at 500-1000 MHz, with a gain of 24 dB, and a noise figure of 1.5 dB. The other amplifier to be used at IF is the AMP-76 from Mini-Circuits. This amplifier has a noise figure of 3.1, and a gain of 26 dB. Both the amplifiers datasheet will be provided in Appendix C.

5.1.6 Filters

The basic function of the filter is to selectively pass, by frequency, the wanted signals and to suppress the unwanted signals. The filters selected will be based on their nature to maximise the output signals at the specific frequencies.

The front-end filter chosen was the T8B bandpass filter from Lorch. This particular filter has a 3 dB bandwidth of 25 MHz. The other filter to be used at IF, which is the BP-10.7 filter from Mini-Circuits. The 3 dB bandwidth of the filter is at 3.8 dB. Datasheets for these filters are attached in the Appendix C.

5.1.7 Signal Level Analysis of the Receiver Design

Once all of the components for the receiver system have been chosen, the signal should be traced through the designed receiver to ensure that non of the components are saturated while the signal travels through the system. The following image is a signal trace through the system to ensure that no saturation exists.

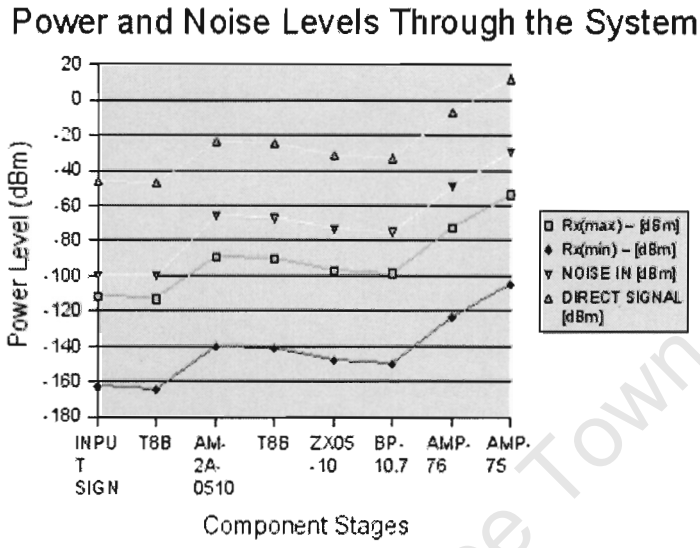

Figure 5.3: Graph showing the signal levels through the receiver.

The low signal levels indicated within Figure 5.3 can be increased. Various methods exist to increase signal levels. Such as increasing the gain of antenna, or the LNA.

5.1.8 Synchronisation Effects

One of the major problems within bistatic radar systems is to be able to synchronise the received signal with the transmitted signal. The receiver is required to reproduce the timings and frequencies of the transmitter waveforms before it can accurately measure the time delays and Doppler shifts of the target echoes.

In practice, a more reliable and accurate system can be achieved by sending the transmitter's frequency and modulation data down a narrow band data link along with the location, orientation and motion data, which is then used to recreate the transmission signal at the receiver side [8]. However, there are other cost-effective methods to achieve synchronisation:

1. Lock the receiver local oscillator to the direct transmitter signal received along the baseline. Platform motion at either end will cause errors because reference signal is Doppler shifted when it arrives.

2. Lock both transmitter and receiver oscillator to external signal or beacon. Renders radar dependent on external signal which might fail or attacked during wartime.

3. Use the frequency at both ends. Expensive, but frequency stability is adequate for Doppler processing requirements [24].

4. To improve the performance of the radar system, a dedicated local oscillator can be designed to make the receiver less reliant on support equipment.

According to the research done by Howland [21], no synchronisation with the television transmitter is required if no timing measurements are made, providing the television carrier frequency is known and stable. The requirement for such a carrier widens the number of possible transmissions which may be exploited. This method does not only include television broadcasts, but also any transmitter of opportunity broadcasting a stable CW, AM, narrowband PM or narrowband FM signal [21].

5.2 Geographical Positioning of the Radar

The receiver will be located in the Menzies building at the University of Cape Town. The exact coordinates of UCT will be taken into account as well as the coordinates for Tygerberg, and various other transmitting sites when doing various calculations. These calculations made are vital for the estimation of signals which will be received at the receiver.

Simulations for these predicted received signals have been created and are discussed in more detail in the following sections. The position of the transmitter, which is at the top of Tygerberg (for initial estimations), is 18.5 km away from UCT (this represents the baseline). The actual locations can be seen in the images created by the simulator which was described in the previous chapter. Initial estimations and calculations are based on the Tygerberg transmitter. Details of other sites are available in the simulator as well.

5.3 A Brief Description of the Antenna System

In any promising radar system, two fundamental parameters for an antenna design which are directly considered with the effectiveness of any receiver system are their coverage and their resolution. In a general sense for radar equations, the required antenna gain is proportional to the square of the range which defines the coverage, but the dependency is twice that of the bistatic case [40]. This factor is considered essential for better radar coverage area. For a passive radar system, the received power can be considered as [40]:

$P_R = P_T + P_{L1} + G_T + P_{L2} + G_R$

whereby their respective properties are:

P_R = received power
P_T = transmitted power
P_{L1} = path loss (transmitter to target)
G_T = gain of the target
P_{L2} = path loss (target to the receiver)
G_R = gain of the receiver

By increasing the gain of a receiving antenna system, you effectively increase the received power. This increase in received power, increases the range of the system respectively. In the above equation, we can see that the antenna gain parameter can be controlled easily. Another important factor in a bistatic radar receiver system would be the angular resolution.

It is well known that by increasing the gain or narrowing the main beam of the antenna system, the overall performance of the receiver can be increased. To achieve this, more elements in the array antenna design should be included. By increasing the array arrangement of the antenna system (therefore increasing the electrical size of the antenna and causing the main beam to narrow, resulting in increased angular resolution), we are also able to take advantage of the Direction of Arrival (DOA) estimation techniques such as Multiple Signal Characterisation (MUSIC) or Analytical Constant Modulus Algorithm (ACMA) techniques [40]. Furthermore, we are able to utilise some array attributes such as super directivity, sidelobe reduction techniques, etc, which results in even better performance [40].

Typical passive radar systems have the requirements of the antenna design. Some features are [40]:

- High Gain or Directivity - peak power for a passive system is typically low, therefore we need an antenna to have a high gain to overcome this, or to increase the elements in the array.
- Low Sidelobes.
- Low Cost.

The antenna array, and structure should be:

- Able to steer nulls at jammers, interferes, direct breakthrough from the transmitter.
- Able to make accurate measurements.
- Covert - located in areas which is not noticeable.

For an increased range measurement, a large receiving aperture would be required, since, although the transmitted power is the same order as some radar systems, it emanates from a low-gain aerial [14]. By comparison, normal monostatic radar systems have large-aperture, high-gain antennas for both transmit, and receive.

For the system to be built, multiple antenna structure will probably be made. One of the antenna structures will be used for the main receiving channel with maximised gain, and directivity to minimise any ghosting effects. Another antenna structure will be used to point a null directly at the transmitter, therefore only receiving signals except the one from the transmitter. This basically makes use of antenna patterns.

Theoretically, this might work, but the paper presented by Griffiths et al. [14], states that this could be a naive move because the required depth of the null is so great that only an adaptive closed-loop technique will be useful. This method is not recommended. These antenna systems could be dedicated to down-converting the received signals to HF. Due to the fact that the system operates in the UHF/VHF frequency band, multipath propagation is still a potential cause, as discussed earlier, and also, the surrounding buildings can add to this effect. These antenna structures should be mounted on a tower off the top of the roof top to avoid any unnecessary multipath effects. In [21], he stated that by placing the array structures close together, could reduce the directional ambiguities, but this causes severe coupling. Much of these concerns for the antenna design have been resolved in depth by my Reiners [31].

5.4 Simulation and Analysis of the Designed Receiver

From the details described in this chapter, a simulation model of the receiver has been designed in Systemview. Figure 5.4 is the block diagram for the simulated receiver design. In Figure 5.4, the simulated tv signal at RF block refers to the simulated signal shown in Figure 3.8 as the input signal to the receiver chain.

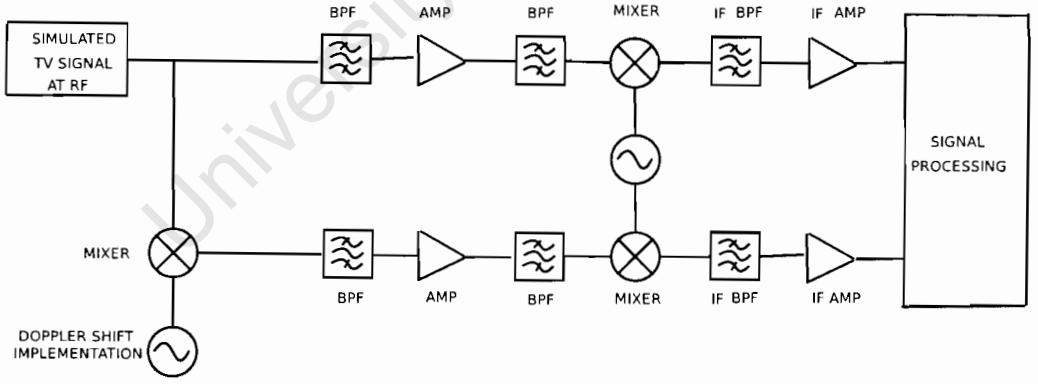

Figure 5.4: Block diagram of the simulated receiver design.

This simulation was executed with the components as mentioned in Section 5.1. The input to the receiver chain is the television signal which was created in Chapter 3. This input signal is then fed into the receiver designed, which downconverts the television signal from RF to an IF signal located at 10.7 MHz. The recorded signal will then be downconverted to baseband in processing.

The FFT of the signal at IF is shown in Figure 5.5 whereby the modulated TV signal is downconverted to 10.7 MHz from RF. The frequency resolution settings in Systemview affects the exact location of the downconverted signal.

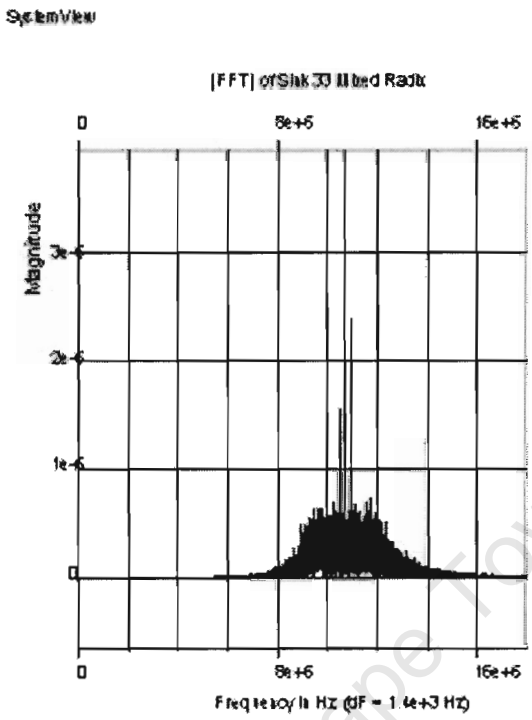

Figure 5.5: FFT of the e-tv signal at IF in Systemview.

The Doppler shift due to the targets movement can be can be extracted from the signal if the frequency supplied by the LO is stable enough. The difference between IF frequency and the LO represents the Doppler shift in the signal received. If no Doppler shift was present, the resultant difference would be zero. The Doppler frequency caused by the target flightpath can be realistically simulated by manipulating the input frequency to the receiver chain. This modification can be made to the input frequency for the simulated television signal. The Doppler shift mixed with the original simulated television signal represents the Doppler shift due to the target. This Doppler shift can be added in the lower channel shown in Figure 5.4.

The shifted signal can then be basebanded to extract the Doppler shift as shown in Figure 5.6. The image shown in Figure 5.6 is for a 700 Hz Doppler shift simulation.

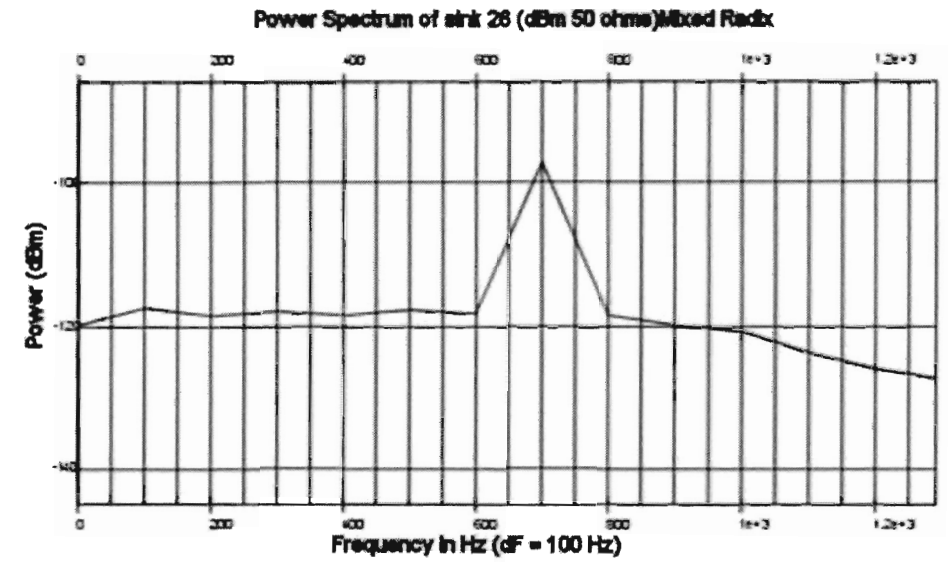

Figure 5.6: FFT of the Doppler shifted television signal.

Certain limitations exists in Systemview which prevents accurate simulations of the receiver system designed for the optimum performance. Most of these limitations occur with the settings for the sampling time within the software, which also affects the frequency resolution.

In order to achieve a decent Doppler resolution for the target flightpath, as calculated Section 3.3, a Doppler resolution of 4 Hz was calculated, which required a total recording time of 250 ms. In order to simulate this correctly, at least 250 ms of data needed to be recorded and simulated in Systemview. This however, would require an immense amount of memory as well as data space for storage of the data. This was one of the major limitations encountered for an accurate simulation of the receiver chain.

In the following section, data will be captured with the use of only a TV card. Doppler shift of target echoes will then be extracted.

5.5 Analysis of the Data Recorded

Real data for targets flying into Cape Town International were recorded. These measurements were taken by the use of the demodulation blocks on an ordinary pc television card. The television card used was the Pinnacle PCTV Rave card. The image of the setup can be shown below.

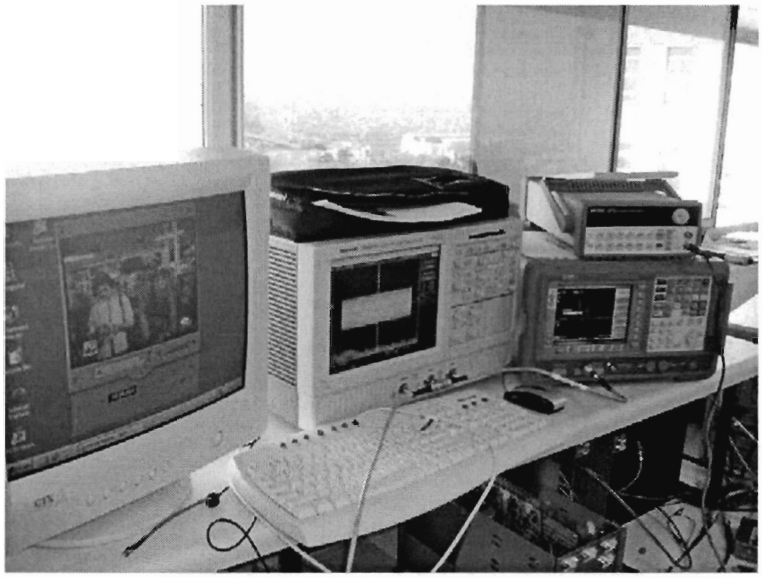

Figure 5.7: Image of the hardware used to capture target data.

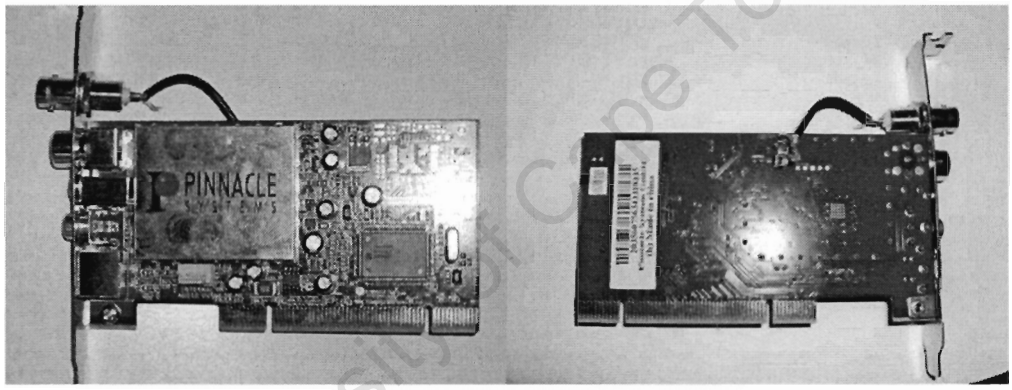

Figure 5.8: Close-up image of the actual TV card.

Television demodulation blocks are available on the card itself, and therefore, the RF signal received from the antenna is downconverted to the IF frequency of the card, which sits roughly at 38.9 MHz. Although it was previously stated that the use of television demodulation blocks were not ideal for the use of a receiver, however, the pc television card is a simple and cheap method of obtaining some real data for Doppler extraction. Figure 5.9 shows the spectrum of the signal at IF of the pc television card.

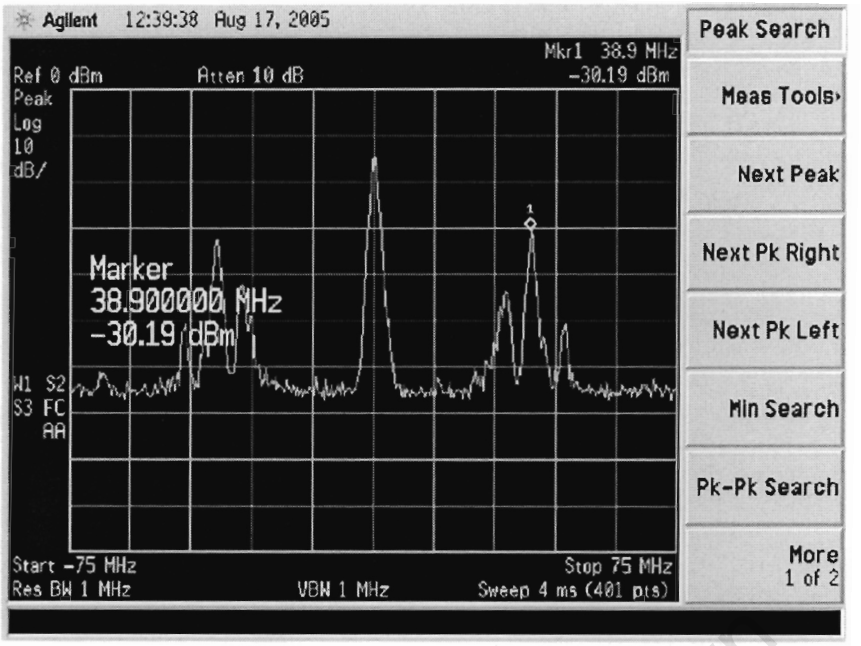

Figure 5.9: Downconverted television signal captured from the TV card.

The vision carrier of the television signal can be seen as the dominant feature in the television signal. The Doppler shift calculated for targets flying around the Cape Town area is calculated to be roughly not more than 1 kHz. In order to extract this 1 kHz signal, a total recording time of at least 1 ms is required. The signal was captured with 400 000 samples at a sampling frequency of 100 MS/sec for a duration of 4 ms, using the Tektronix TDS5000B Digital Phosphor Oscilloscope. With these figures, the effective Doppler resolution of the system is 250 Hz, meaning that targets can only be resolved for a velocity of 55.75 ms^{-1}. This however, is the maximum performance to which the oscilloscope allows.

Considering the fact that the receiver is used to track Boeing's, this is not a bad resolution in the sense that targets would not interfere with one another at 56 m intervals. In order to resolve targets at closer intervals, a finer resolution is required. This can be achieved by taking larger number of samples recorded or a longer recording length. This however cannot be achieved with the equipment made available for the experiment. For short periods of recordings, the LO on the pc tv card should be sufficient to provide a stable clock for the recordings. However, for longer periods of data recordings, a more stabilised LO would be required to reduce any drift which might occur in the LO of the card and the transmitter's LO.

The data recorded at IF was downconverted to baseband and filtered at a bandwidth of 2 kHz around the vision carrier. A Doppler shift of -500 Hz was obtained as shown in Figure 5.10. The Doppler shift extracted was for a target leaving the Cape Town Airport (The target leaving the airport was reflected in the results, as well as observed from the experimental room).

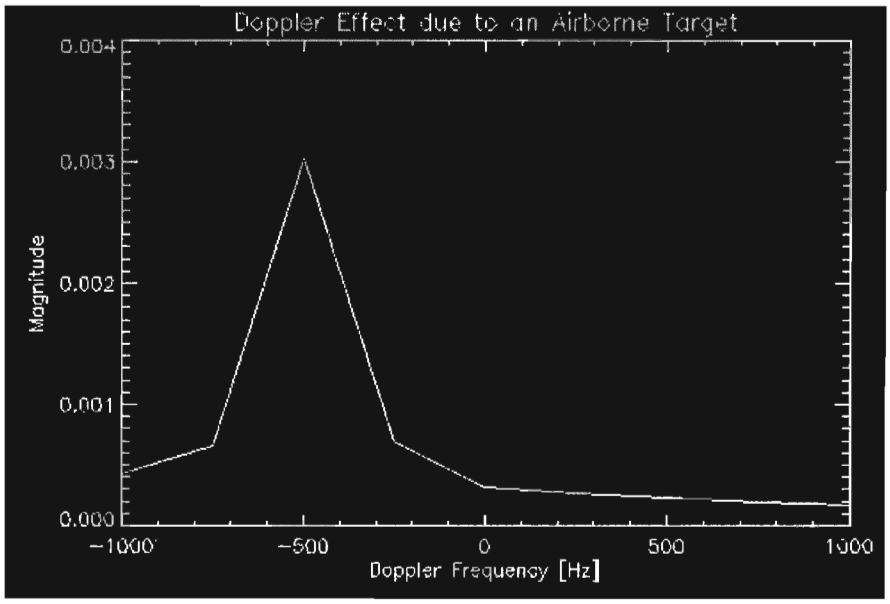

Figure 5.10: Doppler shifted signal of the recorded data off the Pinnacle PCTV Rave card.

5.6 Method of Approach for the Ambiguity Function Analysis on the Recorded Data

Ambiguity functions were defined in detail in Chapter 2, Section 2.10. The various equations used for the analysis study of the data recorded were defined, as well as a study performed by Tsao et al. [41], was discussed.

There are numerous analogue and digital VHF radio and UHF television transmissions available at high power, and such frequencies may be useful for detection of targets. The importance of this is by considering the nature of analogue television modulation, whereby there will be ambiguities within the $64\mu s$ line repetition rate [14]. We also need to know how the ambiguity behaviour depends on the instantaneous modulation of the particular communication signal or programme content, and how it varies against time [12]. It is also important to know how these ambiguity properties vary with time, as variations in the forms of ambiguities will affect the performance of the radar system [12]. Other effects such as radar clutter, which is defined as:

> "Unwanted echoes, typically from the ground, sea, rain or other precipitation, etc. [44]"

can also be taken into consideration for the overall receiver system.

Before the methods of ambiguity studies are performed on the recorded data, some results are shown from a paper, [12], acquired based on ambiguity functions of a system built at

the University College of London (UCL). These measurements were taken by them, and the results are shown in the table below.

Signal	Frequency (MHz)	Range Resolution (km)	Sidelobe Bandwidth (kHz)	Peak Range Sidelobe Level (dB)	Peak Doppler Sidelobe Level (dB)
FM Radio - speech (BBC Radio 4)	93.5	16.5	9.1	-19.1	-46.5
FM Radio - classical music (Classic FM)	100.6	5.8	25.9	-23.9	-32.5
FM Radio - rock music (XFM)	104.9	6.55	22.9	-12.0	-26.0
FM radio - reggae music (choice FM)	107.1	1.8	83.5	-27.0	-39.5
DAB	219.4	1.54	97.1	-11.7	-38.0
Analogue Television Chrominance sub-carrier (ITV 1)	491.55	9.61	15.6	-0.2	-9.1
Digital Television (DVB - T)	505.0	1.72	87.1	-18.5	-34.6
GSM 900	944.6	1.8	83.3	-9.3	-46.7
GSM 1800	1833.6	2.62	57.2	-6.9	-43.8

Table 5.1: Properties of ambiguity functions of various types of broadcast and communications signals

The results shown in Table 5.1, indicates the relative frequencies used, the range resolutions and their instantaneous modulation bandwidths, as well as the peak sidelobe levels.

For an ambiguity analysis to be performed on the recorded data at UCT, there needs to be at least two recording channels. Firstly, we need a channel with its antenna pointed directly at the transmission source, therefore recording the direct transmitted signal. This is used as the reference channel. At the same instant, a second channel would have its antenna pointed in the surveillance region, recording data of any airborne targets. It is essential that the data from both the channels are recorded simultaneously to provide effective information which would be used in the matched filtering.

Once the data from both the channels have been recorded, the direct signal data would be used as the reference channel to create the matched filter, while the surveillance channel is used as the "comparing" signal for detection of the Doppler effect caused by the moving target.

The ambiguity diagram for the recorded data can be created by taking the combination of

a convolution of the two signals, and matched filtering. These diagrams can be used to understand the signal's range and Doppler properties. If however, there were two targets present at the same instant, these target ambiguities can still be resolved. When processed through a matched filter, a well defined (point) target produces an output with a sharp central peak where the targets are located, whereby these targets are separated by τ in time delay [2].

The resultant plot of the ambiguity function would be a 3-D plot, as mentioned before. Figure 5.11 illustrates the front-view of this surface plot.

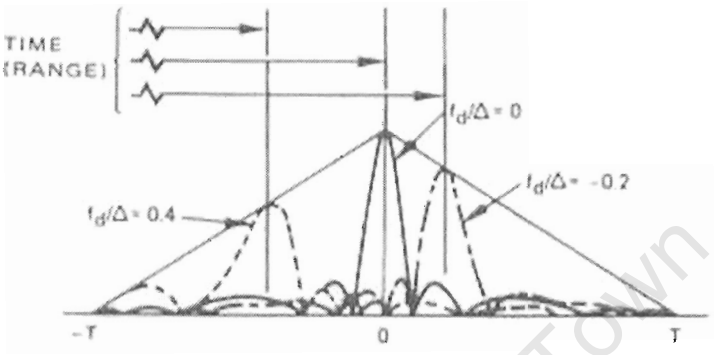

Figure 5.11: Amplitude-Frequency-Time relationship of a pulse compression signal [16].

From the example plot, one is able to determine where or how the target was flying past the receiver antenna. When the target moves, its Doppler shift may affect the time of arrival of the peak signal, therefore causing an ambiguity. From Figure 5.11, it can be shown that for closing targets, with a positive Doppler shift ($f_d > 0$) will appear closer while opening targets with negative Doppler shift ($f_d < 0$) will appear further away. Non-moving targets will have zero Doppler shift ($f_d = 0$). From this analysis, the ambiguity functions produced can be used to tell the user the direction and movement of the target [16].

As mentioned before in Chapter 3, the format of the television signals used in South Africa is the PAL system, which use vestigial sideband amplitude modulation for the picture, and FM for the sound. The bandwidth of the visual signal is roughly 5.5 MHz, this results in a range resolution of 27.25 m. Each picture consists of 625 lines with interlaced scans and a frame rate of 50 Hz. Each line is 64 μs which results in range ambiguities corresponding to a bistatic range of 9600 m. These analysis corresponds to work presented by Griffiths, Baker, et.al [12, 14, 11].

Certain limitations and restrictions were experienced during the ambiguity function analyses. One of the major difficulties experienced was that two channels of data was required to be recorded, but only one pc tv card was available. This therefore only allowed one set of measurements taken.

However, an ambiguity analysis of the recorded data could still be performed by using

the recorded data as the reference data used for the matched filter. Shifting the recorded data in time represents a multiplication with a frequency ramp in the frequency domain, therefore representing the Doppler shift of the target.

The above mentioned processing technique was implemented and both these signals were then basebanded and convolved to produce the ambiguity diagram shown in Figure 5.12 for an e-tv television signal. This signal was filtered with a bandwidth of 1 MHz.

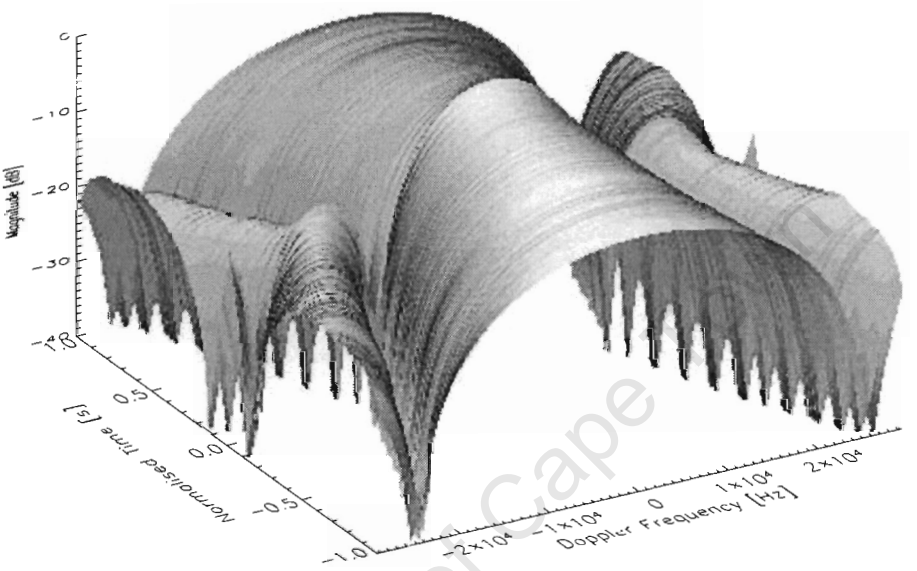

Figure 5.12: Ambiguity diagram of the recorded data from the Pinnacle PCTV rave card.

Another method would be to use only a portion of the actual signal spectrum. However, this would reduce the signal power available. Figure 5.13 shows the ambiguity function for the chrominance subcarrier. The ambiguities associated with the 50 Hz frame rate can be identified here. This was demonstrated by Baker, et al [11].

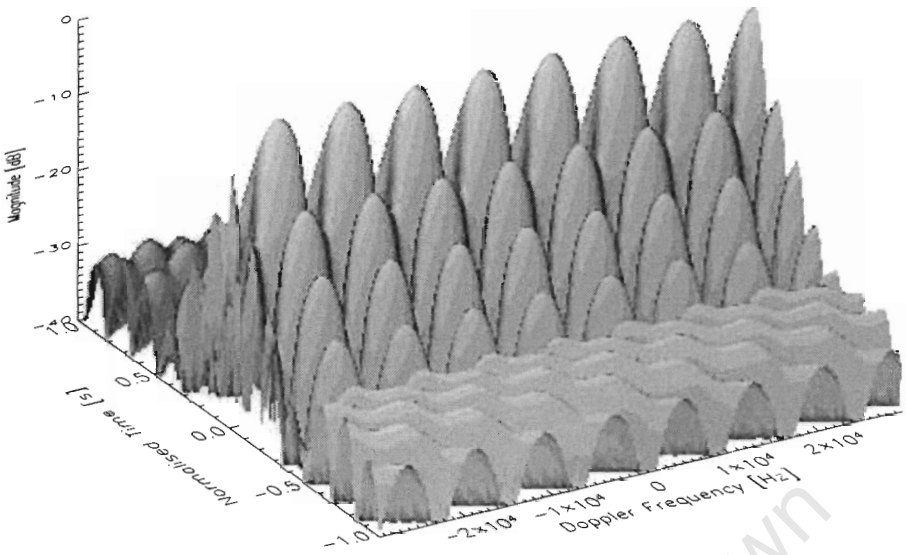

Figure 5.13: Ambiguity function for the chrominance subcarrier.

5.7 Conclusions

This chapter is an implementation of the knowledge of the various types of receiver systems which were built and tested in the past. Howland's method was explained in detail, as well as his system architecture which this research was based. System designs and simulations of the actual receiver were executed, along with an analysis of the recorded data. The components for the receiver designed for the Television Based Bistatic Radar have been provided in this chapter. The design of the receiver chain for the Television-Based bistatic radar system was shown and discussed, and the theory behind the receiver was implemented with the use of a pc TV card.

Results achieved from the simulations were analysed and presented the Doppler shifted signals from the simulation. The Doppler shift for a target leaving the Cape Town airport was extracted, as well as a plot of the ambiguity signal was presented. Much of the details and the estimations for the design of this receiver system was made possible due to the simulation created to estimate possible signal levels to be expected at the receiver.

Chapter 6

Conclusions and Future Work

Various uses of these radar systems, such as military and non-military applications have been presented, as well as the advantages and disadvantages for the system have been discussed in detail, and makes this type of system desirable for certain applications. The geometry and co-operation between the sites have been discussed, and presents a general overview of the structure for the receiver system to be built. It was also shown that the complexity of the bistatic system is greater than that of the monostatic radar as synchronisation between the transmitter and receiver should be achieved for accurate measurements.

A general, and brief overview of television signals has been given. The television waveform was shown, with the section of the actual waveform to be used was discussed. Actual waveforms of the television signal was acquired and processed. Possible solutions and variations to manipulate this signal to our advantage have also been discussed, and a simulation of the television signal was shown in Systemview, which was used as the input signal for the receiver simulation.

The designs for the receiver structure had been shown, and simulations of this system have also been implemented with successful extraction of Doppler information which will be used for target tracking methods. Doppler and DOA estimations were proved to be extracted from the receiver architecture, and processing of some of the recorded data have been done. A simulator has been created for accurate predictions of the SNR values at various distances away from the transmitter and receiver locations. The explanations and verification of the results created by the simulator was presented and discussed.

Recorded data was acquired with the use of a pc Pinnacle PCTV rave card. This data was analysed and signal processing was performed on this data. The Doppler shift for a target leaving the Cape Town airport was extracted, as well as an ambiguity diagram for the television signal used was presented. The ambiguity associated with the chrominance was also extracted and shown.

One of the major problems encountered in this research was the hardware limitations. The hardware available only allowed 4 ms of data to be captured. This only provided a resolution of 250 Hz. However, the Doppler shift of the signal was still successfully

extracted. Recommendations for this is to acquire equipment which allows for taking longer data recordings to achieve a better resolution to resolve closer targets. A second channel of the receiver could also be implemented to acquire measurements for DOA extractions.

Another problem which could be encountered when taking longer data recordings is the ability of the pc TV card's LO locking onto the transmitter's LO to provided a stable enough clock. This is vital to reduce any errors in the Doppler extractions caused due to the drift caused due to the local oscillators. Recommendations for this are to have a GPS system fixed at the transmitter whereby the receiver locks onto this frequency, and therefore recording accurate Doppler information of target flightpath. By doing so, finer resolutions can be accomplished with finer sampling intervals. Other possible scenarios for accurate testing measurements would be to ask for co-operation from the local broadcasting stations to transmit repetitive signals at certain times for measurement recordings.

In a general sense, a relatively cheap and simple Television Based Bistatic Radar receiver system was designed, simulated and tested at the University of Cape Town, for the investigation of bistatic systems.

Appendix A

Software Verification

c	=	$2.998 \times 10^{8}[\mathrm{ms}^{-1}]$
f	=	671.25 [MHz]
$\mathrm{P_T}$	=	200 [W]
$\mathrm{G_T}$	=	1
$\mathrm{G_R}$ (Omni − Directional Antenna)	=	1
$\mathrm{G_R}$ (Directional Antenna)	=	31.623
$\mathrm{t_0}$	=	0.25 [s]
λ	=	$\frac{c}{f}$
σ	=	20 [m^2]
$\mathrm{F_T}$	=	1
$\mathrm{F_R}$	=	1
k	=	1.38×10^{-23}
$\mathrm{T_S}$	=	290 [K]
$\mathrm{R_T}$ (Eqn 1)	=	40370 [m]
$\mathrm{R_R}$ (Eqn 1)	=	41910 [m]
$\mathrm{R_T}$ (Eqn 2)	=	135069 [m]
$\mathrm{R_R}$ (Eqn 2)	=	117261 [m]

Algorithm 1

$$\begin{aligned}\left(\frac{\mathrm{S}}{\mathrm{N}}\right) &= \frac{\mathrm{P_T G_T G_R t_0 \lambda^2 \sigma F_T F_R}}{(4\pi)^3\,\mathrm{k T_S R_T^2 R_R^2}} \\ &= \frac{(200)\,(1)\,(1)\,(0.25)\,(0.446)^2\,(20)\,(1)}{(4\pi)^3\,(1.38 \times 10^{-23})\,(290)\,(40370)^2\,(41910)^2} \\ &= 8.75 \\ &= 9.42\,\mathrm{dB}\end{aligned}$$

Algorithm 2

$$\begin{aligned}\left(\frac{S}{N}\right)_{min} &= \frac{P_T G_T G_R t_0 \lambda^2 \sigma F_T F_R}{(4\pi)^3 k T_S R_T^2 R_R^2} \\ &= \frac{(200)(1)(1)(0.25)(0.446)^2(20)(1)}{(4\pi)^3 (1.38\times10^{-23})(290)(135069)^2(117261)^2} \\ &= 0.099849 \\ &= -10.01\,\text{dB}\end{aligned}$$

Algorithm 3

$$\begin{aligned}\left(\frac{S}{N}\right) &= \frac{P_T G_T G_R t_0 \lambda^2 \sigma F_T F_R}{(4\pi)^3 K T_S R_T^2 R_R^2} \\ &= \frac{(200)(1)(31.623)(0.25)(0.446)^2(20)(1)}{(4\pi)^3 (1.38\times10^{-23})(290)(40790)^2(41230)^2} \\ &= 280.048 \\ &= 24.472\,\text{dB}\end{aligned}$$

Algorithm 4

$$\begin{aligned}\left(\frac{S}{N}\right)_{min} &= \frac{P_T G_T G_R t_0 \lambda^2 \sigma F_T F_R}{(4\pi)^3 K T_S R_T^2 R_R^2} \\ &= \frac{(200)(1)(31.623)(0.25)(0.446)^2(20)(1)}{(4\pi)^3 (1.38\times10^{-23})(290)(135069)^2(117261)^2} \\ &= 3.15753 \\ &= 4.993\,\text{dB}\end{aligned}$$

Appendix B

Doppler & DOA Extraction Verification

In the equations below, it should be noted the LO of the receiver is assumed to be locked onto the transmitter, and therefore is assumed to have the same value as that of the transmitter. This can be achieved by using an extremely stable synthesiser, such as the Rohde and Schwartz synthesiser to provided the stable LO which a reference signal, which can be used to phase lock onto other synthesisers and receivers for the system. $V_{\mathcal{A}}$& $V_{\mathcal{B}}$ are the signals received from the antenna structures. The bearing, or the direction of arrival, as mentioned is represented by θ in the equations.

The DOA bearing, θ, can be calculated by extracting the phase difference, $\Delta\phi$, from the two channels. The phase difference $\Delta\phi$ will be split into $\frac{\Delta\phi}{2}$ and $-\frac{\Delta\phi}{2}$ to simplify the mathematics. The positive and negative portions of this phase difference represents the positive and negative portions for the phase difference on either side of boresight to where the antennas are pointing. For instance, if the target was directly on boresight, there would be no phase difference between the channels, therefore $\Delta\phi = 0$ and $\theta = 0$.

It should also be noted that the amplitudes of the signal has been assumed to be of no great importance. This was established because the phase comparison monopulse system is used for the processing techniques, and the amplitudes will be normalised at the extraction of the phase difference information from the two channels. It is therefore assumed that the amplitude patterns are identical, therefore pure phase sensing can be achieved. This method of sensing was also demonstrated earlier by Rhodes, [32]. Since only the phase of the signals will be considered, the amplitudes of the signals will be represented by A.

$$
\begin{aligned}
V_{\mathcal{A}} &= A(\theta, d, t) \exp^{-j\left((\omega_{tx}t+\omega_d)t+\omega_d t-\frac{\Delta\phi}{2}\right)} \\
V_{\mathcal{B}} &= A(\theta, d, t) \exp^{-j\left((\omega_{tx}t+\omega_d)t+\omega_d t+\frac{\Delta\phi}{2}\right)}
\end{aligned}
$$

$$
f_{\text{out}} \quad \text{LO} = A(\theta, d, t) \exp^{j(\omega_{rx}t+\omega_d)t} \approx A(\theta, d, t) \exp^{j(\omega_{tx}t+\omega_d)t}
$$

$$
\begin{aligned}
V_{\mathcal{A}_{\text{IF}}} &= A(\theta, d, t) \exp^{-j\left((\omega_{tx}t+\omega_d)t+\omega_d t-\frac{\Delta\phi}{2}\right)} \cdot A(\theta, d, t) \exp^{j((\omega_{tx}t+\omega_d)t)} \\
&= A^2(\theta, d, t) \exp^{-j\left(\omega_d t-\frac{\Delta\phi}{2}\right)} \\
V_{\mathcal{B}_{\text{IF}}} &= A(\theta, d, t) \exp^{-j\left((\omega_{tx}t+\omega_d)t+\omega_d t+\frac{\Delta\phi}{2}\right)} \cdot A(\theta, d, t) \exp^{j((\omega_{tx}t+\omega_d)t)} \\
&= A^2(\theta, d, t) \exp^{-j\left(\omega_d t+\frac{\Delta\phi}{2}\right)}
\end{aligned}
$$

$$
\begin{aligned}
\Delta &= A^2(\theta, d, t) \exp^{-j\left(\omega_d t-\frac{\Delta\phi}{2}\right)} - A^2(\theta, d, t) \exp^{-j\left(\omega_d t+\frac{\Delta\phi}{2}\right)} \\
&= A^2(\theta, d, t) \exp^{-j\omega_d t}\left[\exp^{j\frac{\Delta\phi}{2}} - \exp^{-j\frac{\Delta\phi}{2}}\right] \\
\Sigma &= A^2(\theta, d, t) \exp^{-j\left(\omega_d t-\frac{\Delta\phi}{2}\right)} + A^2(\theta, d, t) \exp^{-j\left(\omega_d t+\frac{\Delta\phi}{2}\right)} \\
&= A^2(\theta, d, t) \exp^{-j\omega_d t}\left[\exp^{j\frac{\Delta\phi}{2}} + \exp^{-j\frac{\Delta\phi}{2}}\right]
\end{aligned}
$$

$$
\begin{aligned}
\frac{\Delta}{\Sigma} &= \frac{A^2(\theta, d, t)e^{-j\omega_d t} \times \left[e^{j\frac{\Delta\phi}{2}} - e^{-j\frac{\Delta\phi}{2}}\right]}{A^2(\theta, d, t)e^{-j\omega_d t} \times \left[e^{j\frac{\Delta\phi}{2}} + e^{-j\frac{\Delta\phi}{2}}\right]} \\
&= \frac{\left[e^{j\frac{\Delta\phi}{2}} - e^{-j\frac{\Delta\phi}{2}}\right]}{\left[e^{j\frac{\Delta\phi}{2}} + e^{-j\frac{\Delta\phi}{2}}\right]} \\
&= j\tan\left(\frac{\Delta\phi}{2}\right)
\end{aligned}
$$

Appendix C

Datasheets

The following pages are the datasheets for the components selected for the receiver design.

Coaxial

Frequency Mixers

NEW!

ZX05-SERIES

0.5 to 6000 MHz

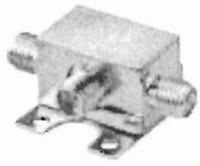

CASE STYLE: FL905

Features

- rugged construction
- small size
- low conversion loss
- high L-R isolation
- multiple patents pending

Applications

- cellular
- PCS
- instrumentation
- satellite communication

Electrical Specifications (T_{AMB}= 25°C)

MODEL NO.	LO level (dBm)	RF @ 1dB compr. (dBm) Typ.	FREQUENCY (MHz) LO/RF f_L-f_U	IF	CONVERSION LOSS (dB) Mid band m $\bar{x}$	σ	Max.	Total Range Max.	LO-RF ISOLATION (dB) L Typ.	Min.	M Typ.	Min.	U Typ.	Min.	LO-IF ISOLATION (dB) L Typ.	Min.	M Typ.	Min.	U Typ.	Min.	IP3@ center band Typ. (dBm)	E FACTOR	PRICE $ Qty. (1-24)
ZX05-1L	+3	0	2-500	DC-500	5.2	0.1	7.2	8.0	68	50	55	30	44	30	55	40	45	30	35	25	16	1.3	37.95
†• ZX05-10L	+4	+1	10-1000	DC-800	7.2	0.1	8.2	8.8	70	55	60	40	47	37	40	26	37	20	24	13	16	1.2	37.95
ZX05-1	+7	+1	0.5-500	DC-500	5.0	0.1	6.5	7.8	70	50	55	35	45	30	65	45	40	25	30	20	15	0.8	37.95
†• ZX05-2	+7	+1	5-1000	DC-1000	6.67	0.26	8.0	9.5	65	50	47	25	35	22	62	35	45	25	32	20	20	1.3	37.95
ZX05-10	+7	+1	10-1000	DC-800	6.8	0.1	7.8	8.3	80	50	60	40	47	37	40	26	33	20	24	13	16	0.9	37.95
†• ZX05-5	+7	+1	5-1500	DC-1000	6.6	0.1	7.5	9.3	50	40	40	25	33	23	50	40	30	20	20	10	15	0.8	37.95
ZX05-11X	+7	+1	10-2000	5-1000	7.1	0.1	8.2	9.8	62	45	36	20	27	18	60	45	37	20	38	20	9	0.2	37.95
• ZX05-C24	+7	+1	300-2400	DC-700	6.1	0.1	8.9	—			40 (typ.)	25 (min.)					25 (typ.)	15(min.)			10	0.3	37.95
ZX05-30W	+7	+1	300-4000	DC-950	6.8	0.2	9.0	9.8			35 (typ.)	17 (min.)					16 (typ.)	7(min.)			12	0.5	37.95
ZX05-C42	+7	+1	1000-4200	DC-1500	6.1	0.1	8.9	—			35 (typ.)	23 (min.)					20 (typ.)	12(min.)			10	0.3	37.95
• ZX05-C60	+7	+1	**1600-6000**	**DC-2000**																			
			1600-4400	DC-2000	6.3	0.2	8.3	—			32 (typ.)	20 (min.)					17 (typ.)	—			9	0.2	37.95
			4400-6000	DC-2000	6.2	0.3	8.5	—			23 (typ.)	17 (min.)					18 (typ.)	—			8	0.1	37.95
ZX05-1LHW	+10	+5	2-750	DC-750	5.3	0.1	6.8	8.5	66	50	52	35	46	27	64	40	50	27	40	20	15	0.5	38.95
• ZX05-C24LH	+10	+5	300-2400	DC-700	6.5	0.1	8.9	—			40 (typ.)	25 (min.)					30 (typ.)	15 (min.)			13	0.3	38.95
ZX05-C42LH	+10	+5	1000-4200	DC-1500	6.0	0.1	8.9	—			38 (typ.)	23 (min.)					20 (typ.)	11 (min.)			12	0.2	38.95
• ZX05-C60LH	+10	+5	**1600-6000**	**DC-2000**																			
			1600-4400	DC-2000	6.3	0.1	7.9	—			35 (typ.)	23 (min.)					17 (typ.)	—			13	0.3	38.95
			4400-6000	DC-2000	6.0	0.1	8.3	—			27 (typ.)	20 (min.)					21 (typ.)	—			11	0.1	38.95
†• ZX05-1MHW	+13	+9	0.5-600	DC-600	5.2	0.1	6.9	8.0	63	50	53	32	43	20	56	40	44	25	30	20	17	0.4	39.95
ZX05-12MH	+13	+9	10-1200	DC-1200	6.3	0.1	8.0	9.3	62	45	45	32	40	26	68	40	42	27	30	20	22	0.9	39.95
• ZX05-C24MH	+13	+9	300-2400	DC-700	6.1	0.1	8.6	—			40 (typ.)	20 (min.)					25 (typ.)	14 (min.)			13	0	39.95
ZX05-25MH	+13	+9	5-2500	5-1500	6.9	0.1	8.8	9.6	47	28	34	23	34	23	34	23	32	18	23	17	18	0.5	39.95
ZX05-42MH	+13	+9	5-4200	5-3500	7.5	0.2	9.8	11.6	47	26	29	20	30	15	34	23	26	17	23	17	19	0.6	39.95
ZX05-C42MH	+13	+9	1000-4200	DC-1500	6.2	0.1	8.9	—			35 (typ.)	15 (min.)					20 (typ.)	10 (min.)			16	0.3	39.95
• ZX05-C60MH	+13	+9	**1600-6000**	**DC-2000**																			
			1600-4400	DC-2000	6.9	0.1	8.5	—			32 (typ.)	26 (min.)					17 (typ.)	—			15	0.2	39.95
			4400-6000	DC-2000	6.0	0.1	8.5	—			22 (typ.)	18 (min.)					15 (typ.)	—			15	0.2	39.95
ZX05-1HW	+17	+14	5-750	DC-750	6.0	0.1	8.6	9.0	64	45	48	35	42	28	50	35	40	30	30	20	26	0.9	41.95
†• ZX05-10H	+17	+14	10-1000	DC-800	7.6	0.1	8.5	9.5	68	52	55	38	47	25	46	30	32	20	26	13	22	0.5	41.95
ZX05-17H	+17	+14	100-1700	50-1500	7.2	0.1	8.5	9.5	32	20	—	—	36	22	32	20	—	—	37	22	25	0.8	41.95
ZX05-20H	+17	+14	1500-2000	DC-300	5.2	0.2	7.8	—			31 (typ.)	22 (min.)					34 (typ.)	20 (min.)			22	0.5	41.95

E FACTOR= [IP3(dBm)-LO Power(dBm)]/10

† Models noted have positive phase detection. Phase detection negative for all other models

• Conversion loss specification at 30 MHz IF. For performance vs. IF See our website.

L = low range [f_L to 10 f_L] M = mid range [10f_L to f_U/2] U = upper range [f_U/2 to f_U]

m = mid band [2f_L to f_U/2]

REV. OR
M062306
ED-10927
ZX05-SERIES
RVM/CP
030528
page 1 of 2

Mini-Circuits®
INTERNET http://www.minicircuits.com
P.O. Box 350166, Brooklyn, New York 11235-0003 (718) 934-4500 Fax (718) 332-4661
Distribution Centers NORTH AMERICA 800-654-7949 • 417-335-5935 • Fax 417-335-5945 • EUROPE 44-1252-832600 • Fax 44-1252-837010
ISO 9001 CERTIFIED

ZX05-10 MIXER

AMPLIFIERS BY FREQUENCY (CONT.)

FREQUENCY (MHz)	MODEL NUMBER	GAIN (dB) (Min.)	VAR. (±dB) (Max.)	VSWR (Max.)	IMPED. IN/OUT (Ohms)	NOISE FIGURE (dB, Max.) F_1	F_0	F_2	P1 dB (dBm) (Min.)	VOLTS	NOM. DC POWER (mA)	OUTLINE NO.
50 – 1000	AM-1538	13	1.0	2.0:1	50/50	7.0	7.0	7.0	17	15	165	2
50 – 1000	AM-1510	13	1.25	2.0:1	50/50	7.0	7.0	7.0	20	15	250	2
50 – 1000	AM-1539	18	1.25	2.0:1	50/50	7.5	7.5	7.5	15	15	130	2
50 – 1000	AMP-1381	30	1.5	2.0:1	50/50	5.0	4.0	4.2	28	21	660	13
50 – 1000	AMP-1512	36	1.75	2.0:1	50/50	5.0	4.5	4.5	28	21	750	13
50 – 1200	AM-1141	10	1.0	2.0:1	50/50	6.0	6.0	6.0	8	15	45	7
100 – 180	AU-1372-140	7	0.2	1.5:1	50/50	8.0	8.0	8.0	13	15	65	1
100 – 180	AU-1552-140	10	0.25	1.5:1	75/75	5.0	5.0	5.0	20	15	85	1
100 – 180	AU-1576-140	12	0.25	1.3:1	75/50	9.0	9.0	9.0	14	15	180	2
100 – 180	AU-1510-140	13	0.2	1.5:1	50/50	7.0	7.0	7.0	22	15	250	2
100 – 180	AU-1538-140	13	0.2	1.5:1	50/50	7.0	7.0	7.0	17	15	165	2
100 – 180	AU-1049-140	14	0.2	1.5:1	50/50	2.7	2.7	2.7	10	15	40	1
100 – 180	AU-1046-140	19	0.2	1.5:1	50/50	2.7	2.7	2.7	10	15	40	1
100 – 180	AU-1499-140	21	0.2	1.5:1	50/50	8.0	8.0	8.0	17	15	195	3
100 – 180	AU-1541-140	24	0.2	1.5:1	75/75	2.5	2.5	2.5	20	15	180	2
100 – 180	AU-1459-140	26	0.2	1.5:1	50/50	3.0	3.0	3.0	14	15	130	3
100 – 180	AU-1469-140	28	0.2	1.5:1	50/50	7.5	7.5	7.5	15	15	240	3
100 – 180	AU-1127-140	29	0.2	1.5:1	75/75	1.3	1.3	1.3	7	15	55	2
100 – 180	AU-1092-140	29	0.2	1.5:1	75/75	3.2	3.2	3.2	19	15	125	3
100 – 180	AU-1092	29	0.25	1.3:1	75/75	3.2	3.2	3.2	18	15	125	3
100 – 180	AU-1293	29	0.25	1.3:1	75/75	1.5	1.5	1.5	7	15	55	2
100 – 180	AU-1006-140	30	0.2	1.5:1	50/50	1.3	1.3	1.3	8	15	50	2
100 – 180	AU-1158-140	30	0.2	1.5:1	50/50	2.9	2.9	2.9	19	15	125	3
100 – 180	AU-1093-140	32	0.2	1.5:1	50/50	3.0	3.0	3.0	17	15	135	3
100 – 180	AU-1555-140	34	0.2	1.5:1	50/50	1.4	1.4	1.4	14	15	130	3
100 – 180	AU-1466-140	35	0.25	1.5:1	50/50	1.2	1.2	1.2	7	15	45	2
100 – 180	AU-1571-140	38	0.2	1.5:1	50/50	1.3	1.3	1.3	18	15	225	3
100 – 180	AU-1263-140	43	0.2	1.5:1	50/50	1.5	1.5	1.5	19	15	140	4
100 – 180	AU-1027-140	44	0.2	1.5:1	50/50	1.4	1.4	1.4	10	15	75	3
100 – 180	AU-1415-140	44	0.25	1.5:1	50/50	1.4	1.4	1.4	19	15	140	4
100 – 180	AU-1360-140	45	0.2	1.5:1	75/75	2.0	2.0	2.0	19	15	140	4
100 – 180	AU-1204-140	52	0.2	1.5:1	50/50	2.0	2.0	2.0	19	15	130	3
100 – 180	AU-1575-140	54	0.25	1.5:1	50/75	2.0	2.0	2.0	15	15	225	4
100 – 180	AU-1494-140	56	0.25	1.5:1	50/50	1.2	1.2	1.2	12	15	70	3
100 – 450	AU-2A-1045	30	0.5	1.5:1	50/50	1.4	1.5	1.6	7	15	50	2
100 – 450	AU-3A-1045	44	0.5	1.5:1	50/50	1.4	1.5	1.6	10	15	75	3
100 – 550	AU-1330	7	0.5	2.0:1	50/50	6.5	6.5	6.5	23	15	135	2
100 – 1000	AM-1358	25	1.75	2.0:1	50/50	4.0	4.0	4.0	20	15	375	15-2
100 – 1000	AM-1530	35	1.75	2.0:1	50/50	4.5	3.7	3.7	20	15	375	15-2
100 – 1000	AM-1331	35	0.75	2.0:1	50/50	1.4	1.6	1.8	14	15	140	8
100 – 1000	AM-1412	35	0.75	2.0:1	50/50	1.4	1.6	1.8	14	15	140	3
100 – 2000	AMMIC-1420	12	1.5	2.2:1	50/50	6.0	6.0	6.0	12	15	135	7
100 – 2000	AMMIC-1348	13	1.0	2.2:1	50/50	5.0	4.3	4.6	14	15	150	7
100 – 2500	AM-1585	26	2.0	2.0:1	50/50	3.6	3.6	3.6	18	15	185	2
100 – 3000	AM-1526	9	1.0	2.0:1	50/50	8.0	5.5	5.5	20	15	160	1
100 – 3000	AM-1544	20	1.0	2.0:1	50/50	9.0	5.0	5.0	26	15	360	15-2
100 – 3000	AM-1373	30	1.75	2.0:1	50/50	6.0	5.0	5.0	19	15	390	15-2
100 – 3000	AM-1554	33	2.0	2.0:1	50/50	9.0	5.0	5.0	20	15	470	15-3
200 – 300	AU-1180	40	0.25	1.5:1	50/50	1.3	1.4	1.5	11	15	80	3
200 – 2000	AMMIC-1427	20	1.5	2.2:1	50/50	4.2	4.3	4.6	14	15	210	7
200 – 2000	AM-1569	20	1.5	2.2:1	50/50	4.2	4.3	4.6	14	15	210	2
225 – 400	AU-1501	35	0.25	2.0:1	50/50	2.0	2.0	2.0	21	15	240	3
500 – 1000	AMMIC-1141	10	0.5	1.5:1	50/50	6.0	6.0	6.0	10	15	45	7
500 – 1000	AM-1385	18	0.5	2.0:1	50/50	3.2	3.4	3.6	10	15	75	2
500 – 1000	AM-2A-0510	24	0.5	2.0:1	50/50	1.4	1.5	1.6	0	15	50	2
500 – 1000	AM-1518	30	0.5	2.0:1	50/50	1.8	2.0	2.2	15	15	155	3
500 – 1000	AM-1409	38	0.5	2.2:1	50/50	2.1	2.2	2.4	20	15	280	4
500 – 1000	AM-3A-0510	38	0.5	2.0:1	50/50	1.4	1.5	1.6	9	15	80	3
500 – 1000	AM-1556-0510	39	0.5	2.0:1	50/50	1.4	1.5	1.6	10	15	140	4
500 – 1000	AMP-1502	41	0.5	2.0:1	50/50	2.2	2.2	2.2	21	15	250	4
500 – 1000	AM-4A-0510	53	0.5	2.0:1	50/50	1.4	1.5	1.6	10	15	90	4
500 – 1500	AM-2A-0515	19	0.5	2.0:1	50/50	1.5	1.8	2.2	-5	15	50	2
500 – 1500	AM-3A-0515	29	0.5	2.0:1	50/50	1.5	1.8	2.2	4	15	85	3
500 – 1500	AM-4A-0515	40	0.75	2.0:1	50/50	1.5	1.8	2.2	5	15	95	4
500 – 1500	AM-5A-0515	50	0.75	2.0:1	50/50	1.5	1.8	2.2	5	15	90	5
500 – 2000	AM-1522	11	1.0	2.2:1	50/50	4.5	2.7	2.7	16	15	110	1
500 – 2000	AM-2A-0520	18	0.75	2.2:1	50/50	1.4	1.9	2.4	-6	15	50	2
500 – 2000	AM-3A-0520	29	0.75	2.0:1	50/50	1.4	1.9	2.4	3	15	85	3
500 – 2000	AM-1556-0520	39	0.75	2.0:1	50/50	1.5	1.9	2.4	10	15	140	4
500 – 2000	AM-4A-0520	40	1.0	2.0:1	50/50	1.4	1.9	2.4	5	15	95	4
500 – 2000	AM-5A-0520	50	1.25	2.0:1	50/50	1.4	1.9	2.4	5	15	90	5

13

AM-2A-0510 AMPLIFIER

LOW-NOISE AMPLIFIERS 50Ω

BROADBAND, LINEAR 0.1 to 2700 MHz


AMP

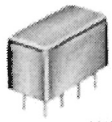
MAN

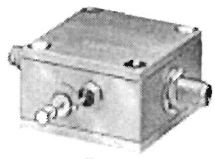
ZFL


TO

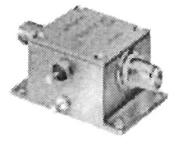
ZEL

up to +16 dBm output

MODEL NO.	FREQ. (MHz) f_L-f_U	NF (dB) Typ.	GAIN (dB) Min.	Flatness m	Flatness Max.	MAXIMUM POWER (dBm) Output (1 dB Comp.)	MAXIMUM POWER (dBm) Input (no damage)	INTERCEPT POINT (dBm) IP3 Typ.	VSWR Typ. In	VSWR Typ. Out	DC POWER Volt (V)	DC POWER Current (mA)	CASE STYLE Note B	CONNECTORS	PRICE $ Qty. (1-9)
AMP-15	5-1000	2.8	13	±0.6	±1.2	+8	+13	+22	2.1	2.1	15	29	PP120	cd	49.95
AMP-75	5-500	2.4	19	±0.4	±1.0	+12	+13	+28	2.1	2.1	15	31	PP120	cd	49.95
AMP-76	5-500	3.1	26	±0.7	±1.0	+13.5	+6	+28	2.1	2.1	15	71	PP120	cd	78.95
AMP-77	5-500	3.3	15	±0.4	±1.0	+16	+13	+32	2.1	2.1	15	56	PP120	cd	55.95
MAN-1LN**	0.5-500	3.0	28	±0.5	±1.4	+7	+15	+18	1.8:1	1.8:1	12	60	A05	cc	19.95
MAN-1HLN	10-500	3.7	16	±0.5	±0.8	+15	+15	+30	1.8:1	1.8:1	12	70	A06	cc	19.95
ZFL-500HLN	10-500	3.8	19	—	±0.4	+16	+15	+30	2:1	2:1	15	110	Y460	—	99.95
ZFL-500LN*	0.1-500	2.9	24	—	±0.5	+5	+5	+14	1.5:1	1.6:1	15	60	Y460	—	79.95
ZFL-1000LN	0.1-1000	2.9	20	—	±0.5	+3	+5	+14	1.5:1	2:1	15	60	Y460	—	89.95

m = mid range [2 f_L to $f_U/2$]

features

- very low noise
- ideal for printed-circuit designs (AMP,MAN & TO series)
- high dynamic range (ZHL- HLN & ZQL series)
- smooth response over entire band, no external resonances
- low impedance, less susceptible to EMI
- easy to use, 50 ohm input/output
- all models are cascadable

NOTES:

* VSWR 1.6:1 maximum from 0.1 to 0.2 MHz. Also available with BNC connectors.
** Below 5 MHz, 1 dB compression point decreases to 6.5 dBm.
▲ Available only with SMA connectors.
B. Connector types and case mounted options, case finishes are given in section 0, see "Case styles & outline drawings"
C. Prices and specifications subject to change without notice.
D. For Quality Control Procedures see Table of Contents, Section 0, "Mini-Circuits Guarantees Quality" article. For Environmental Specifications see Amplifier Selection Guide.
1. Absolute maximum power, voltage and current rating:
   1a. AMP models, 17V DC. 1b. MAN models, 12.5V DC. 1c. ZQL models, 17V DC.
2. Open load is not recommended, potentially can cause damage. With no load, derate max input power by 20 dB.
3. ZEL and TO models, NF specified at room temperature, increases to 2 dB typical at +85 deg C.
4. ZHL models, NF specified at room temperature, increases to 2.3 dB maximum at +65 deg C.

NSN GUIDE

MCL NO.	NSN
AMP-15	5895-01-350-9550
AMP-75	5895-01-350-9551
AMP-77	5895-01-350-9549
ZEL-1724LN	5996-01-450-0781
ZFL-1000LN	5998-01-412-3031

030605

Mini-Circuits®
INTERNET http://www.minicircuits.com
P.O. Box 350166, Brooklyn, New York 11235-0003 (718) 934-4500 Fax (718) 332-4661
Distribution Centers NORTH AMERICA 800-654-7949 • 417-335-5935 • Fax 417-335-5945 • EUROPE 44-1252-832600 • Fax 44-1252-837010
ISO 9001 CERTIFIED

AMP-76 AMPLIFIER

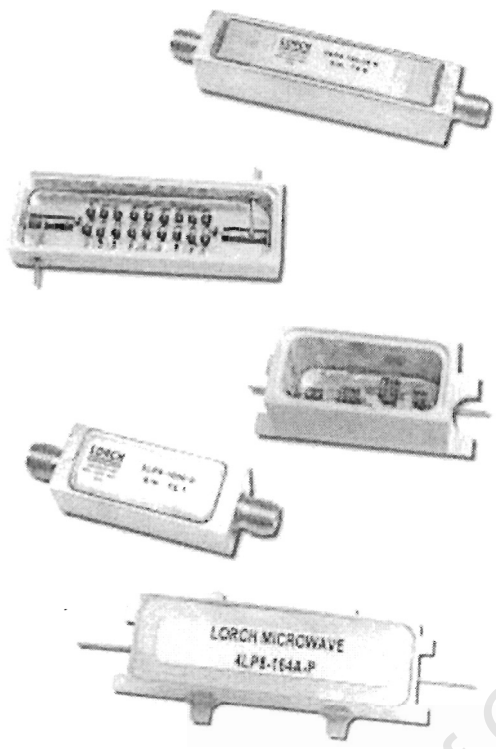

- *5 MHz to 10 GHz*
- *3 dB Bandwidths from 1% to > 100%*
- *Computer-Aided Designs*
- *10 Stock Series*
- *Custom & Dielectric Resonator Designs*

Lorch Microwave's miniature discrete component filters are designed to give optimal performance where small size is critical. Electrical and mechanical requirements for each design are computer generated, taking into consideration realizable "Q" and environmental conditions, then analyzed using our unique software, thereby reducing the amount of trial and error alignment.

Lorch Microwave's filter designs are available to satisfy bandpass, lowpass, highpass, or bandreject applications. We have found through our years of service that one design does not fit all needs. In order to achieve today's required electrical performance, Lorch Microwave's engineers use a variety of electrical circuits ranging from coupled tank, mesh, resonant ladder, highpass/lowpass, or helical to achieve the desired performance. In some cases, a combination of circuit designs is used. This enables our engineers to provide you with the highest performance filters available.

Lorch Microwave has developed a series of package types to satisfy the majority of industry needs. These range from small TO packages to 1/4-wave designs. Actual package selection will depend upon your specific performance needs. All machining is done on computer-controlled machines, thereby reducing error and assuring repeatability of critical processes. Our designs incorporate high "Q" air wound or toroidal inductors and monolithic ceramic capacitors.

Discrete Component Bandpass Filters

P/N	Freq. Range (MHz)	% 3 dB Bandwidth	VSWR (nominal)	Number of Sections	Avg. Power (watts)	Operating Temp. (°C)	Relative Humidity
BP2	5 - 100	3 - 100	1.5:1	2 - 10	10	-55 to +85	95%
BP3	25 - 200	3 - 100	1.5:1	2 - 10	10	-55 to +85	95%
BP4	15 - 200	3 - 100	1.5:1	2 - 10	10	-55 to +85	95%
BP5	5 - 200	3 - 100	1.5:1	2 - 10	10	-55 to +85	95%
BP6	50 - 10000	3 - 100	1.5:1	2 - 10	1	-55 to +85	95%
BP7	50 - 10000	3 - 100	1.5:1	2 - 10	1	-55 to +85	95%
BP8	50 - 10000	3 - 100	1.5:1	2 - 10	1	-55 to +85	95%
BP9	25 - 5000	5 - 100	1.5:1	2 - 10	1	-55 to +85	95%
MH	60 - 3000	1 - 5	1.5:1	2 - 10	1	-55 to +85	95%
T8B	70 - 1000	5 - 30	1.5:1	2 - 4	1	-55 to +85	95%

Shock 10 G
Vibration 20 G

See pages 20-24 for mechanical outlines and dimensions.
Contact factory for specific requirements not listed above

LORCH MICROWAVE
1725 N. Salisbury Blvd. • PO Box 2828 • Salisbury, MD 21802
P: 800-780-2169, 410-860-5100 • F: 410-860-1949 • www.lorch.com • lorchsales@lorch.com

ZX05-10 MIXER

BANDPASS 10.7 to 70 MHz

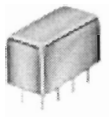

PIF
PBP
PBLP

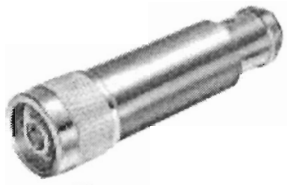

NIF
NBP
NBLP

constant impedance

MODEL NO.	CENTER FREQ. MHz	PASSBAND, MHz (loss < 1dB)	STOP BANDS (loss > 10 dB) at MHz	STOP BANDS (loss > 20 dB) at MHz	VSWR, 1.3:1, Typ. TOTAL BAND, MHz	CASE STYLE Note B	CONNECTION	PRICE $ (note 2a) Qty. (1-9)
_IF-21.4	21.4	18-25	4.9 & 85	1.3 & 150	DC-220	V	cs	14.95
_IF-30	30	25-35	7 & 120	1.9 & 210	DC-330	V	cs	14.95
_IF-40	42	35-49	10 & 168	2.6 & 300	DC-400	V	cs	14.95
_IF-50	50	41-58	11.5 & 200	3.1 & 360	DC-440	V	cs	14.95
_IF-60	60	50-70	14 & 240	3.8 & 400	DC-500	V	cs	14.95
_IF-70	70	58-82	16 & 280	4.4 & 480	DC-550	V	cs	14.95

For connector selection, add prefix letter P, B, N or S to _IF where applicable (see note 2)

elliptic response

MODEL NO.	CENTER FREQ. MHz	PASSBAND, MHz I.L. 1.5 dB Max. MHz	3 dB BANDWIDTH Typical MHz	STOP BANDS (I. Loss > 20 dB) at MHz	STOP BANDS (I. loss > 35 dB) at MHz	PASSBAND VSWR Max.	STOP BAND VSWR Typ.	CASE STYLE Note B	CONNECTION	PRICE $ (note 2b) Qty. (1-9)
_BP-10.7	10.7	9.5-11.5	8.9-12.7	7.5 & 15	0.6 & 50-1000	1.7:1	16:1	V	cr	18.95
_BP-21.4	21.4	19.2-23.6	17.8-25.3	15.5 & 29	3.0 & 80-1000	1.7:1	16:1	V	cr	18.95
_BP-30	30	27.0-33.0	25-35	22 & 40	3.2 & 99-1000	1.7:1	16:1	V	cr	18.95
_BP-60	60	55.0-67.0	49.8-70.5	44 & 79	4.6 & 190-1000	1.7:1	16:1	V	cr	18.95
_BP-70	70	63.0-77.0	58.0-82.0	51 & 94	6.0 & 193-1000	1.7:1	16:1	V	cr	18.95

For connector selection, add prefix letter P, B, N or S to _BP where applicable (see note 2)

BANDPASS, CONSTANT IMPEDANCE
TYPICAL FREQUENCY RESPONSE

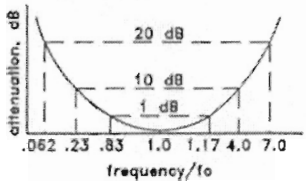

BANDPASS, ELUPTICAL
TYPICAL FREQUENCY RESPONSE

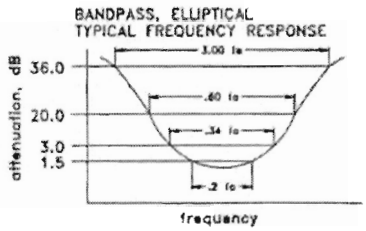

NSN GUIDE

MCL NO.	NSN
SIF-30	5915-01-464-8971

020711

200

_BP-10.7 FILTER

Bibliography

[1] *An experimental bistatic radar trails system*. ABC Press (Pty) Ltd, 1981.

[2] Barton DK. *Modern Radar System Analysis*. Artech House, Jan 1988.

[3] Bostian C W, Raab F H, Krauss Herbert L. *Solid State Radio Engineering*. John Wiley and Sons, Jan 1980.

[4] Burke G.J. Numerical electromagnetics code - NEC-4 method of moment part I: Users manual. Technical report, Lawrence Livermore National Laboratory, Jan 1992.

[5] Carrara B, Tourtier P, Pecot M. "Le radar MUET (radar multistatique utilisant des emetteurs de television)". *International Conference on Radar, Paris*, pages 426–431, May 1994.

[6] Chang CW. Television-Based Bistatic Radar. Technical report, University of Cape Town, RRSG, 2004.

[7] Del Mistro M. A Study of Bistatic Radar and the Development of an Independent Bistatic Radar Receiver. Master's thesis, University of Cape Town, 1992.

[8] Dunsmore MRB. *Bistatic Radars in Advanced Radar Techniques and Systems*. ABC Press (Pty) Ltd, 1993.

[9] Glaser J I. Fifty Years of Bistatic and Multistatic Radar. *Proceedings of the IEE*, 133(7):596–603, Dec 1986.

[10] Glossary AMS. Glossary of Meteorology - http://amsglossary.allenpress.com/glossary/ , November 2005.

[11] Griffiths H D, Baker C J. Measurement and Analysis of Ambiguity Functions of Passive Radar Transmissions. In *Proceedings IEEE International Radar Conference*, 2005.

[12] Griffiths H D, Baker CJ, Ghaleb H, Ramakrishnan R, Willman E. Measurement and Analysis of Ambiguity Functions of Off-Air Signals for Passive Coherent Location. *Electronics Letters*, 39(13):1005–1007, Jun 2003.

[13] Griffiths H D, Garnett A. J. Bistatic radar using satellite-borne illuminators of opportunity. *In IEE Conference Publications (Radar-92)*, pages 276–279, 1992.

[14] Griffiths H D, Long NRW. Television-Based Bistatic Radar. In *IEE Proceedings*, volume 133, pages 649 – 657, Dec 1986.

[15] Hanle E, Ing Dr, Gunputh HR. Survey of Bistatic and Multistatic Radar. *IEE Proceedings*, 133(Pt F No 7):587 – 595, Dec 1986.

[16] Hovanessian SA. *Introduction to Synthetic Array and Imaging Radars*. Artech House, Jan 1980.

[17] Hovanessian SA. *Radar System Design and Analysis*. Artech House, Jan 1984.

[18] Howland P E. A passive metric radar using a transmitter of opportunity. *in IEE Conference Publications (Radar-94)*, pages 251–256, May 1994.

[19] Howland P E. Passive Tracking of Airborne Targets Using Only Doppler and DOA Information. *IEE colloquium on algorithms for target tracking*, 1995.

[20] Howland P E. *Television Based Bistatic Radar*. PhD thesis, University of Birmingham, 1997.

[21] Howland P E. Target Tracking Using Television-Based Bistatic Radar. *IEE Proceedings on Radar, Sonar and Navigation*, 146(3):166–174, Jun 1999.

[22] Inggs M R, Del Mistro M. Performance of a L-Band Bistatic Radar Receiver. In *Proceedings of the 1991 IEEE South Africa AP/MTT Symposium*, volume AP/MTTS-91, pages 162–169, Aug 1991.

[23] Jackson M C. The Geometry of Bistatic Radar Systems. In *IEE Proceedings*, volume 133, pages 604–612, Dec 1986.

[24] Kingsley Simon, Quegan Shaun. *Understanding Radar Systems*. McGraw-Hill Book Company, Jan 1992.

[25] McHarg J. The Ambiguity Diagram - http://www.owlnet.rice.edu, July 2005.

[26] Mini-circuits. *RF/IF Designer's Handbook*. Mini-circuits Division of Scientific Components, 1992.

[27] Pell C, Hanle E. Bistatic and Multistatic Radar. *Proceedings of the IEE*, 133(7):585–586, Dec 1986.

[28] Poullin D, Lesturgie M. Radar Multistatic a Emissions Non Cooperatives. *IEE Conference Publications (Radar)*, pages 370–375, May 1994.

[29] Pozar DM. *Microwave and RF Design of Wireless Systems*. John Wiley and Sons, 2001.

[30] Ramshamole K. Modelling of Bistatic tracking radar. Technical report, University of Cape Town, RRSG, 2005.

[31] Reiners S. Front-End Implementation for a Television-Based Bistatic Radar. Technical report, University of Cape Town, RRSG, 2004.

[32] Rhodes Donald R. *Introduction to Monopulse*. McGraw-Hill Book Company, Jan 1959.

[33] Schoenenberger J.G. Totally independent bistatic radar receiver with real-time microprocessor correction. *IEE Conference Publications (Radar)*, pages 380–386, 1980.

[34] Sherman S M. *Monopulse Principles and Techniques*. Artech House, Apr 1985.

[35] Skolnik M I. An Analysis of Bistatic Radar. *Transactions on Communications Technology*, pages 19–27, 1961.

[36] Skolnik M I. *Introduction to Radar Systems, 2nd Edition*. McGraw-Hill Book Company, Jan 1980.

[37] Skolnik M I. *Radar Handbook, Second Edition*. McGraw-Hill Book Company, Jan 1990.

[38] Slater J. *Modern Television Systems to HDTV and Beyond*. PITMAN PUBLISHING, 1991.

[39] Stremler FG. *Introduction to Communication Systems: 3rd Edition*. Addison-Wesley Publishing Company, Jan 1990.

[40] Terzouli, Jr AJ, Calikoglu B. Evaluation and analysis of array antennas for passive coherent location systems. Technical report, Dayton Graduate Studies Institute (DAGSI), 2004.

[41] Tsao T. Ambiguity Function for a Bistatic Radar. *IEEE Trans on Aerospace and Electronic Systems*, 33(3):1041–1051, Jul 1997.

[42] Wikipedia. Wikipedia, the free encyclopedia - http://en.wikipedia.org/wiki/Passive Radar , November 2005.

[43] Wikipedia. Wikipedia, the free encyclopedia - http://en.wikipedia.org/wiki/Vestigial Sideband , November 2005.

[44] Willis NJ. *Bistatic Radar*. Artech House, 1995.